The Design and Tuning of Boronate-Tetraazaadamantane Covalent Adaptable Networks

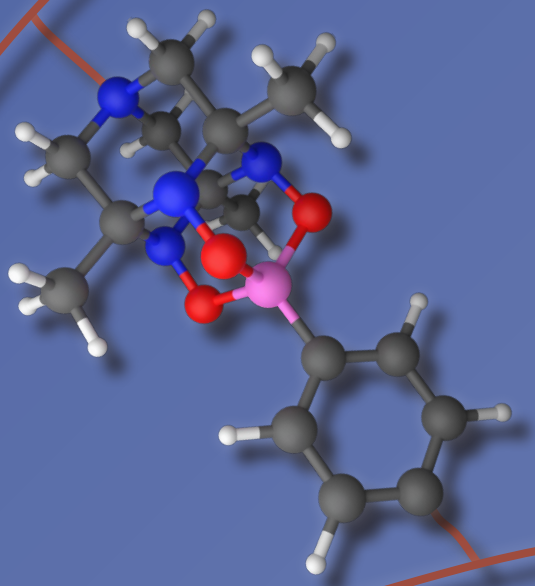

Simon van Hurne

Propositions

1. Without reversible RAFT (de)polymerization there is no future for recyclable, thermosetting polymer networks.
   (this thesis)

2. Large-scale implementation of (bio)degradable plastics will lead to yet another ecological disaster.
   (this thesis)

3. The publishing of research data in preprints before proper peer review will slow down science.

4. Replacing 85% of boronic esters in a covalent adaptable network with $-CF_3$ dipole-dipole interactions is a step towards unsustainability.
   (Mah et al., *Chem. Asian J.* **2024**, e202400143)

5. Engagement in role playing (video)games promotes empathy.

6. The strong focus on symptom relief over addressing underlying medical causes by medical professionals is detrimental to society.

Propositions belonging to the thesis, entitled

The Design and Tuning of Boronate-Tetraazaadamantane Covalent Adaptable Networks

Simon van Hurne
Wageningen, 17 September 2024

The Design and Tuning of Boronate-Tetraazaadamantane Covalent Adaptable Networks

Simon van Hurne

Thesis committee

Promotor
Prof. Dr H. Zuilhof
Professor of Organic Chemistry
Wageningen University & Research

Co-promotor
Dr M. M. J. Smulders
Associate professor at the Laboratory of Organic Chemistry
Wageningen University & Research

Other members
Prof. Dr J. van der Gucht, Wageningen University & Research
Dr E. Maaskant-Reilink, Wageningen University & Research
Dr K. V. Bernaerts, Maastricht University
Dr L. Pitet, Hasselt University

This research was conducted under the auspices of the VLAG Graduate School (Biobased, Biomolecular, Chemical, Food and Nutrition Science).

The Design and Tuning of Boronate-Tetraazaadamantane Covalent Adaptable Networks

Simon van Hurne

Thesis
submitted in fulfilment of the requirements for the degree of doctor
at Wageningen University
by the authority of the Rector Magnificus,
Prof. Dr C. Kroeze,
in the presence of the
Thesis Committee appointed by the Academic Board
to be defended in public
on Tuesday 17 September 2024
at 1 p.m. in the Omnia Auditorium.

Simon van Hurne
The Design and Tuning of Boronate-Tetraazaadamantane Covalent Adaptable Networks,
157 pages.

PhD thesis, Wageningen University, Wageningen, the Netherlands (2024)
With references, with summary in English and Dutch

DOI https://doi.org/10.18174/661580

Contents

1 General Introduction **1**

2 Electronic Effects in Covalent Adaptable Furan-Maleimide Networks **33**

3 Covalent Adaptable Networks using Boronate Linkages by incorporating Tetraazaadamantanes **65**

4 Tuning Material Properties of Covalent Adaptable Networks Containing Boronate-TAAD Bonds Through Systematic Variation in Electron Density of Ring Substituents **81**

5 Recyclable Covalent Adaptable Polystyrene-Networks using Boronates and Tetraazaadamantanes **103**

6 General Discussion **127**

7 Summary/Samenvatting **143**

8 Acknowledgements **149**

9 About the author **153**

Chapter 1

General Introduction

1.1 Background

In modern society polymers have achieved a prominent position, mostly in the form of plastic materials.[1,2] These plastics can be found in almost every cornerstone of society, be it as plastic bags in supermarkets for people to put their groceries in, or as cheap parts in toys or small devices, to even parts of high-end machinery in for example the automotive and computer industry. Plastics attained such widespread use because of their cheap, up-scalable production and their versatility.[3,4]
Plastic consists of polymers. There are many synthetic polymers that are produced to fulfil various functions nowadays. One of the first and most well-known examples of a synthetic polymer is bakelite.[5,6] Bakelite was invented by Leo Henricus Arthur Baekeland in 1907 by reacting phenol with formaldehyde.
Besides synthetic polymers, biopolymers are also an important group. Here one can think of lignin,[7,8] but also of cellulose[9] and starch.[10] Proteins[11,12] and DNA[13,14]/RNA[15,16] are very important polymers in the field of biology since they govern the functioning of living cells. These biopolymers can also be used to make various (bio)plastics.[17–19]

1.2 Polymer types and recycling

Despite the many advantages associated to polymers, their use also has negative impact on our society: there is a clear outstanding challenge on what to do with a polymer after its lifetime, *i.e.*, when it becomes waste. It has been estimated that annually 359 million tons of polymers have been produced in the last few years, with the actual amount likely being even larger.[20] Especially the synthetic polymers can be difficult to recycle or degrade. In this regard, it becomes important to distinguish between the main overarching types of plastics.
First, we have the thermoplastics, which are generally composed of loose polymer chains that have weak, non-covalent interactions with each other. Around 80% of all consumed plastics are considered thermoplastics.[21] Thermoplastics can be molten and reprocessed into a different shape.[22] As a result, thermoplastics tend to be easily recyclable. However, the absence of strong interchain crosslinks also means that these polymers typically have poor mechanical properties, excluding their use in high-strength applications.[23]

Second, there are thermosets.[24] In 2022 around 12% of all produced plastics (44 million tons) were thermosets.[25] Thermosets consist of covalently crosslinked polymers. Due to their covalent crosslinks these plastics are generally stronger, enabling their use in demanding applications and conditions. The bonds limit molecular movement, thus preventing chains from getting pulled apart akin to a fishing net. Because the chains are crosslinked into a permanent network, these plastics are not able to melt and thus cannot be reprocessed.[26] This means that thermosets can only be incinerated or shredded at the end of their life cycle.[20]
The increasing tonnage of polymer that is produced every year is causing serious problems.[3,27] Plastic waste management still has a lot of problems partly due to the low profitability of plastic recycling. In 2018 around only 9% of annually produced plastics consisted of recycled plastics.[28] Plastics are not always properly disposed of and as such exit the circular economy as waste instead of being properly recycled.[29,30] For thermosets, their crosslinked structure prevents thermal recycling, leading to incineration or landfilling, with the occasional shredding and downcycling as filler material.[31,32] A potential solution for these non-recyclable thermosets are covalent adaptable networks (CANs).[26,32–34]

1.3 Covalent adaptable networks

Covalent adaptable networks are crosslinked polymer networks that make use of dynamic covalent chemistry.[35–38] These adaptable networks utilise covalent crosslinks, thus giving these networks good mechanical properties, however these crosslinks can link/unlink or exchange in the presence of certain stimuli.[39–41] Using this principle, it is possible to create recyclable thermoset-like materials which combine the recyclability of thermoplastics and the mechanical performance of thermosets (**Figure 1.1**). This is a slight simplification though, as there is usually a trade-off between the recyclability of the material and its mechanical strength.[42]

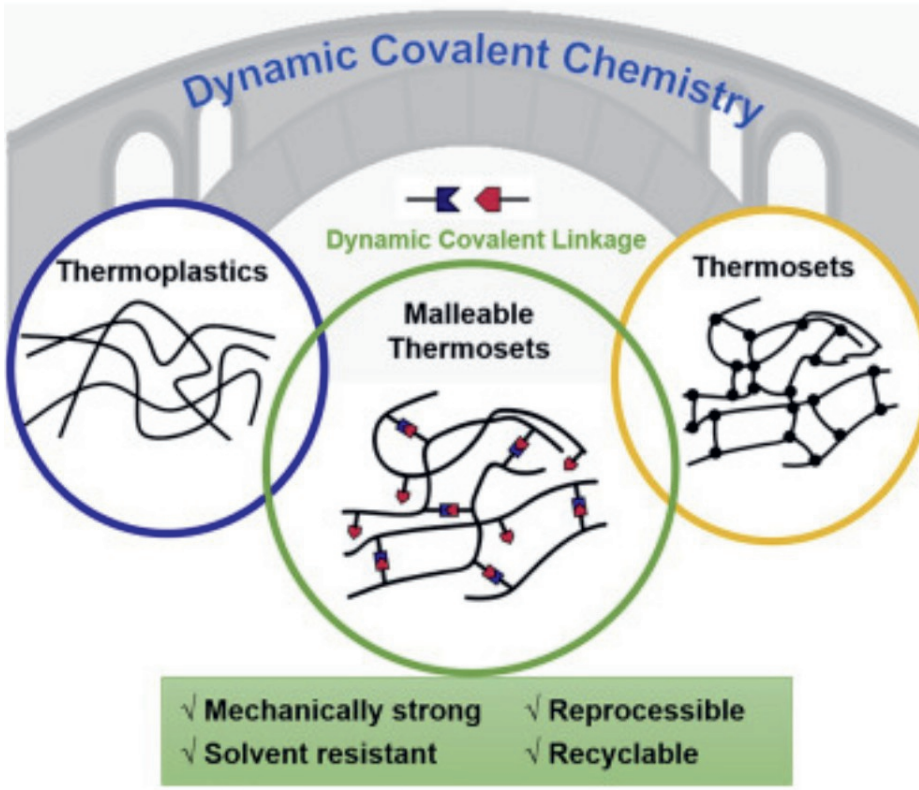

Figure 1.1: *The malleable thermosets, or covalent adaptable networks, bridging the gap between thermoplastics and thermosets. Figure adapted from Jin et al. (2019).*[33]

1.4 Dynamic covalent chemistry

There is a wide variety of reversible covalent chemistries that can be used to form covalent adaptable networks. These can be sorted into two categories based on the mechanism by which they are able to exchange: namely associative and dissociative networks, as illustrated in **Scheme 1.1**.[43] However, it should be kept in mind that some dynamic chemistries have multiple possible modes of exchange when exposed to different conditions.[44,45]

Dissociative networks require the crosslinks to first decouple before recoupling at a different site. This means that the crosslink density (the number of crosslinks per volume of material) changes over time. The crosslink density temporarily decreases when the linkage decouples and is restored upon recoupling at another position. Since the crosslink density is coupled to the mechanical strength of the material, the mechanical strength of such a material can thus also fluctuate as function of temperature. When taken to the extreme and all crosslinks are simultaneously decoupled, the network ceases to exist and the material melts, thus resembling conventional thermoplastics. This temperature-responsive bonding or debonding allows dissociative networks to switch between a thermoplastic-like state and a thermoset-like state.[46] Examples of dissociative chemistries are Diels-Alder reactions,[47–49] anilinium salts,[50,51] alkoxyamines[52–54] or triazolinedione-indole reactions.[55,56]

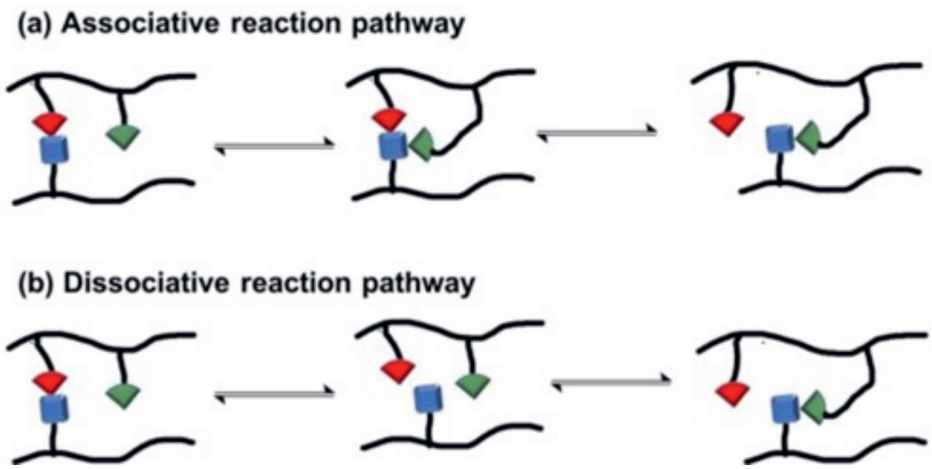

Scheme 1.1: *Dynamic bond exchange pathways: a) Associative reaction mechanism and b) dissociative reaction mechanism. Scheme adapted from Wanasinghe et al. (2022).*[43]

Within associative networks bond exchange reactions occur differently. Here, the dynamic crosslinks are able to exchange without the need to decouple first. This means that the crosslink density remains constant over time, since no crosslinks are broken. Instead, such a network becomes increasingly softer with increasing temperature as the exchange rate of the dynamic bonds speeds up. Examples of associative chemistries are imines,[57,58] esters,[59,60] boronic esters,[61–63] disulphides,[64,65] vinylogous urethanes,[66,67] thiol-Michael,[68,69] thiol-ene,[70,71] thiol-yne,[72,73] phosphate esters[74,75] and silyl ethers.[76,77]

Associative networks are often also called vitrimers.[78,79] Vitrimers are polymer materials that behave like glasses or metals in that they flow like viscoelastic liquids at high temperature and as glasses at low temperature, with a stable crosslinking degree.[42] This behaviour comes from the temperature-dependent bond exchange rate, which increases with temperature. By constructing an Arrhenius plot the activation energy of such thermally activated process can be calculated.[80] There has been some debate in the scientific community about whether only associative networks can be called vitrimers or if dissociative networks can also display vitrimer, or vitrimer-like, material behaviour.[51,81] Within this thesis, the term covalent adaptable network with the possible specification of associative or dissociative bond exchange will be used, since those terms are less likely to garner miscommunication when discussing these networks.

The catalogue of dynamic covalent motifs is still expanding, with additions such as the oxime metathesis,[82] diamide-imide[83,84] and TAD-indole[85] motifs (**Scheme 1.2**). Adapting these motifs for incorporation in CANs requires the necessary functional groups to be attached to multi-arm frameworks, such as linkers with two or more arms or as side chain to polymers, to enable crosslinking of the network. An additional consideration for the dynamic bond exchange reaction in CANs, compared to dynamic reactions in solution, is the reduced diffusion of reactive groups caused by the polymer matrix. This can limit reactive groups from efficiently reacting and exchanging.[86]

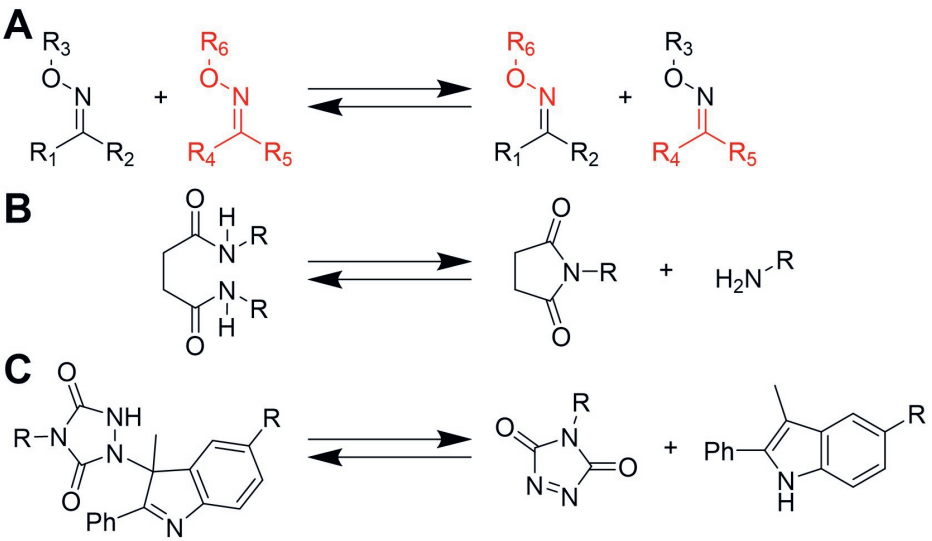

Scheme 1.2: *(A) The dynamic oxime metathesis motif as reported by Pettazzoni et al. (2024).*[82] *(B) The dynamic diamide-imide motif as reported by Lijsebetten et al. (2021).*[84] *(C) The dynamic TAD-indole motif as reported by Unal et al. (2018).*[85]

1.5 Boronic esters

The boronic ester is an interesting type of associative dynamic covalent bond. It can be present in a range of different states depending on the surrounding pH and on the presence of diols (or other poly-ols).[87–90] Boronic acids and esters are pH responsive. At high pH the coupling of boronic acids and diols to form boronic esters is favoured. Boronic esters will decouple at low pH to release the free boronic acid and diol. The pH-dependent equilibrium constant of the boronic ester formation depends on the pK_a of both the boronic acid and the diol.[91–93] At high pH both the boronic acid and boronic ester can take up an OH^- anion. This results in a negative charge on the boron to form a boronate, which drastically slows down the formation and exchange of the esters. A general overview of these equilibria can be seen in **Scheme 1.3**.

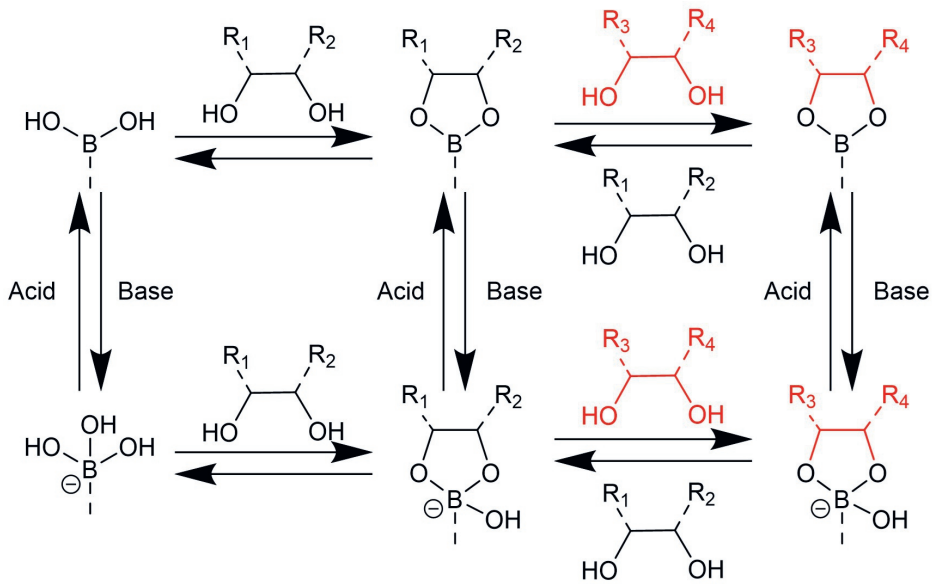

Scheme 1.3: *A general overview of the different states that a boronic acid can be found in. The state of the boronic acid is dependent on the pH and the presence of diols which can bind with the boronic acid.*

Boronic acids can have quite a range of possible uses, as will be described in this paragraph.[94,95] One of the most well-known uses of boronic acids is its use in the Suzuki coupling reaction. In this reaction a palladium catalyst can form a carbon-carbon bond between an organoboron and a halide.[96] In 2010 Akira Suzuki received a shared Nobel prize in chemistry for this type of carbon bond coupling chemistry. Boronic acids are also used in affinity chromatography.[97–99] Here, boronic acids bound onto silica particles can be used to make separation columns. Boronic acids have different interactions with a wide variety of (biological) compounds and can thus be used to separate a mixture.[100,101] Within the context of polymer chemistry, boronic esters are most commonly used in the formation of (hydro)gels.[102] The boronic ester is also susceptible to hydrolysis by water. In life outside of the laboratory, people might come in contact with boronic acids in the form of borax in laundry detergent or in toy slime. Boronic acids are considered biocompatible.[103,104] This biocompatibility, together with the numerous interactions boronic acids can have with biomolecules, makes boronic acids of interest in medicinal applications,[105–107] such as injectable gels[108] or drug delivery nanoparticles.[109–111]

There are many unique and creative implementations of boronic acid-based covalent adaptable networks,[112] but here I will now give two notable examples of previous research performed into these networks.[105,113–116] These examples showcase the great potential of boronic ester networks and left a big impact on this subfield of covalent adaptable networks.

Cash *et al.* nicely reported some self-healing boronic ester networks they created by reacting a vinylphenyl dioxaborolane with thiol linkers through irradiation at 365 nm to create a network. This network was then compared to a control network without dynamic bonds (**Figure 1.2**).[117] Cash *et al.* prepared a network with a more hydrophobic character as an attempt to limit water uptake and subsequent hydrolysis of the boronic esters. The formed network also healed quite well over the course of a couple days by wetting the interface and reconnecting the parts, as can be seen in **Figure 1.2C**, which illustrates the effect of the dynamic covalent bonds. The control network, which did not contain any dynamic covalent bonds, was not able not heal.

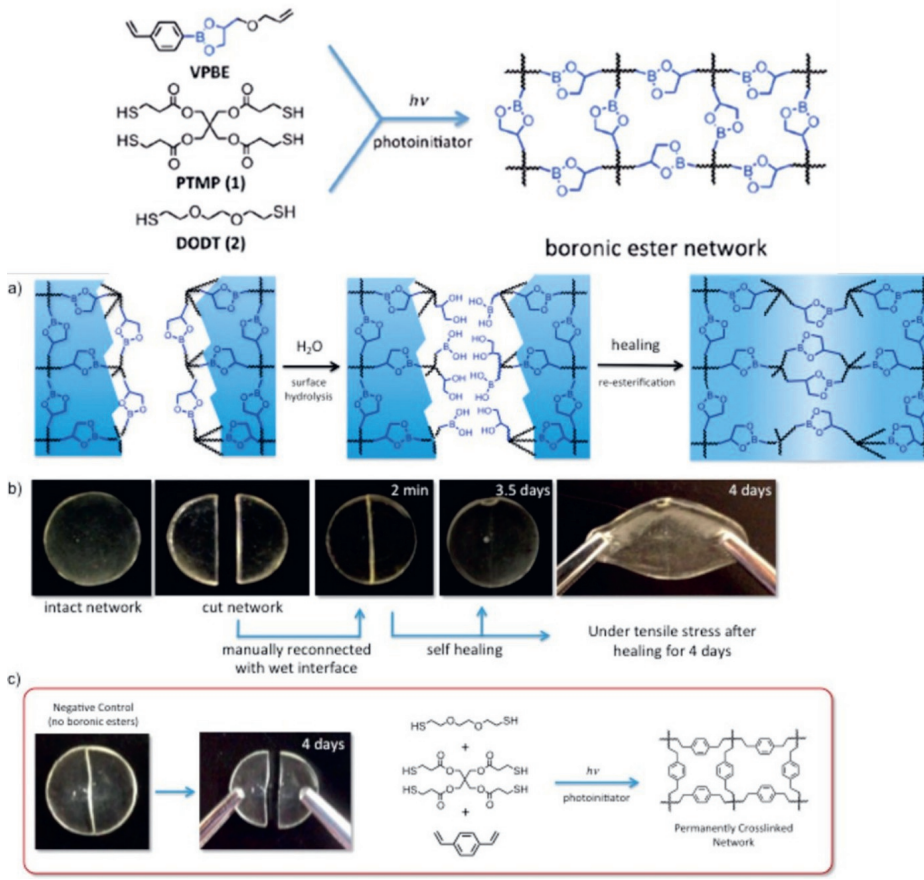

Figure 1.2: *A flexible, self-healing boronic acid-based hydrogel made by Cash et al. (2015).*[117] *(A) The breaking and healing of the hydrogel. (B) The self-healing ability of this covalent adaptable network. (C) A negative control using a normal covalent network.*

Röttger *et al.* reported a method to redesign high density polyethylene (HDPE) into a covalent adaptable network by introducing dynamic boronic ester linkages, as shown in **Figure 1.3**.[118] The dynamic linkages were introduced by either designing polymers from monomeric building blocks or by grafting dioxaborolanes onto existing polymers through reactive processing, thus creating a crosslinked CAN from a thermoplastic polymer. This can be used to obtain CANs with desired properties similar to the original thermoplastic polymer. Their new dynamic plastic showed great mechanical strength and stability. Additionally, the networks showed good creep resistance, yet were still able to exchange and relax stress at moderate temperatures. This allowed these dynamic polymers to be re-

processed. This work showed the potential of boronic acid-based networks and even showed some work on vitrimer interexchange, by effectively using the internal dynamic covalent bonds to weld a HDPE to a PMMA network.

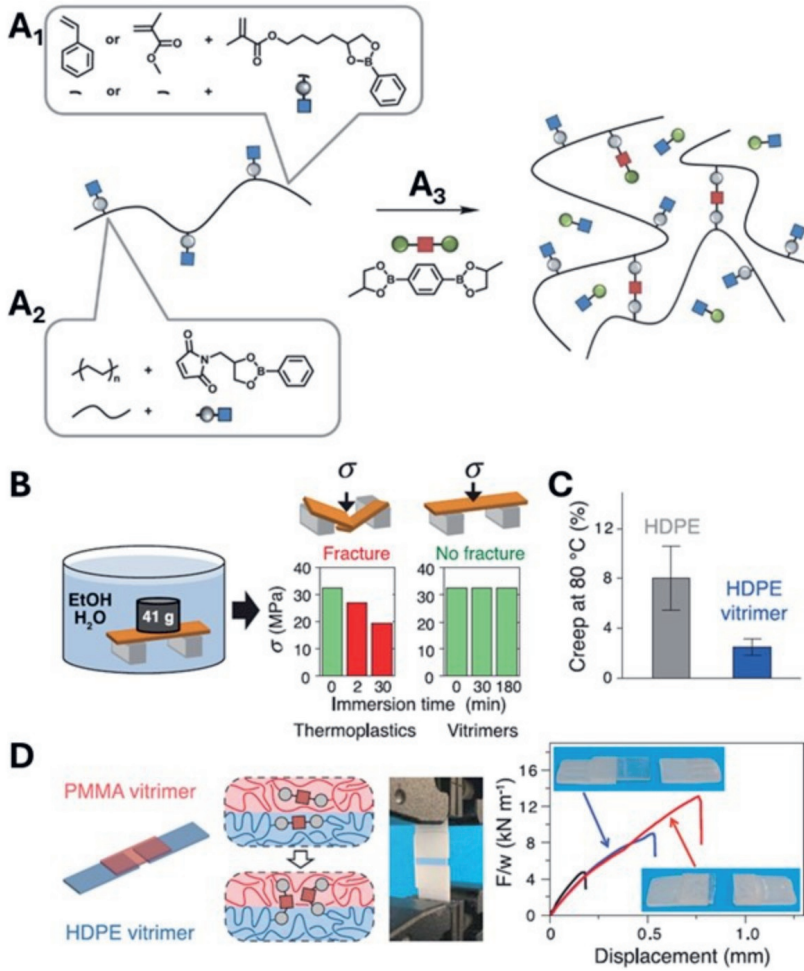

Figure 1.3: *High density polyethylene (HDPE) network containing dynamic boronic ester bonds reported by Röttger et al. (2017).*[118] *Panel A shows the polymerisation (A_1) or the grafting of dioxaborolanes onto existing polymers through reactive processing (A_2) followed by crosslinking with dioxaborolane. Panel B shows the mechanical strength of the material after different immersion times in a mixture of ethanol and water. Panel C shows the enhanced creep resistance of the boronic network at 80 °C compared to the conventional HDPE. Panel D shows the adhesion of the HDPE network to a PMMA network. The black curve is the negative control (10 min contact); the blue and red curves (10 and 20 min contact respectively) show the lap shear testing of the networks.*

1.6 Diels-Alder chemistry

The second dynamic covalent bond investigated in the work reported in this thesis is the dissociative Diels-Alder reaction between furan and maleimide. Diels-Alder (DA) reactions are well established within chemistry. First reported by Otto Diels and Kurt Alder in the year 1928,[47] a Diels-Alder reaction is a pericyclic reaction between a conjugated diene and a dienophile. One such couple is furan and maleimide. The furan and maleimide undergo a Diels-Alder reaction to form a six-membered ring at relatively low temperatures and decouple in a reverse Diels-Alder reaction at higher temperatures, generally around 120 °C. This also gives the reaction a temperature-dependent equilibrium.
The six-membered ring that is formed as Diels-Alder product can have two different configurations: an *endo* and an *exo* isomer, as can be seen in **Figure 1.4**. The endo isomer is the kinetic product. The *exo* isomer has a slightly higher activation energy, but is the thermodynamically most stable product. Depending on the structure of the diene and the dienophile and the reaction conditions a different ratio of *endo/exo* product will be obtained.[119–121] The ratio of *endo/exo* isomer can also influence the final conversion of the reaction and thus the crosslink density of the network.[122] The glass transition temperature of the network can also be influenced by this ratio if the temperature at which the *endo* and *exo* adduct undergo a thermal transition is far enough apart to be differentiated.[48]

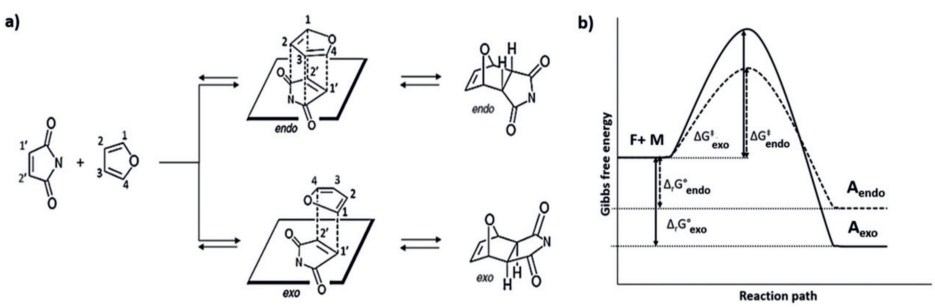

Figure 1.4: *A schematic representation of the Diels-Alder reaction between furan and maleimide made by Cuvellier et al. (2019).*[122] *(A) The reversible Diels-Alder reaction between furan and maleimide and the resulting endo and exo states of the product. (B) The Gibbs free energy profiles of the endo and exo product formations.*

Throughout the years many furan-maleimide Diels-Alder networks have been reported.[123–126] Here I will give two notable examples of reported reversible furan-maleimide networks, as these provide a clear overview of the properties and potential of furan-maleimide networks.
Dam *et al.* reported a thermally self-healing network derived from a four-armed furan linker and a trifunctional maleimide linker (**Figure 1.5A**).[127] They investigated the thermal reversibility of the furan-maleimide DA reaction in the network by following the conversion over several cycles of high and low temperature. The conversion showed a zig-zag pattern as shown in **Figure 1.5B**, indicative of a reversible process. As can be seen in **Figure 1.5C** the material could regain part of its original strength after fracture by subjecting it to a thermal treatment and 'healing' the sustained damage. This self-healing behaviour is a direct consequence of the exchange of the dynamic DA bonds within the material. Using SEM images (**Figure 1.5D**) of the material after healing, where they compare a scraped surface with an as-healed surface, they were able to show that the healing of the material is not limited to the surface of the material and that healing also takes place in the bulk of the material.

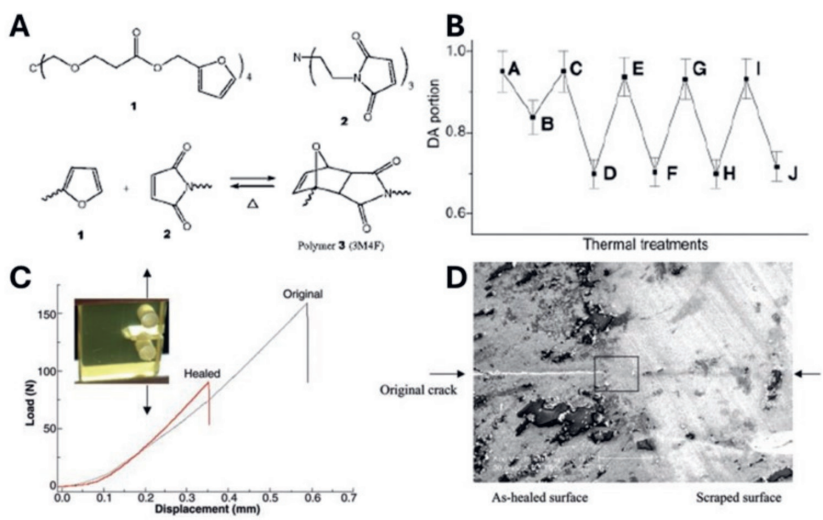

Figure 1.5: *A furan-maleimide material reported by Dam et al. (2002).[127] (A) the chemical structure for the furan and maleimide linkers. (B) Conversion of the Diels-Alder reaction followed over multiple thermal treatments to showcase the thermoreversibility of the network. (C) The mechanical strength of the material before and after healing, as measured with a compact tension test. (D) A SEM image of the healed material. By scraping the surface Dam et al. show that the healing is not limited to the surface layer of the material.*

Figure 1.6 displays a furan-maleimide network prepared by Kuang *et al.* showcasing the thermoreversibility of the furan-maleimide bond.[128] These authors also investigated the effect of the crosslink density on the thermal properties of the network. DSC heating curves showed a shift in the T_g towards higher temperatures when higher crosslink densities were used, going from 10 to 2 furans per maleimide (**Figure 1.6C**). By using temperature sweeps, they were also able to show that the height of the rubbery plateau correlated to the crosslink density of the dynamic network with a higher crosslink densities resulting in a higher rubbery plateau, as can be seen in **Figure 1.6D**.

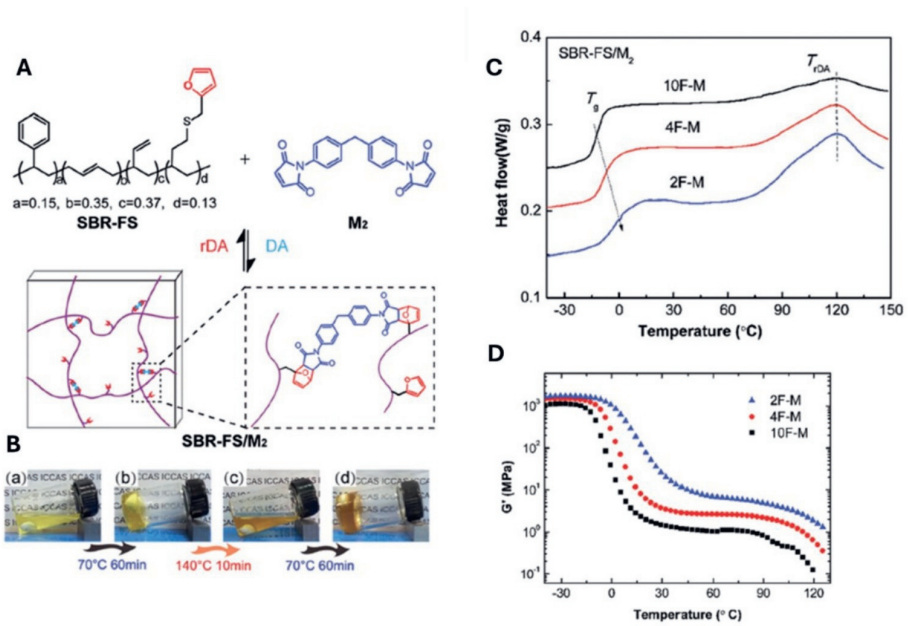

Figure 1.6: *(A) The structures of the furan-functionalised styrene-butadiene rubber (SBR) and bismaleimide crosslinker, and their reversible reaction to forming a network. (B) Photos showing the reversible gelation of the furan-maleimide network. (C) DSC curves showing a shift in T_g of the networks towards higher temperatures with increasing crosslink density of the network. The sample names, e.g., 10F-M represent the ratio of furan/maleimide used in the network, in this case 10 furans per maleimide. (D) Temperature sweeps of the networks with different furan/maleimide ratios. The height of the rubbery plateau increases with increasing crosslink density of the network. Figures adapted from Kuang et al. (2017).*[128]

1.7 Material tuning

If covalent adaptable networks are to compete with conventional plastics, they must show to be just as versatile and broadly applicable. One of the ways to show this, is to investigate possible methods that can be used to tune the material properties of CANs.[129] In recent years many new CANs have been developed. However, besides discovering new CANs, exploring the potential of already existing CANs is just as, if not more, important. Unlocking the potential of existing CANs will also increase our understanding of the specific dynamic covalent bond(s) used in the network as well as the properties of CANs as a whole.

1.8 Classical material tuning

Since CANs are polymer materials their properties can be tuned by conventional approaches used for the tuning of the properties of thermoplastics and thermosets. Materials can be tuned by changing, *e.g.*, the crosslinking degree,[128,130] introducing sterically bulky groups to hinder bond exchange,[131] the polymer matrix[132] and the degree of branching of the crosslinker.[133]

Another way to tune the properties of a material is by changing the spacer length[134,135] of the crosslinkers, as reported by Luo *et al.* in Diels-Alder networks.[136] They showed that short linkers resulted in stiffer networks, while longer linkers gave more flexible and dynamic materials. In **Figure 1.7** three different crosslinkers with different lengths were compared. The longest crosslinker, OBM, showed better healing and performance when compared to the two shorter linkers. This shows that including some flexibility into the network can promote the effect of molecular-level bond exchange to visible changes in macroscopic dynamic-mechanical properties.

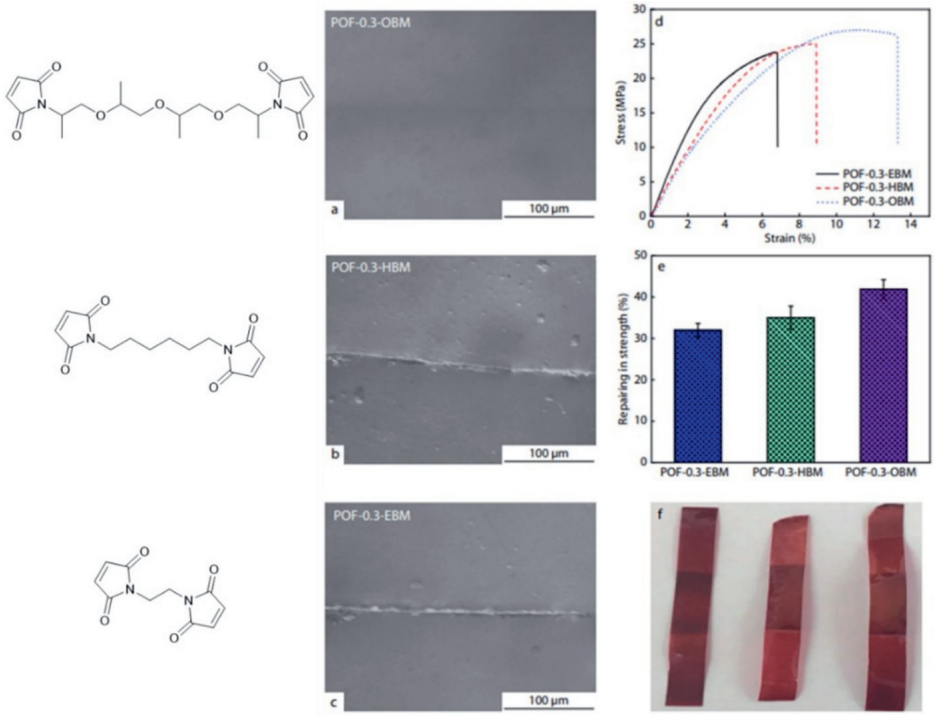

Figure 1.7: *A comparison of mechanic strength between furan-maleimide networks with differently sized spacers reported by Luo et al. (2020).*[136]

1.9 Internal/external catalysis

Since CANs utilise dynamic chemistry in their networks it is possible to catalyse the exchange reaction and thus influence the properties of the network. Depending on the dynamic chemistry used different catalysts could be used.[63,137–139]

An interesting example of catalysis in CANs was reported by Podgórski *et al.*, who showed how different catalysts influence the dielectric characteristics of a thiol-succinic anhydride network, as can be seen in **Figure 1.8**.[140] Podgórski *et al.* proposed a mechanism for the catalysis of reversible thiol-anhydride additions. They then tested thiol-anhydride CANs with either TEMPO, DMAP or DBU mixed in as organocatalyst to investigate whether that would influence the properties of the network. Using DMA, they show that the rubbery modulus (E_R) of the networks has a different drop-off temperature depending on the catalyst used (**Figure 1.8B**). The drop-off temperature of the E_R correlated to the strength (or

stability) of the dynamic bonds. In this example a higher pK_a is destabilising the dynamic bond, thus increasing the exchange rate and lowering the drop-off temperature of the E_R. In **Figure 1.8C**, **D** and **E** a comparison of the dielectric modulus as function of frequency at different temperatures for each of the catalysed networks is shown. It can be seen that the frequency at which the plateau of the dielectric modulus breakdowns is different for each catalysed network.

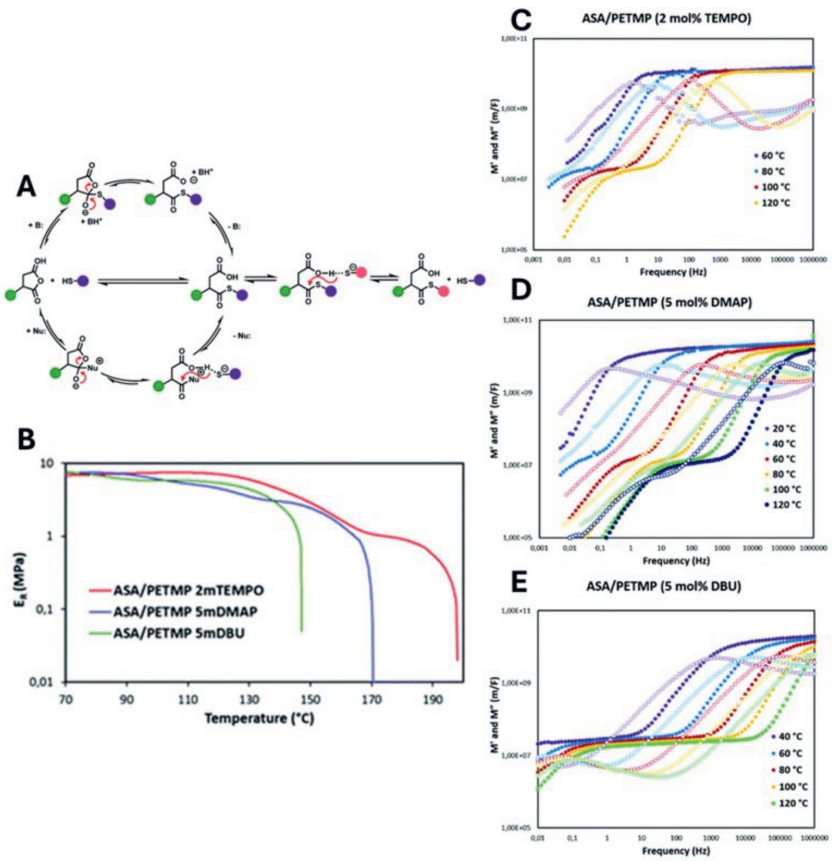

Figure 1.8: *(A) The proposed mechanism for the reversible catalysed reaction between thiols and anhydrides, and the reversible reaction between thiols and thioesters. (B) The rubbery modulus (E_R) of the thiol-anhydride CAN with different catalysts mixed in as measured by DMA. The dielectric modulus (filled) and loss (open) as function of frequency for thiol-succinic anhydride networks with TEMPO (B), DMAP (C) and DBU (D) as catalysts, as reported by Podgórski et al. (2020).*[140]

1.10 Stoichiometry of reactants

By influencing the stoichiometry of the reactants in a covalent adaptable network the equilibrium can be shifted towards a favoured side. An example of using stoichiometry to influence network properties can be found in the work of Safaei *et al.*, who prepared and tested maleimide-furan networks with varying ratios of maleimide/furan.[141] They found that for their networks the fracture stress showed a seemingly linear growth upon increasing the maleimide/furan ratio from a stoichiometry of 0.4 to 1, as can be seen in **Figure 1.9B**. This increase in the network's fracture stress is caused by the formation of a higher number of crosslinks in the network. The Young's modulus of the networks also increased with increasing maleimide/furan ratio, but reached a plateau at high ratios ($r > 0.7$), as shown in **Figure 1.9C**. Here the stiffness of the material barely increased at high ratios, for the network was already highly entangled and crosslinked.

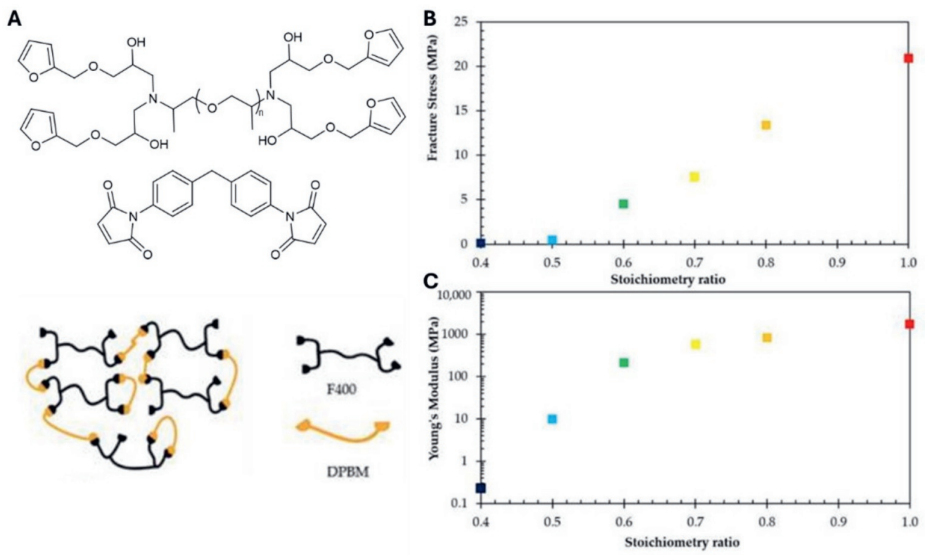

Figure 1.9: *(A) structure of a furan-maleimide network. (B) A graph showing the relation of the fracture stress of the network to the stoichiometry of the furan and maleimide groups in the network. (C) A graph showing the relation of the Young's modulus of the network to the stoichiometry of the furan and maleimide groups in the network. The ratio used is maleimide/furan. Figure adapted from Safaei et al. (2021).*[141]

1.11 Phase separation

The (micro-)environment of the incorporated dynamic bonds can also play a role in the dynamics of the network. Depending on the used network components phase separation can be found in the network.[142,143] A nice example of this can be seen in the work of Lessard *et al.* (**Figure 1.10**), who compared the material properties of a statistical and a phase-separated network, based on the dynamic covalent vinylogous urethane bond. The two blocks of the block copolymer were incompatible with each other and phase separated, whereas the statistical polymers showed a more or less homogenous distribution of network components. The phase-separated network showed longer relaxation, improved strain recovery and a slightly higher activation energy compared to the statistical network. This was attributed to a higher local crosslink structure and a restriction of strand diffusion, due to the phase separation.[66]

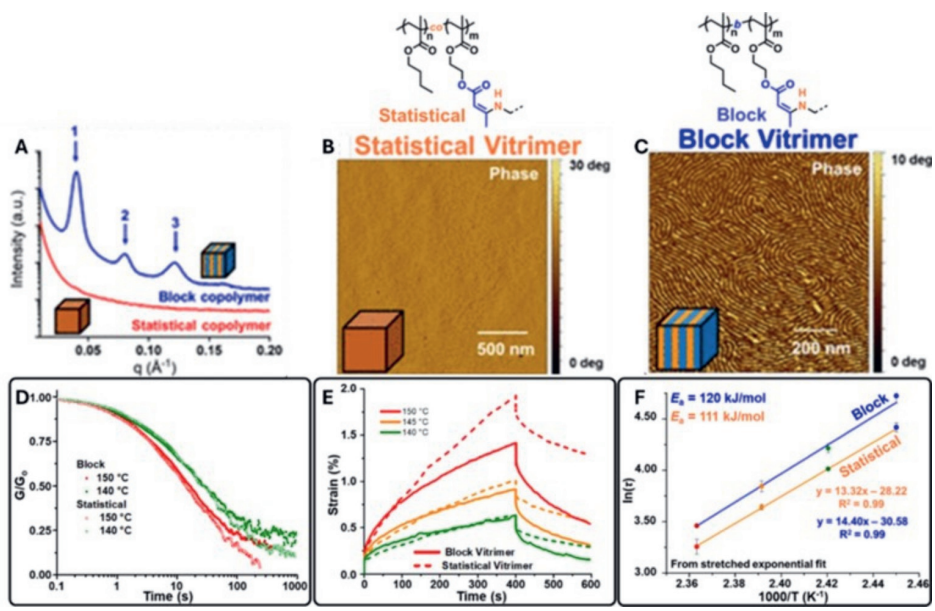

Figure 1.10: *(A) SAXS profile of bulk statistical (red) and block (blue) copolymers. (B) AFM image of a crosslinked and annealed statistical vitrimer. (C) AFM image of a crosslinked and annealed block vitrimer. (D) Stress relaxation of both statistical and block vitrimers at 140 and 150 °C and constant 0.3% strain. (E) Creep recovery of both statistical and block vitrimers at 140, 145 and 150 °C and a constant force of 5 kPa. (F) Arrhenius plot with activation energies for the statistical and block vitrimer. This figure was adapted from Lessard et al. (2020).*[66]

1.12 Electronic substituents

Electronic effects of neighbouring groups can also be used to tune the properties of materials. This electronic effect is based on the electron donating or withdrawing nature of aromatic ring substituents at the *meta*- or *para*-position compared to a hydrogen atom. By influencing the electronics around the dynamic bond it is possible to change its reactivity.
In **Figure 1.11** Schoustra *et al.* showed how making small molecular changes to dianiline linkers can influence the properties of a dynamic imine network.[57] By replacing the bridging substituent between the two phenyl rings of the dianiline the dynamic imine exchange could be tuned, as was observed in a dependence of the activation energy for stress relaxation as a function of electronic nature of the substituent (which was expressed by the corresponding Hammett parameter).[144] This could then also affect the macroscopic relaxation and creep resistance of the network. Creep being the time and temperature-dependent recoverable deformation of the material under constant load. Covalent adaptable networks are susceptible to creep, since even at low temperature their dynamic crosslinks are still exchanging. This allows the network to deform, and thus creep.

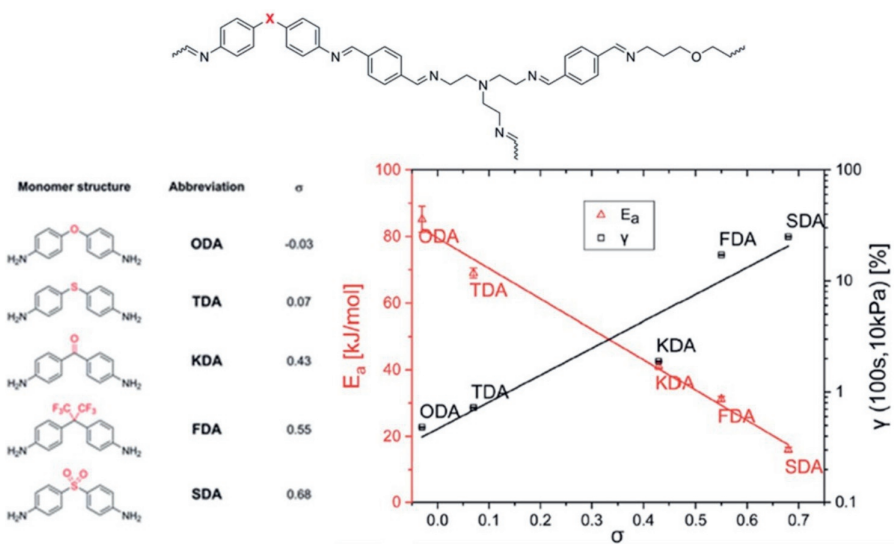

Figure 1.11: *The influence of substituents on the properties of imine-based covalent adaptable network (from Schoustra et al. (2020).*[145]

A similar effect can be seen in **Figure 1.12**, where Demchuk *et al.* showed that the substitution of boronic acids can influence the material properties of the network they are incorporated into.[146] They incorporated four differently substituted boronic acids, with –F, –Cl, –H or $–OCH_3$ at the *meta* position relative to the boronic acid, in boronic ester networks to create four distinct CANs. In **Figure 1.12B** DSC curves of differently substituted boronic ester networks are shown. Demchuk *et al.* showed that the F-containing and Cl-containing networks have a similar T_g, with the H-containing network having a lower T_g, followed by the OCH_3-containing network. This can be approximately be explained by –F and –Cl having roughly the same σ_m value (–Cl = 0.37; –F = 0.34) with –H (0.00) and $–OCH_3$ (0.12) having lower σ_m values. Stronger electron withdrawing substituents can lower the electron density on the boronic acid, thus making it less dynamic. The resulting reduced exchange rate shifts the thermal transition to higher temperatures. This can also be seen in **Figure 1.12C** where the activation energy is determined for each substituted network. The networks with electron withdrawing substituents are shown to generally have a higher activation energy, however it is difficult to determine an exact trend from this dataset.

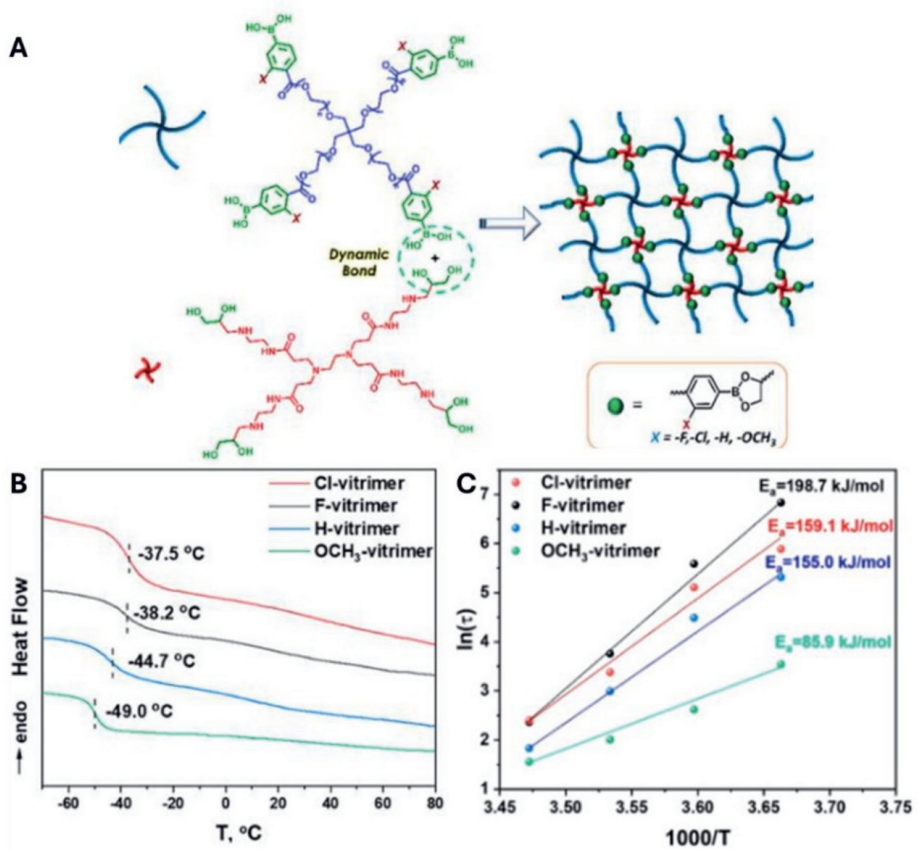

Figure 1.12: *(A) Network components of the boronic ester vitrimer. The meta substituent of the boronic acid is varied between –F, –Cl, –H and –OCH_3. (B) DSC curves of the different vitrimers. The T_g values are indicated per vitrimer. (C) Apparent E_a profiles obtained from relaxation experiments for the different vitrimers. Adapted from Demchuk et al. (2023).*[146]

1.13 Aim of this thesis

In recent years much research has been done on covalent adaptable networks, with many novel dynamic motifs being incorporated in polymeric networks. However, there are still issues with control over the dynamics of dynamic covalent bonds in networks and still a need for knowledge on how the dynamicity of the dynamic covalent bonds relates to the observed macroscopic properties of CANs. Both are needed for them to become more viable for (industrial) applications.

In this thesis project the main goal is to investigate covalent adaptable networks and to develop methods to tune the material properties by making changes on the molecular level. The attention is divided between networks containing boronic esters and networks containing the Diels-Alder couple furan-maleimide.

Chapter 2 reports an investigation regarding the possibility of tuning macroscopic material properties of furan-maleimide networks through variation of the electronic nature of aromatic ring substituents in maleimide linkers. A series of five differently substituted maleimide linkers is prepared and incorporated in furan-maleimide networks. These networks are investigated and compared using IR and rheology.

Chapter 3 discusses the development of a novel type of boronic ester-based CAN by introduction of TetraAzaADamantane (TAAD) moieties. TAAD is an adamantane-like structure with three nitrogen atoms in the bottom ring and one nitrogen atom on top. The bottom nitrogen atoms in the bottom ring have a hydroxyl group, thus making the TAAD a triol.[147,148] Golovanov *et al.* showed that the boronate-TAAD couple displayed strong binding and good hydrolytic stability.[148] This chapter describes the research on how to extend the work by Golovanov *et al.* to covalent adaptable networks.

Chapter 4 expands on the boronate-TAAD-based CAN by making a side-by-side comparison between a conventional boronate-diol-based CAN and the novel boronate-TAAD-based CAN. On top of that, the tunability of boronate-TAAD-based CANs through variations in electronic groups on the *meta*-position of the phenylboronic acid is investigated.

Chapter 5 takes the concept of the boronate-TAAD linkage and applies it to a polystyrene-based system with a permanent backbone to make recyclable, yet crosslinked polystyrene. Here a TAAD-functionalised polystyrene variant is prepared with a high styrene content and crosslinked with a bisboronic acid crosslinker. The material was characterised on its rheological behaviour, reprocessability and swelling behaviour. The tunability was also studied in the form of variations in the crosslinking degree and the incorporation of an external acid catalyst.

Chapter 6 discusses the topics in earlier chapters in a broader context and presents some interesting future prospects, such as Tetraazaadamantane derivatisation and the possibility for tuning boronic esters through metal-ion coordination.

References

[1] D. Feldman, *Des. Monomers Polym.* **2008**, *11*, 1–15, DOI 10.1163/156855508x292383.

[2] R. Geyer, J. R. Jambeck, K. L. Law, *Sci. Adv.* **2017**, *3*, e1700782, DOI 10.1126/sciadv.1700782.

[3] R. C. Thompson, C. J. Moore, F. S. vom Saal, S. H. Swan, *Philos. Trans. R. Soc. Lond. B Biol. Sci.* **2009**, *364*, 2153–66, DOI 10.1098/rstb.2009.0053.

[4] A. L. Andrady, M. A. Neal, *Philos. Trans. R. Soc. B Biol. Sci.* **2009**, *364*, 1977–84, DOI 10.1098/rstb.2008.0304.

[5] L. H. Baekeland, *Ind. Eng. Chem.* **1909**, *1*, 149–161, DOI 10.1021/ie50003a004.

[6] D. Crespy, M. Bozonnet, M. Meier, *Angew. Chem. Int. Ed. Engl.* **2008**, *47*, 3322–8, DOI 10.1002/anie.200704281.

[7] D. S. Bajwa, G. Pourhashem, A. H. Ullah, S. G. Bajwa, *Ind. Crops and Prod.* **2019**, *139*, 111526, DOI 10.1016/j.indcrop.2019.111526.

[8] Y. Zhang, M. Naebe, *ACS Sustain. Chem. Eng.* **2021**, *9*, 1427–1442, DOI 10.1021/acssuschemeng.0c06998.

[9] A. C. O'Sullivan, *Cellulose* **1997**, *4*, 173–207, DOI 10.1023/a:1018431705579.

[10] A. Apriyanto, J. Compart, J. Fettke, *Plant Sci.* **2022**, *318*, 111223, DOI 10.1016/j.plantsci.2022.111223.

[11] K. Numata, *Polym. J.* **2020**, *52*, 1043–1056, DOI 10.1038/s41428-020-0362-5.

[12] P. Gupta, K. K. Nayak, *Polym. Eng. Sci.* **2015**, *55*, 485–498, DOI 10.1002/pen.23928.

[13] O. Thum, S. Jäger, M. Famulok, *Angew. Chem. Inter. Ed.* **2001**, *40*, 3990–+, DOI 10.1002/1521-3773(20011105)40:21<3990::Aid-Anie3990>3.0.Co;2-0.

[14] J. D. Watson, F. H. Crick, *Nature* **1953**, *171*, 737–8, DOI 10.1038/171737a0.

[15] G. L. Conn, D. E. Draper, *Curr. Opin. Struct. Biol.* **1998**, *8*, 278–85, DOI 10.1016/s0959-440x(98)80059-6.

[16] S. A. Mortimer, M. A. Kidwell, J. A. Doudna, *Nat. Rev. Genet.* **2014**, *15*, 469–79, DOI 10.1038/nrg3681.

[17] J. Han, Y. Guo, H. Wang, K. Zhang, D. Yang, *J. Am. Chem. Soc.* **2021**, *143*, 19486–19497, DOI 10.1021/jacs.1c08888.

[18] A. Shafqat, A. Tahir, A. Mahmood, A. B. Tabinda, A. Yasar, A. Pugazhendhi, *Biocatal. Agric. Biotechnol.* **2020**, *27*, 101540, DOI 10.1016/j.bcab.2020.101540.

[19] J. H. Huang, W. F. Liu, X. Q. Qiu, *ACS Sustain. Chem. Eng.* **2019**, *7*, 6550–6560, DOI 10.1021/acssuschemeng.8b04936.

[20] H. Jiao, S. S. Ali, M. H. M. Alsharbaty, T. Elsamahy, E. Abdelkarim, M. Schagerl, R. Al-Tohamy, J. Sun, *Ecotoxicol. Environ. Saf.* **2024**, *271*, 115942, DOI 10.1016/j.ecoenv.2024.115942.

[21] M. Kazemi, S. F. Kabir, E. H. Fini, *Resour. Conserv. and Recy.* **2021**, *174*, 105776, DOI 10.1016/j.resconrec.2021.105776.

[22] S. S. Ali, T. Elsamahy, R. Al-Tohamy, D. Zhu, Y. A. Mahmoud, E. Koutra, M. A. Metwally, M. Kornaros, J. Sun, *Sci. Total Environ.* **2021**, *780*, 146590, DOI 10.1016/j.scitotenv.2021.146590.

[23] P. Jagadeesh, S. Mavinkere Rangappa, S. Siengchin, M. Puttegowda, S. M. K. Thiagamani, G. Rajeshkumar, M. Hemath Kumar, O. P. Oladijo, V. Fiore, M. M. Moure Cuadrado, *Polym. Compos.* **2022**, *43*, 5831–5862, DOI 10.1002/pc.27000.

[24] H. Dodiuk, S. H. Goodman in *Handbook of Thermoset Plastics*, (Ed.: H. Dodiuk), William Andrew Publishing, Boston, **2022**, pp. 1–11, DOI 10.1016/b978-0-12-821632-3.00009-9.

[25] E. Morici, N. T. Dintcheva, *Polymers-Basel* **2022**, *14*, 4153, DOI 10.3390/polym14194153.

[26] W. Post, A. Susa, R. Blaauw, K. Molenveld, R. J. I. Knoop, *Polym. Rev.* **2020**, *60*, 359–388, DOI 10.1080/15583724.2019.1673406.

[27] M. R. Johansen, T. B. Christensen, T. M. Ramos, K. Syberg, *J. Environ. Manage.* **2022**, *302*, 113975, DOI 10.1016/j.jenvman.2021.113975.

[28] P. Jagadeesh, S. Mavinkere Rangappa, S. Siengchin, M. Puttegowda, S. M. K. Thiagamani, G. Rajeshkumar, M. Hemath Kumar, O. P. Oladijo, V. Fiore, M. M. Moure Cuadrado, *Polym. Compos.* **2022**, *43*, 5831–5862, DOI 10.1002/pc.27000.

[29] J. P. Lange, *ACS Sustain. Chem. Eng.* **2021**, *9*, 15722–15738, DOI 10.1021/acssuschemeng.1c05013.

[30] S. M. Al-Salem, P. Lettieri, J. Baeyens, *Waste Management* **2009**, *29*, 2625–43, DOI 10.1016/j.wasman.2009.06.004.

[31] A. Rahimi, J. M. García, *Nat. Rev. Chem.* **2017**, *1*, 0046, DOI 10.1038/s41570-017-0046.

[32] L. Imbernon, S. Norvez, *Eur. Polym. J.* **2016**, *82*, 347–376, DOI 10.1016/j.eurpolymj.2016.03.016.

[33] Y. H. Jin, Z. P. Lei, P. Taynton, S. F. Huang, W. Zhang, *Matter* **2019**, *1*, 1456–1493, DOI 10.1016/j.matt.2019.09.004.

[34] G. M. Scheutz, J. J. Lessard, M. B. Sims, B. S. Sumerlin, *J. Am. Chem. Soc.* **2019**, *141*, 16181–16196, DOI 10.1021/jacs.9b07922.

[35] C. Bowman, F. Du Prez, J. Kalow, *Polym. Chem.* **2020**, *11*, 5295–5296, DOI 10.1039/d0py90102d.

[36] N. Zheng, Y. Xu, Q. Zhao, T. Xie, *Chem. Rev.* **2021**, *121*, 1716–1745, DOI 10.1021/acs.chemrev.0c00938.

[37] S. Huang, X. Kong, Y. S. Xiong, X. R. Zhang, H. Chen, W. Q. Jiang, Y. Z. Niu, W. L. Xu, C. G. Ren, *Eur. Polym. J.* **2020**, *141*, 110094, DOI 10.1016/j.eurpolymj.2020.110094.

[38] F. Garcia, M. M. J. Smulders, *J. Polym. Sci. A Polym. Chem.* **2016**, *54*, 3551–3577, DOI 10.1002/pola.28260.

[39] Y. Jin, C. Yu, R. J. Denman, W. Zhang, *Chem. Soc. Rev.* **2013**, *42*, 6634–54, DOI 10.1039/c3cs60044k.

[40] P. T. Corbett, J. Leclaire, L. Vial, K. R. West, J. L. Wietor, J. K. Sanders, S. Otto, *Chem. Rev.* **2006**, *106*, 3652–711, DOI 10.1021/cr020452p.

[41] S. J. Rowan, S. J. Cantrill, G. R. Cousins, J. K. Sanders, J. F. Stoddart, *Angew. Chem. Int. Ed. Engl.* **2002**, *41*, 898–952, DOI 10.1002/1521-3773(20020315)41:6<898::aid-anie898>3.0.co;2-e.

[42] J. M. Winne, L. Leibler, F. E. Du Prez, *Polym. Chem.* **2019**, *10*, 6091–6108, DOI 10.1039/c9py01260e.

[43] S. V. Wanasinghe, O. J. Dodo, D. Konkolewicz, *Angew. Chem. Int. Ed. Engl.* **2022**, *61*, e202206938, DOI 10.1002/anie.202206938.

[44] F. Elizalde, R. H. Aguirresarobe, A. Gonzalez, H. Sardon, *Polym. Chem.* **2020**, *11*, 5386–5396, DOI 10.1039/d0py00842g.

[45] A. G. Orrillo, R. L. E. Furlan, *Angew. Chem. Int. Ed. Engl.* **2022**, *61*, e202201168, DOI 10.1002/anie.202201168.

[46] G. Griffini, B. Rigatelli, S. Turri, *Macromol. Mater. Eng.* **2023**, *308*, 2300133, DOI 10.1002/mame.202300133.

[47] O. Diels, K. Alder, *Justus Liebigs An. Chem.* **1928**, *460*, 98–122, DOI 10.1002/jlac.19284600106.

[48] F. Orozco, J. Li, U. Ezekiel, Z. Niyazov, L. Floyd, G. M. R. Lima, J. G. M. Winkelman, I. Moreno-Villoslada, F. Picchioni, R. K. Bose, *Eur. Polym. J.* **2020**, *135*, 109882, DOI 10.1016/j.eurpolymj.2020.109882.

[49] B. J. Adzima, H. A. Aguirre, C. J. Kloxin, T. F. Scott, C. N. Bowman, *Macromolecules* **2008**, *41*, 9112–9117, DOI 10.1021/ma801863d.

[50] P. Chakma, Z. A. Digby, M. P. Shulman, L. R. Kuhn, C. N. Morley, J. L. Sparks, D. Konkolewicz, *ACS Macro Lett.* **2019**, *8*, 95–100, DOI 10.1021/acsmacrolett.8b00819.

[51] P. Chakma, C. N. Morley, J. L. Sparks, D. Konkolewicz, *Macromolecules* **2020**, *53*, 1233–1244, DOI 10.1021/acs.macromol.0c00120.

[52] Y. Higaki, H. Otsuka, A. Takahara, *Macromolecules* **2006**, *39*, 2121–2125, DOI 10.1021/ma052093g.

[53] F. Wang, M. Z. Rong, M. Q. Zhang, *J. Mater. Chem.* **2012**, *22*, 13076–13084, DOI 10.1039/c2jm30578j.

[54] K. Jin, L. Li, J. M. Torkelson, *Adv. Mater.* **2016**, *28*, 6746–50, DOI 10.1002/adma.201600871.

[55] M. Du, H. A. Houck, Q. Yin, Y. Xu, Y. Huang, Y. Lan, L. Yang, F. E. Du Prez, G. Chang, *Nat. Commun.* **2022**, *13*, 3231, DOI 10.1038/s41467-022-30972-7.

[56] S. Billiet, K. De Bruycker, F. Driessen, H. Goossens, V. Van Speybroeck, J. M. Winne, F. E. Du Prez, *Nat. Chem.* **2014**, *6*, 815–21, DOI 10.1038/nchem.2023.

[57] S. K. Schoustra, J. A. Dijksman, H. Zuilhof, M. M. J. Smulders, *Chem. Sci.* **2020**, *12*, 293–302, DOI 10.1039/d0sc05458e.

[58] Y. J. Liu, Z. H. Tang, J. L. Chen, J. K. Xiong, D. Wang, S. Wang, S. W. Wu, B. C. Guo, *Polym. Chem.* **2020**, *11*, 1348–1355, DOI 10.1039/c9py01826c.

[59] M. Hayashi, *Acs Appl. Polym. Mater.* **2020**, *2*, 5365–5370, DOI 10.1021/acsapm.0c01099.

[60] D. Montarnal, M. Capelot, F. Tournilhac, L. Leibler, *Science* **2011**, *334*, 965–8, DOI 10.1126/science.1212648.

[61] Y. Yang, F. S. Du, Z. C. Li, *ACS Appl. Polym. Mater.* **2020**, *2*, 5630–5640, DOI 10.1021/acsapm.0c00941.

[62] C. Seidler, D. Y. W. Ng, T. Weil, *Tetrahedron* **2017**, *73*, 4979–4987, DOI 10.1016/j.tet.2017.06.066.

[63] M. Piest, X. Zhang, J. Trinidad, J. F. J. Engbersen, *Soft Matter* **2011**, *7*, 11111–11118, DOI 10.1039/c1sm06230a.

[64] W. B. Kong, Y. Y. Yang, A. Q. Yuan, L. Jiang, X. W. Fu, Y. C. Wang, H. L. Xu, Z. M. Liu, J. X. Lei, *Energy* **2021**, *232*, 121070, DOI 10.1016/j.energy.2021.121070.

[65] J. Canadell, H. Goossens, B. Klumperman, *Macromolecules* **2011**, *44*, 2536–2541, DOI 10.1021/ma2001492.

[66] J. J. Lessard, G. M. Scheutz, S. H. Sung, K. A. Lantz, 3. Epps, T. H., B. S. Sumerlin, *J. Am. Chem. Soc.* **2020**, *142*, 283–289, DOI 10.1021/jacs.9b10360.

[67] W. Denissen, G. Rivero, R. Nicolaÿ, L. Leibler, J. M. Winne, F. E. Du Prez, *Adv. Funct. Mat.* **2015**, *25*, 2451–2457, DOI 10.1002/adfm.201404553.

[68] B. R. Zhang, Z. A. Digby, J. A. Flum, P. Chakma, J. M. Saul, J. L. Sparks, D. Konkolewicz, *Macromolecules* **2016**, *49*, 6871–6878, DOI 10.1021/acs.macromol.6b01061.

[69] K. C. Koehler, K. S. Anseth, C. N. Bowman, *Biomacromolecules* **2013**, *14*, 538–47, DOI 10.1021/bm301789d.

[70] O. Konuray, S. Moradi, A. Roig, X. Fernández-Francos, X. Ramis, *Acs Appl. Polym. Mater.* **2023**, *5*, 1651–1656, DOI 10.1021/acsapm.2c02136.

[71] K. Cheng, A. Chortos, J. A. Lewis, D. R. Clarke, *ACS Appl. Mater. Interfaces* **2022**, *14*, 4552–4561, DOI 10.1021/acsami.1c22287.

[72] N. Van Herck, D. Maes, K. Unal, M. Guerre, J. M. Winne, F. E. Du Prez, *Angew. Chem. Int. Ed. Engl.* **2020**, *59*, 3609–3617, DOI 10.1002/anie.201912902.

[73] M. A. Jedrzejczyk, P. D. Kouris, M. D. Boot, E. J. M. Hensen, K. V. Bernaerts, *Acs Appl. Polym. Mater.* **2022**, *4*, 2544–2552, DOI 10.1021/acsapm.1c01853.

[74] S. Majumdar, H. Zhang, M. Soleimani, R. A. T. M. van Benthem, J. P. A. Heuts, R. P. Sijbesma, *ACS Macro Lett.* **2020**, *9*, 1753–1758, DOI 10.1021/acsmacrolett.0c00636.

[75] X. M. Feng, G. Q. Li, *Chem. Eng. J.* **2021**, *417*, 129132, DOI 10.1016/j.cej.2021.129132.

[76] Y. Nishimura, J. Chung, H. Muradyan, Z. Guan, *J. Am. Chem. Soc.* **2017**, *139*, 14881–14884, DOI 10.1021/jacs.7b08826.

[77] C. A. Tretbar, J. A. Neal, Z. Guan, *J. Am. Chem. Soc.* **2019**, *141*, 16595–16599, DOI 10.1021/jacs.9b08876.

[78] B. Krishnakumar, R. V. S. P. Sanka, W. H. Binder, V. Parthasarthy, S. Rana, N. Karak, *Chem. Eng. J.* **2020**, *385*, 123820, DOI 10.1016/j.cej.2019.123820.

[79] L. Porath, B. Soman, B. B. Jing, C. M. Evans, *ACS Macro Lett.* **2022**, *11*, 475–483, DOI 10.1021/acsmacrolett.2c00038.

[80] F. Meng, M. O. Saed, E. M. Terentjev, *Nat. Commun.* **2022**, *13*, 5753, DOI 10.1038/s41467-022-33321-w.

[81] B. R. Elling, W. R. Dichtel, *ACS Cent. Sci.* **2020**, *6*, 1488–1496, DOI 10.1021/acscentsci.0c00567.

[82] L. Pettazzoni, M. Ximenis, F. Leonelli, G. Vozzolo, E. Bodo, F. Elizalde, H. Sardon, *Chem. Sci.* **2024**, *15*, 2359–2364, DOI 10.1039/d3sc06011j.

[83] Y. Chen, H. Zhang, S. Majumdar, R. A. T. M. van Benthem, J. P. A. Heuts, R. P. Sijbesma, *Macromolecules* **2021**, *54*, 9703–9711, DOI 10.1021/acs.macromol.1c01389.

[84] F. Van Lijsebetten, Y. Spiesschaert, J. M. Winne, F. E. Du Prez, *J. Am. Chem. Soc.* **2021**, *143*, 15834–15844, DOI 10.1021/jacs.1c07360.

[85] K. Unal, D. Maes, L. Stricker, K. Lorenz, F. E. Du Prez, L. Imbernon, J. M. Winne, *ACS Appl. Polym. Mater.* **2024**, *6*, 2604–2615, DOI 10.1021/acsapm.3c02791.

[86] L. M. Fenimore, M. J. Suazo, J. M. Torkelson, *Macromolecules* **2024**, *57*, 2756–2772, DOI 10.1021/acs.macromol.3c02515.

[87] H. S. Geethanjali, R. M. Melavanki, D. Nagaraja, P. Bhavya, R. A. Kusanur, *J. Mol. Liq.* **2017**, *227*, 37–43, DOI 10.1016/j.molliq.2016.11.097.

[88] A. R. Narkar, B. Barker, M. Clisch, J. Jiang, B. P. Lee, *Chem. Mater.* **2016**, *28*, 5432–5439, DOI 10.1021/acs.chemmater.6b01851.

[89] C. C. Deng, W. L. A. Brooks, K. A. Abboud, B. S. Sumerlin, *ACS Macro Lett.* **2015**, *4*, 220–224, DOI 10.1021/acsmacrolett.5b00018.

[90] G. Springsteen, B. H. Wang, *Tetrahedron* **2002**, *58*, 5291–5300, DOI 10.1016/S0040-4020(02)00489-1.

[91] Y. Furikado, T. Nagahata, T. Okamoto, T. Sugaya, S. Iwatsuki, M. Inamo, H. D. Takagi, A. Odani, K. Ishihara, *Chemistry* **2014**, *20*, 13194–202, DOI 10.1002/chem.201403719.

[92] W. L. A. Brooks, C. C. Deng, B. S. Sumerlin, *ACS Omega* **2018**, *3*, 17863–17870, DOI 10.1021/acsomega.8b02999.

[93] S. Kheirjou, A. Abedin, A. Fattahi, *Comput. Theor. Chem.* **2012**, *1000*, 1–5, DOI 10.1016/j.comptc.2012.08.012.

[94] K. Lacina, P. Skládal, T. D. James, *Chem. Cent. J.* **2014**, *8*, 60, DOI 10.1186/s13065-014-0060-5.

[95] D. G. Hall in *Boronic Acids*, **2011**, pp. 1–133, DOI 10.1002/9783527639328.ch1.

[96] N. Miyaura, K. Yamada, A. Suzuki, *Tetrahedron Lett.* **1979**, *20*, 3437–3440, DOI 10.1016/S0040-4039(01)95429-2.

[97] X. Liu, W. H. Scouten in *Affinity Chromatography*, Springer, **2000**, pp. 119–128.

[98] P. R. Westmark, L. S. Valencia, B. D. Smith, *J. Chromatogr. A* **1994**, *664*, 123–128, DOI Doi10.1016/0021-9673(94)80637-3.

[99] S. Soundararajan, M. Badawi, C. M. Kohlrust, J. H. Hageman, *Anal. Biochem.* **1989**, *178*, 125–34, DOI 10.1016/0003-2697(89)90367-9.

[100] R. Nishiyabu, Y. Kubo, T. D. James, J. S. Fossey, *Chem. Commun. (Camb.)* **2011**, *47*, 1106–23, DOI 10.1039/c0cc02920c.

[101] S. D. Bull, M. G. Davidson, J. M. van den Elsen, J. S. Fossey, A. T. Jenkins, Y. B. Jiang, Y. Kubo, F. Marken, K. Sakurai, J. Zhao, T. D. James, *Acc. Chem. Res.* **2013**, *46*, 312–26, DOI 10.1021/ar300130w.

[102] S. Cho, S. Y. Hwang, D. X. Oh, J. Park, *J. Mater. Chem. A* **2021**, *9*, 14630–14655, DOI 10.1039/d1ta02308j.

[103] D. Hall, *Boronic Acids: Preparation and Applications in Organic Synthesis, Medicine and Materials*, Wiley, J. & Sons, **2012**.

[104] J. Weir, R. J., R. S. Fisher, *Toxicol. Appl. Pharmacol.* **1972**, *23*, 351–64, DOI 10.1016/0041-008x(72)90037-3.

[105] W. L. Brooks, B. S. Sumerlin, *Chem. Rev.* **2016**, *116*, 1375–97, DOI 10.1021/acs.chemrev.5b00300.

[106] J. Plescia, N. Moitessier, *Eur. J. Med. Chem.* **2020**, *195*, 112270, DOI 10.1016/j.ejmech.2020.112270.

[107] J. N. Cambre, B. S. Sumerlin, *Polymer* **2011**, *52*, 4631–4643, DOI 10.1016/j.polymer.2011.07.057.

[108] V. Yesilyurt, M. J. Webber, E. A. Appel, C. Godwin, R. Langer, D. G. Anderson, *Adv. Mater.* **2016**, *28*, 86–91, DOI 10.1002/adma.201502902.

[109] Z. Zhao, X. Yao, Z. Zhang, L. Chen, C. He, X. Chen, *Macromol. Biosci.* **2014**, *14*, 1609–18, DOI 10.1002/mabi.201400251.

[110] H. Takata, K. Ono, N. Iwasawa, *Chem. Commun. (Camb.)* **2020**, *56*, 5613–5616, DOI 10.1039/d0cc01441a.

[111] B. Cai, Y. Luo, Q. Guo, X. Zhang, Z. Wu, *Carbohydr. Res.* **2017**, *445*, 32–39, DOI 10.1016/j.carres.2017.04.006.

[112] A. P. Bapat, B. S. Sumerlin, A. Sutti, *Mater. Horiz.* **2020**, *7*, 694–714, DOI 10.1039/c9mh01223k.

[113] M. Gosecki, M. Gosecka, *Polymers-Basel* **2022**, *14*, 842, DOI 10.3390/polym14040842.

[114] A. P. Bapat, B. S. Sumerlin, A. Sutti, *Mater. Horiz.* **2020**, *7*, 694–714, DOI 10.1039/c9mh01223k.

[115] B. Marco-Dufort, M. W. Tibbitt, *Mater. Today Chem.* **2019**, *12*, 16–33, DOI 10.1016/j.mtchem.2018.12.001.

[116] Y. Guan, Y. Zhang, *Chem. Soc. Rev.* **2013**, *42*, 8106–21, DOI 10.1039/c3cs60152h.

[117] J. J. Cash, T. Kubo, A. P. Bapat, B. S. Sumerlin, *Macromolecules* **2015**, *48*, 2098–2106, DOI 10.1021/acs.macromol.5b00210.

[118] M. Rottger, T. Domenech, R. van der Weegen, A. Breuillac, R. Nicolay, L. Leibler, *Science* **2017**, *356*, 62–65, DOI 10.1126/science.aah5281.

[119] R. C. Boutelle, B. H. Northrop, *J. Org. Chem.* **2011**, *76*, 7994–8002, DOI 10.1021/jo201606z.

[120] J. A. Berson, Z. Hamlet, W. A. Mueller, *J. Am. Chem. Soc.* **2002**, *84*, 297–304, DOI 10.1021/ja00861a033.

[121] V. Froidevaux, M. Borne, E. Laborbe, R. Auvergne, A. Gandini, B. Boutevin, *RSC Adv.* **2015**, *5*, 37742–37754, DOI 10.1039/c5ra01185j.

[122] A. Cuvellier, R. Verhelle, J. Brancart, B. Vanderborght, G. Van Assche, H. Rahier, *Polym. Chem.* **2019**, *10*, 473–485, DOI 10.1039/C8PY01216D.

[123] C. R. Ratwani, A. R. Kamali, A. M. Abdelkader, *Prog. Mater. Sci.* **2023**, *131*, 101001, DOI 10.1016/j.pmatsci.2022.101001.

[124] V. Gaina, M. Nechifor, C. Gaina, O. Ursache, *Polym.-Plast. Technol. Mater.* **2021**, *60*, 253–270, DOI 10.1080/25740881.2020.1811315.

[125] B. Briou, B. Ameduri, B. Boutevin, *Chem. Soc. Rev.* **2021**, *50*, 11055–11097, DOI 10.1039/d0cs01382j.

[126] A. Gandini, *Prog. Polym. Sci.* **2013**, *38*, 1–29, DOI 10.1016/j.progpolymsci.2012.04.002.

[127] X. Chen, M. A. Dam, K. Ono, A. Mal, H. Shen, S. R. Nutt, K. Sheran, F. Wudl, *Science* **2002**, *295*, 1698–702, DOI 10.1126/science.1065879.

[128] X. Kuang, G. M. Liu, X. Dong, D. J. Wang, *Mater. Chem. Front.* **2017**, *1*, 111–118, DOI 10.1039/c6qm00094k.

[129] B. Marco-Dufort, R. Iten, M. W. Tibbitt, *J. Am. Chem. Soc.* **2020**, *142*, 15371–15385, DOI 10.1021/jacs.0c06192.

[130] Y. Yang, F. S. Du, Z. C. Li, *Polym. Chem.* **2020**, *11*, 1860–1870, DOI 10.1039/c9py01546a.

[131] F. B. Chen, F. Gao, X. R. Guo, L. Shen, Y. J. Lin, *Macromolecules* **2022**, *55*, 10124–10133, DOI 10.1021/acs.macromol.2c01378.

[132] Y. Spiesschaert, C. Taplan, L. Stricker, M. Guerre, J. M. Winne, F. E. Du Prez, *Polym. Chem.* **2020**, *11*, 5377–5385, DOI 10.1039/D0PY00114G.

[133] P. Raffa, A. Kassi, J. Gosschalk, N. Migliore, L. M. Polgar, F. Picchioni, *Macromol. Mater. Eng.* **2021**, *306*, 2000755, DOI 10.1002/mame.202000755.

[134] Q. Zhou, Z. Sang, K. K. Rajagopalan, Y. Sliozberg, F. Gardea, S. A. Sukhishvili, *Macromolecules* **2021**, *54*, 10510–10519, DOI 10.1021/acs.macromol.1c01662.

[135] J. D. Mayo, A. Adronov, *J. Polym. Sci. Part A: Polym. Chem.* **2013**, *51*, 5056–5066, DOI 10.1002/pola.26937.

[136] K. J. Luo, L. B. Huang, Y. Wang, J. R. Yu, J. Zhu, Z. M. Hu, *Chinese J. Polym. Sci.* **2020**, *38*, 268–277, DOI 10.1007/s10118-019-2328-7.

[137] B. Kang, J. A. Kalow, *ACS Macro Lett.* **2022**, *11*, 394–401, DOI 10.1021/acsmacrolett.2c00056.

[138] F. Cuminet, S. Caillol, É. Dantras, É. Leclerc, V. Ladmiral, *Macromolecules* **2021**, *54*, 3927–3961, DOI 10.1021/acs.macromol.0c02706.

[139] O. R. Cromwell, J. Chung, Z. Guan, *J. Am. Chem. Soc.* **2015**, *137*, 6492–5, DOI 10.1021/jacs.5b03551.

[140] M. Podgórski, N. Spurgin, S. Mavila, C. N. Bowman, *Polym. Chem.* **2020**, *11*, 5365–5376, DOI 10.1039/d0py00091d.

[141] A. Safaei, S. Terryn, B. Vanderborght, G. Van Assche, J. Brancart, *Polymers* **2021**, *13*, 2522, DOI 10.3390/polym13152522.

[142] M. H. P. de Heer Kloots, S. K. Schoustra, J. A. Dijksman, M. M. J. Smulders, *Soft Matter* **2023**, *19*, 2857–2877, DOI 10.1039/D3SM00047H.

[143] S. K. Schoustra, M. H. P. de Heer Kloots, J. Posthuma, D. van Doorn, J. A. Dijksman, M. M. J. Smulders, *Macromolecules* **2022**, *55*, 10341–10355, DOI 10.1021/acs.macromol.2c01595.

[144] C. Hansch, A. Leo, R. W. Taft, *Chem. Rev.* **1991**, *91*, 165–195, DOI 10.1021/cr00002a004.

[145] Z. Demchuk, X. Zhao, Z. Shen, S. Zhao, A. P. Sokolov, P. F. Cao, *ACS Mater. Au.* **2024**, *4*, 185–194, DOI 10.1021/acsmaterialsau.3c00074.

[146] I. S. Golovanov, A. Y. Sukhorukov, Y. V. Nelyubina, Y. A. Khomutova, S. L. Ioffe, V. A. Tartakovsky, *J. Org. Chem.* **2015**, *80*, 6728–36, DOI 10.1021/acs.joc.5b00892.

[147] A. N. Semakin, A. Y. Sukhorukov, A. V. Lesiv, S. L. Ioffe, K. A. Lyssenko, Y. V. Nelyubina, V. A. Tartakovsky, *Org. Lett.* **2009**, *11*, 4072–5, DOI 10.1021/ol9015157.

[148] I. S. Golovanov, G. S. Mazeina, Y. V. Nelyubina, R. A. Novikov, A. S. Mazur, S. N. Britvin, V. A. Tartakovsky, S. L. Ioffe, A. Y. Sukhorukov, *J. Org. Chem.* **2018**, *83*, 9756–9773, DOI 10.1021/acs.joc.8b01296.

Chapter 2

Electronic Effects in Covalent Adaptable Furan-Maleimide Networks

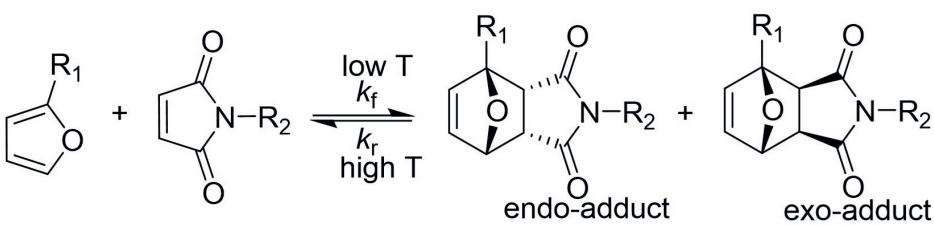

$$K = \frac{[\text{Adduct}]}{[\text{Furan}][\text{Maleimide}]} = \frac{k_f}{k_r}$$

2.1 Abstract

The use of polymers in modern society has become widespread due to their cheap production and wide applicability. However, society is now facing environmental issues caused by the massive amounts of (thermosetting) polymer waste. Thermosetting polymer networks are difficult to recycle, due to their permanent crosslinks. This low recyclablility can be improved by changing the permanent crosslinks into dynamic covalent bonds. One such dynamic covalent bond is the thermally reversible furan-maleimide bond. Here, we investigate how varying ring substituents on maleimide linkers can be used to tune the properties of a covalent adaptable network based on furan-maleimide bonds. Five maleimide linkers are prepared with different electronic properties and incorporated into furan-maleimide covalent adaptable networks. Using IR, reaction enthalpy and entropy values are calculated for the dynamic networks and fitted against Hammett σ_p values, resulting in a positive trend being found. However, no such trend is observed when correlating the macroscopic stress relaxation behaviour and the σ_p values. This suggests that, while the molecular parameters of the dynamic exchange can be tuned through variations in aromatic ring substituents, these variations of ring substituents are not the main contributor in the tuning of the macroscopic stress relaxation of these networks.

2.2 Introduction

Polymers are an important class of materials in modern society with their widely varying applications and cheap production costs. However, the massive amounts of polymers being produced have also sparked a need to recycle polymers, which is still proving especially challenging for thermosetting polymers, due to their network structure.[1–4] In recent years covalent adaptable networks (CANs) have received increasing interest as a possible solution to the problems regarding the recycling of thermosetting polymer networks.[5–7] By using dynamic covalent chemistry, CANs can be used to make strong and covalently crosslinked, yet still recyclable networks, thus reducing the need for strong, but non-recyclable thermosets.[8–11]

There are numerous types of dynamic covalent bonds that can be used to prepare CANs. Examples of dynamic covalent bonds are imines,[12,13] diketoenamines,[14,15] esters,[16,17] disulfides,[18–20] X-yne,[21,22] boronic es-

ters,[23–25] nucleophilic alkylation reactions[26,27] and Diels-Alder chemistry.[28–31] In this chapter we report a study that focusses on networks that make use of the Diels-Alder reaction, as this reversible pericyclic reaction allows for bonding and debonding of the created network.[32] This debonding of the network can aid in the recycling of the created networks by reverting the network (partially) back into its individual starting components.[33] A commonly used Diels-Alder reaction for the formation of CANs is the reaction between furan and maleimide, which is the focus of the current study.[34] One of the reasons for this is that furan derivatives can be easily accessed from biobased sources.[35,36] In addition, the switching temperature for this reversible reaction is in a practical window (see below), that allows debonding to happen at elevated temperatures at which irreversible polymer decomposition is not yet an issue.

Furan and maleimide can undergo a Diels-Alder reaction with the furan acting as the diene and the maleimide as the dienophile. Upon reacting, either the kinetic *endo* adduct or the thermodynamically favoured *exo* adduct are formed, as shown in **Scheme 2.1**.[37] This is an equilibrium reaction, which at low temperatures (<100 °C) favours the formation of the Diels-Alder adduct and at high temperatures (≥120 °C) favours the reverse Diels-Alder reaction yielding furan and maleimide back again. It should be noted that maleimide tends to self-polymerise at higher temperatures (above 150 °C), thus creating irreversible linkages.[38,39]

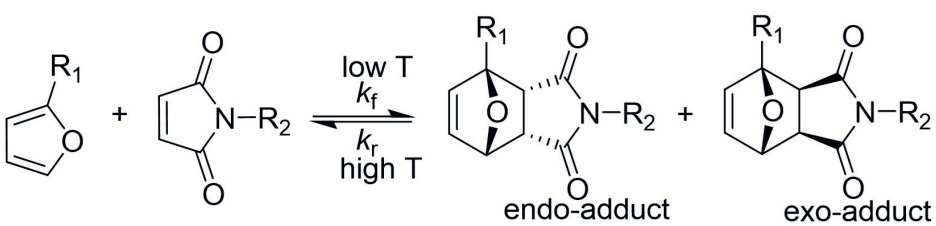

Scheme 2.1: *The Diels-Alder reaction between furan and maleimide.*

In order to make Diels-Alder CANs attractive stand-alone alternative materials or components of conventional thermosetting polymer networks, research must be performed to tune the material properties of these dynamic materials. Such tuning allows for optimisation towards specific (industrial) applications. Studies have already considered the effects of, *e.g.*, linker length,[40–42] crosslinking branching,[43] stoichiometry[44] and

the crosslinking density[45] of furan-maleimide networks on the properties of the network. However, studies into the electronic effect of electron-donating or withdrawing ring substituents on aromatic dienes and/or dienophiles in a Diels-Alder reaction have mostly been limited to small-molecule studies.[46–59] These studies were able to successfully construct Hammett plots with linear trends for both the reaction equilibria[60] and kinetics,[61] although for the kinetics σ had to be switched to σ^+.[61] Translating this to a crosslinked network prepared using Diels-Alder reactions implies that (at a fixed temperature) the extent of crosslinking, and thus also the crosslinking density, would be influenced by the substituent. The progression of the reaction would be dependent on, among other factors, the temperature and the σ value of the substituent. The ability to tune material properties using substituents would be interesting since there is a wide spread of substituents and corresponding σ values, thus potentially allowing for fine-tuned control over the material properties. It has already been shown that substituents with varying electronic properties can have an effect on the thermodynamics and even the material properties for other CANs, such as those based on imines[62] or thiol-ynes.[21]

The aim of this study is to investigate the influence of substituents on the material properties of furan-maleimide networks. Here we focused on the use of bismaleimides with different electronic groups. To do this, we chose to adapt the network studied by Adzima *et al.* as our first choice for it is a well-studied and well-behaved system with easily synthesised building blocks (**Figure 2.1**).[63] In their original work, Adzima *et al.* studied a network consisting of a trifunctional furan linker and 1,1'-(methylenedi-4,1-phenylene)bismaleimide, with its –CH_2– group between the two phenyl rings. In this study we will expand the variety of bismaleimide linkers by preparing different maleimide linkers with a varying X group between the two phenyl rings, where X is CH_2, CO, O, S and later also SO_2 as depicted in **Figure 2.1**. The networks made with these new bismaleimide linkers will be tested and compared based on their difference in substitution. Our expectation is to find a dependency of the crosslinking degree and the (dissociative) exchange rate in the networks on the σ value of the substituent.

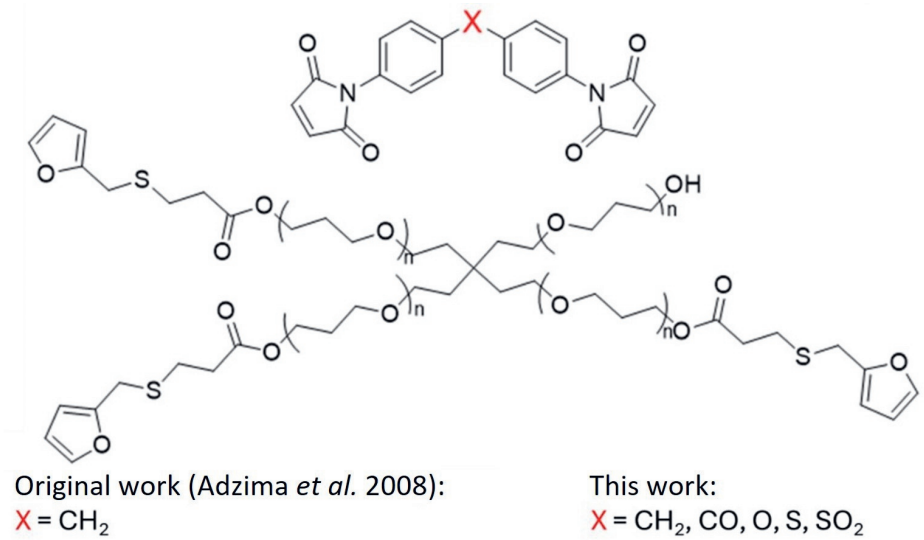

Figure 2.1: *The two building blocks of the furan-maleimide network consisting of a bismaleimide and a tri-functional furan linker prepared from pentaerythritol propoxylalate triacrylate and furfuryl mercaptan. X = CH_2 in the original work. The figure was adapted with permission from Adzima et al. (2008). Copyright 2008 American Chemical Society.*[63]

2.3 Results & Discussion

In order to study the effect of electronic groups in furan-maleimide networks a set of linkers with different electronic groups within one of the two monomers had to be synthesised. There were two possible approaches for this study: variations on the furan part of the network or on the maleimide part. Here we chose to look at variations in maleimide linkers, since they can be readily synthesised from commercially available precursors with a good variety of electronic groups, which was lacking for furan. A group of five maleimide linkers, prepared from 4,4-diaminophenyl precursors, with a good spread of electronic groups was selected: **bMCH$_2$**, **bMCO**, **bMO**, **bMS** and **bMSO$_2$** (**1-5**, **Figure 2.2**), named after the bismaleimide and the electronic group in its middle. The proposed linkers were synthesised by refluxing the corresponding 4,4-diaminophenyl precursor with maleic anhydride in acetic acid overnight, followed by purification via extraction and precipitation in cold water with a yield around 50-70%, as described in the appendix (section 2.1.1). **bMCH$_2$** was commercially available; the ^{1}H NMR spectra of the other four linkers are displayed in **Figure 2.2**. Further characterisation is available in the appendix.

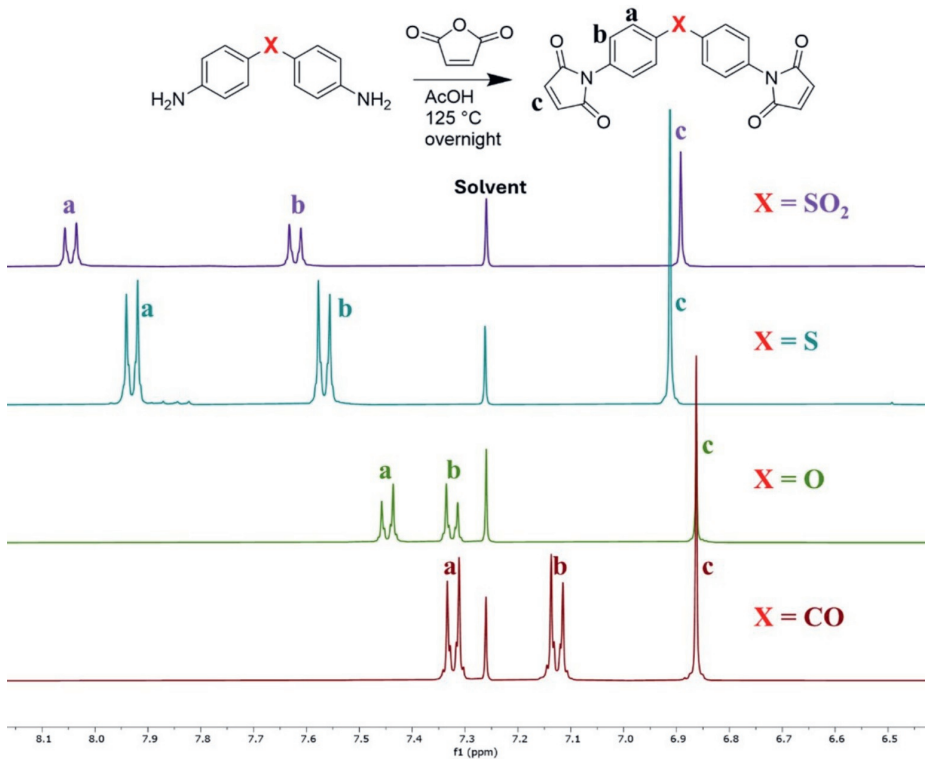

Figure 2.2: *Stacked ^{1}H-NMR plots of the synthesised linkers (top to bottom):* ***bMSO$_2$***, ***bMCO***, ***bMS*** *and* ***bMO*** *in $CDCl_3$ (400 MHz, 25 °C).*

To assess the (electronic) effects of a variable linker in the bridging group of the bismaleimide on the Diels-Alder equilibrium, an NMR study was performed. Each of the linkers was reacted with a two fold excess of furan relative to maleimide groups at 100 °C (in DMSO-d_6) in an NMR tube after which the reaction was followed over time until equilibrium had been reached. From the NMR data the K values were calculated and plotted against the σ_p of the electronic group of the bismaleimide linkers, as shown in **Figure 2.3**. It can be seen that there seems to be a difference in the K value for the σ_p values of the electronic groups in the linkers. Despite some experimental error in the data, these measurements suggest that different electronic groups influence the reaction between furan and maleimide, in line with literature reports.[60] The **bMSO$_2$** linker was not included in these preliminary experiments, for it was only added to the series in a later stage to increase the scope and go from four different linkers to five linkers. It should be noted that attempts to determine also

the value for the forward rate constant k_f, failed due to impracticalities with prolonged measurements at high temperature within our available setup.

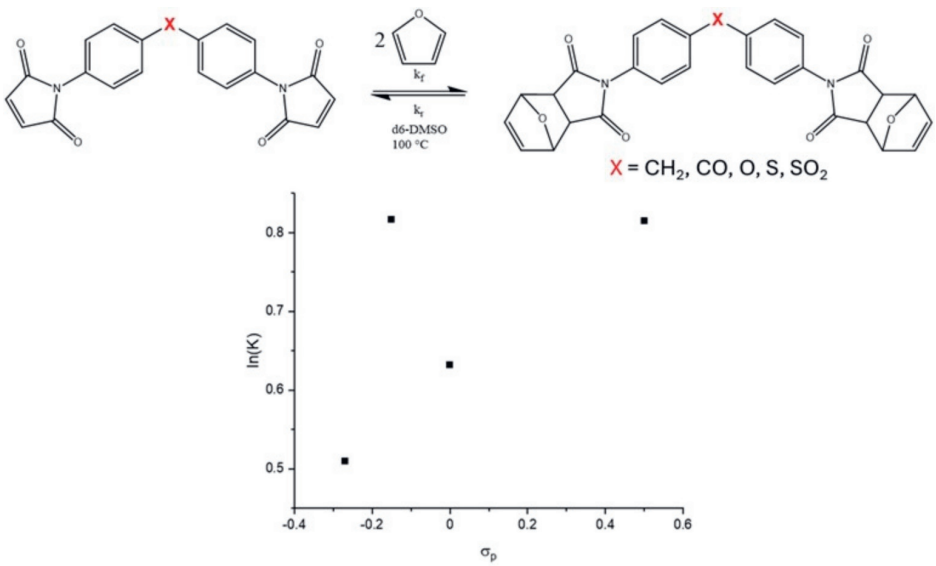

Figure 2.3: *K values obtained from small-molecule NMR study at 100 °C in DMSO-d_6 for the* ***bMCH$_2$***, ***bMCO***, ***bMO*** *and* ***bMS*** *linkers reacting with furan. Furan was added in excess.*

To gain some more insight into the effect of electronic groups on the reaction between furan and maleimide, a B3LYP/6-311+g(d,p) DFT study was performed on the reaction of one furan molecule undergoing a Diels-Alder reaction with one side of a bismaleimide linker.[57] Solvent interactions were not taken into consideration for the calculations. A wide variety of bismaleimide linkers was chosen to get a more complete idea of the correlation between the reaction formation energy and the electronic groups. As can be seen in **Figure 2.4**, the DFT calculations paint a complex relationship between the electronic groups and the formation energy. Important to note is that there are differences based on the electronics. When σ_p is in a range from ca. –1 to 0 there seems to be a somewhat stable plateau. Going to higher σ_p values gives an increase in the reaction enthalpy (ΔH becomes less negative) for both the *endo* and *exo* product. It is likely that these enthalpy values are also influenced by other factors, possibly by sterics-induced differences in the orbital overlap.

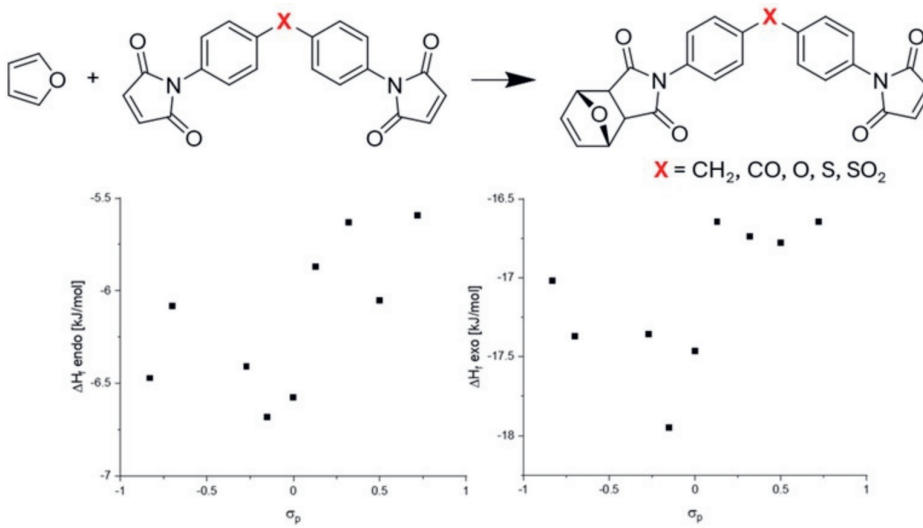

Figure 2.4: *Reaction enthalpies for the endo (bottom left) and exo (bottom right) adduct of the Diels-Alder reaction between furan and bismaleimides with varying substituents (top), as calculated with basis set b3lyp/6-311+g(d,p).*

As the preliminary NMR experiments and DFT calculations hinted to an (possibly non-linear) Hammett effect on the Diels-Alder reaction between furan and (bis)maleimide, it was decided to continue to investigate the dynamic bond in an actual polymer network. The work of Adzima *et al.* was taken as a starting point, since it uses one of the same bismaleimide linkers and an easy to synthesise 3-armed furan linker (**6**) using acrylates and furfuryl mercaptan (**Scheme 2.2**).[63] Unfortunately, the exact same 3-armed triacrylate precursor for their furan linker was not commercially available in Europe. However, pentaerythritol triacrylate with its slightly shorter arms was available. For this reason, a switch was made to this new, slightly shorter linker (details can be found in appendix section 2.1.2). As it turned out, this slightly shorter trifunctional furan linker caused the formed networks to be much stiffer than reported in the original work. Thus an effort was made to include a linear furan linker as well, to reduce the crosslink density of the network. This linear furan linker (**7**) was prepared by reacting furfuroyl chloride with 1,8-diamineoctane. The synthesis is shown in **Scheme 2.2** (details can be found in appendix section 2.1.3).

Following monomer synthesis, the corresponding networks were prepared by dissolving the components (*i.e.*, one of the five bismaleimide monomers **1**–**5**, the trifunctional furan **6**, and the linear bis-furan **7**) in

DMF and casting the networks in plastic round sample tubes with a diameter of 1 cm. The solvent was then evaporated in an oven at 70 °C. The materials were thermally equilibrated at the selected temperatures for measurements for at least two days. These networks were named the **FA3-alkyl** networks.

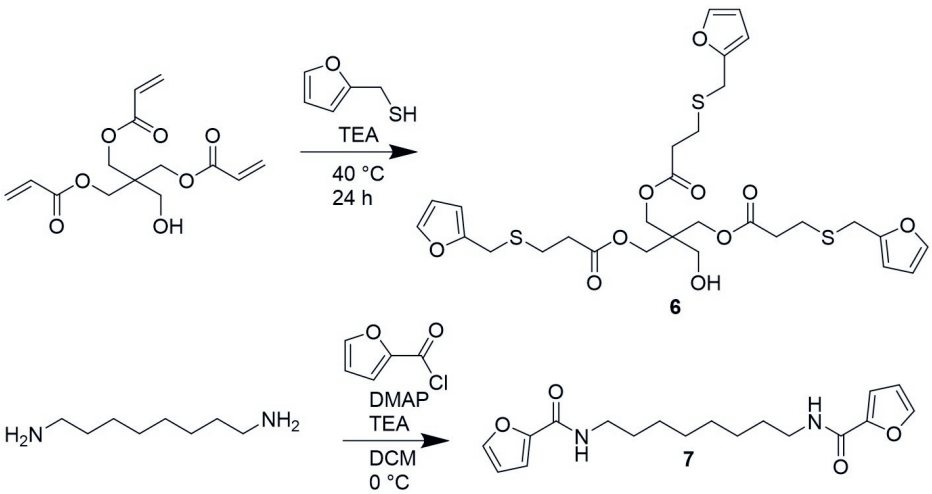

Scheme 2.2: *Synthesis of the of the tri- and bifunctional furan linkers for the* ***FA3-alkyl*** *networks.*

By dropcasting the **FA3-alkyl** networks on KBr pellets the temperature-dependent Diels-Alder equilibrium could be studied using FTIR spectroscopy. By measuring (in triplicate) the dropcast materials at different temperatures the equilibrium of the Diels-Alder reaction could be studied. The conversion was determined by following the maleimide signal at 690 cm^{-1} as shown in **Figure 2.5** before network formation and after equilibrating the networks at selected temperatures. By determining the equilibrium at different temperatures by normalising the maleimide signal using measurements before crosslinking, we could make Van 't Hoff plots, and thus obtain the reaction enthalpy ($\Delta_r H°$) and entropy ($\Delta_r S°$) for the different materials. In **Figure 2.5** the resulting the $\Delta_r H°$ and $\Delta_r S°$ for the different materials are shown. As can be seen there is a clear correlation between the Hammett parameter σ_p and the enthalpy and entropy, fitted here with a linear correlation. Both the $\Delta_r H°$ and $\Delta_r S°$ become less negative with stronger electron-withdrawing groups, in line with expectations, since electron withdrawing groups on the maleimide component lower the LUMO of the dienophile and thus reduce the relevant HOMO-LUMO energy gap.[64]

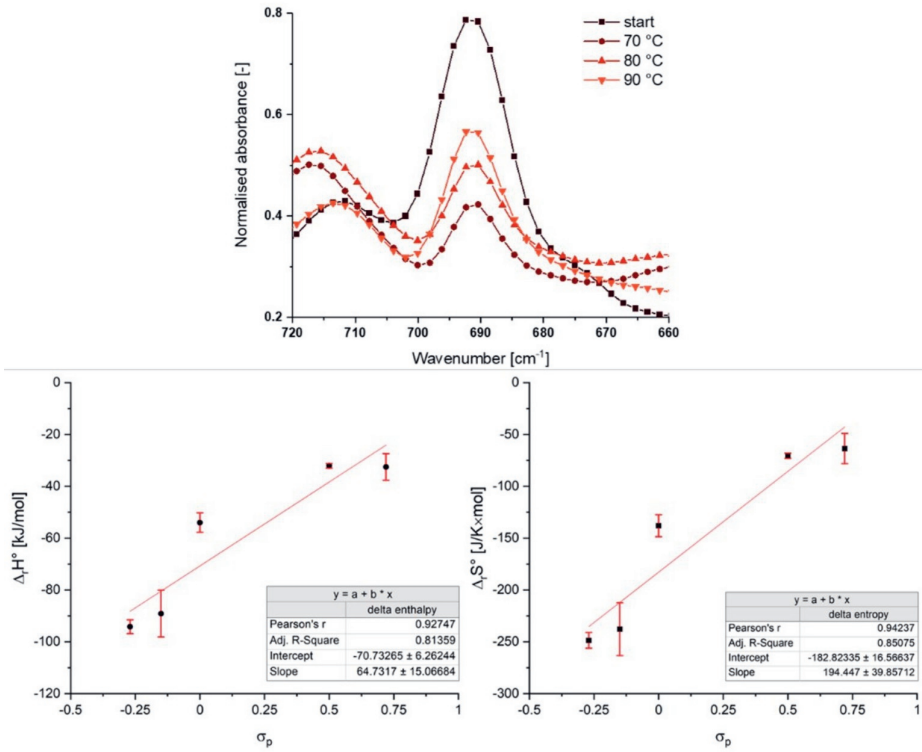

Figure 2.5: *Representative IR spectra of the maleimide signal at 690 cm^{-1} of a* ***FA3-alkyl*** *network before and after equilibration at different temperatures (top). Calculated $\Delta_r H°$ and $\Delta_r S°$ for the different furan-maleimide networks based on IR determined equilibria at 70, 80 and 90 °C through Van 't Hoff plots (bottom).*

Encouraged by these IR results, we set out to explore if the Hammett-dependence in the Diels-Alder equilibrium could also be found in the material properties of the corresponding Diels-Alder networks by studying their rheological properties. However, rheology on the **FA3-alkyl** networks proved difficult. The materials were quite stiff, thus limiting the strain that could be applied. This resulted in noisy and often irreproducible data. An example is shown in **Figure 2.6**, where duplicate relaxation curves of a **bMS FA3-alkyl** network at 100 °C are shown. This meant that the rheological data from these networks was not usable for analysis.

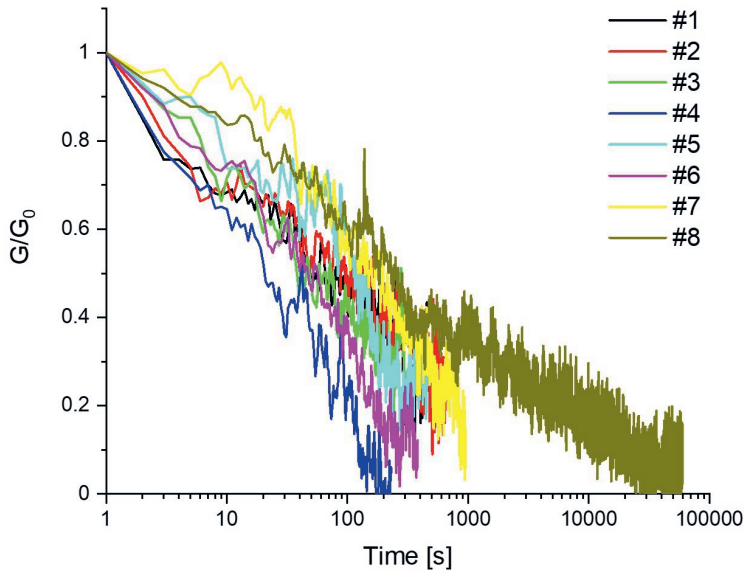

Figure 2.6: *Relaxation repeats of the* ***bMS*** *network at 100 °C with a strain = 0.02%.*

To make the network more flexible, the linear furan linker (**7**) was replaced by a PPG2000 variant (**8**), as can be seen in **Scheme 2.3**.

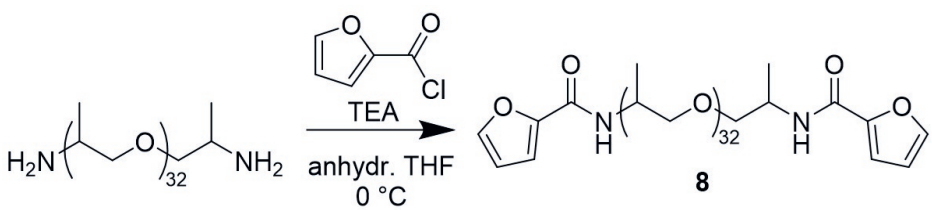

Scheme 2.3: *Synthesis of furan-PPG linker for the* ***FA3-PPG*** *networks.*

The rheological data obtained from the **FA3-PPG** networks, while still containing quite some noise, was far more reproducible, as can be seen in **Figure 2.7**. This was due to the materials being more flexible, thus allowing for measurements at higher strains. However, the sample preparation itself proved to be non-reproducible for these materials. Cast samples would not always crosslink to form materials, which seemed to be occurring at random. Various possible factors, such as impurities, inhomogeneity, casting method and crosslinking protocol were tested and ruled out. This placed some doubts on the reproducibility of the results obtained from these materials and thus this approach was not continued.

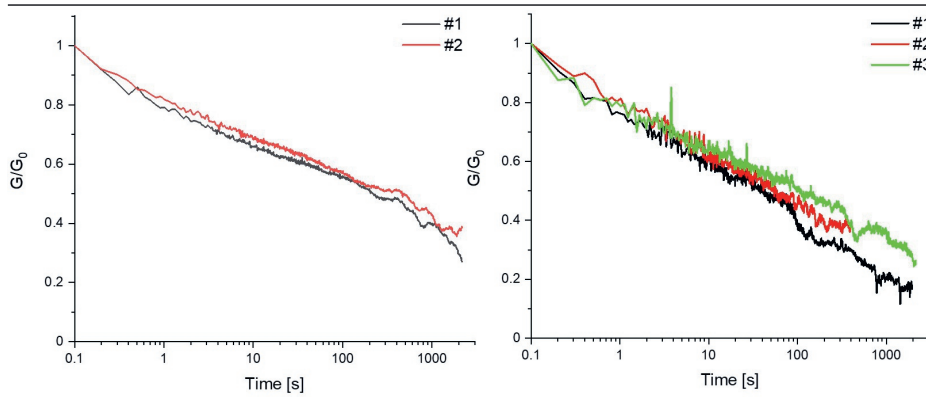

Figure 2.7: *Relaxation curves with repeats at 70 °C and 0.5% strain for networks with PPG-furan linker* ***8*** *with 5% crosslinker (left) and 10% crosslinker (right).*

Since the main recurring issue with measuring these types of networks was that the materials were quite stiff, we redesigned our Diels-Alder networks, guided by published work on a furan-maleimide network with reported rheology experiments: McReynolds *et al.* prepared networks using the same general bismaleimide and crosslinking it with a four-armed furan linker (**9**), based on Jeffamine ED-600 and furfuryl glycidyl ether.[38] The synthesis is shown in **Scheme 2.4** (details can be found in appendix section 2.1.6). This network was named the **FA4** network and was prepared by dissolving the components in DMF and casting the material in molds, taking a maleimide/furan ratio of 0.6. Higher maleimide/furan ratios resulted in stiffer networks, and strongly reduced the effective thermal range over which (rheological) experiments could be performed.

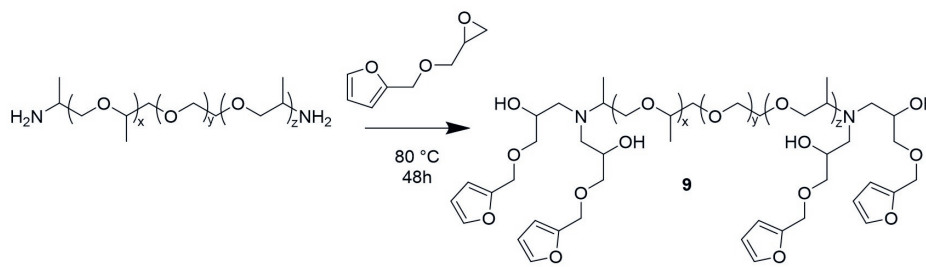

Scheme 2.4: *Synthesis of the four-armed furan linker* ***FA4*** *used for the* ***FA4*** *networks.*

The kinetics and equilibrium conditions of the **FA4** network formation were measured by dropcasting a small amount of material on a Teflon sheet, quickly drying it under air flow and transferring it to an IR spec-

trometer with a heating plate. The IR spectra were recorded every minute for 70-110 °C with 10 °C intervals for the five different bismaleimide linkers. After analysing the data, it became apparent that reactions were much faster than reported in literature, with equilibria generally being reached in minutes instead of hours.[65,66] An attempt was made to construct Arrhenius plots for the bismaleimide linkers, however the reaction kinetics in particular at higher temperatures were too fast for accurate determination of the forward reaction constant (data not shown).
In contrast to the unavailability of reliable kinetic data, using the IR data to estimate the conversion at equilibrium and calculating the K value at the specified temperatures did allow for Van 't Hoff plots to be constructed in order to determine the $\Delta_r H°$ and $\Delta_r S°$ for the **FA4** networks (**Figure 2.8**). As the Van 't Hoff relationship also predicts, the data suggest a linear increase in $\ln(K)$ over $1/T$, allowing the determination of the $\Delta_r H°$ and $\Delta_r S°$ for this reaction.

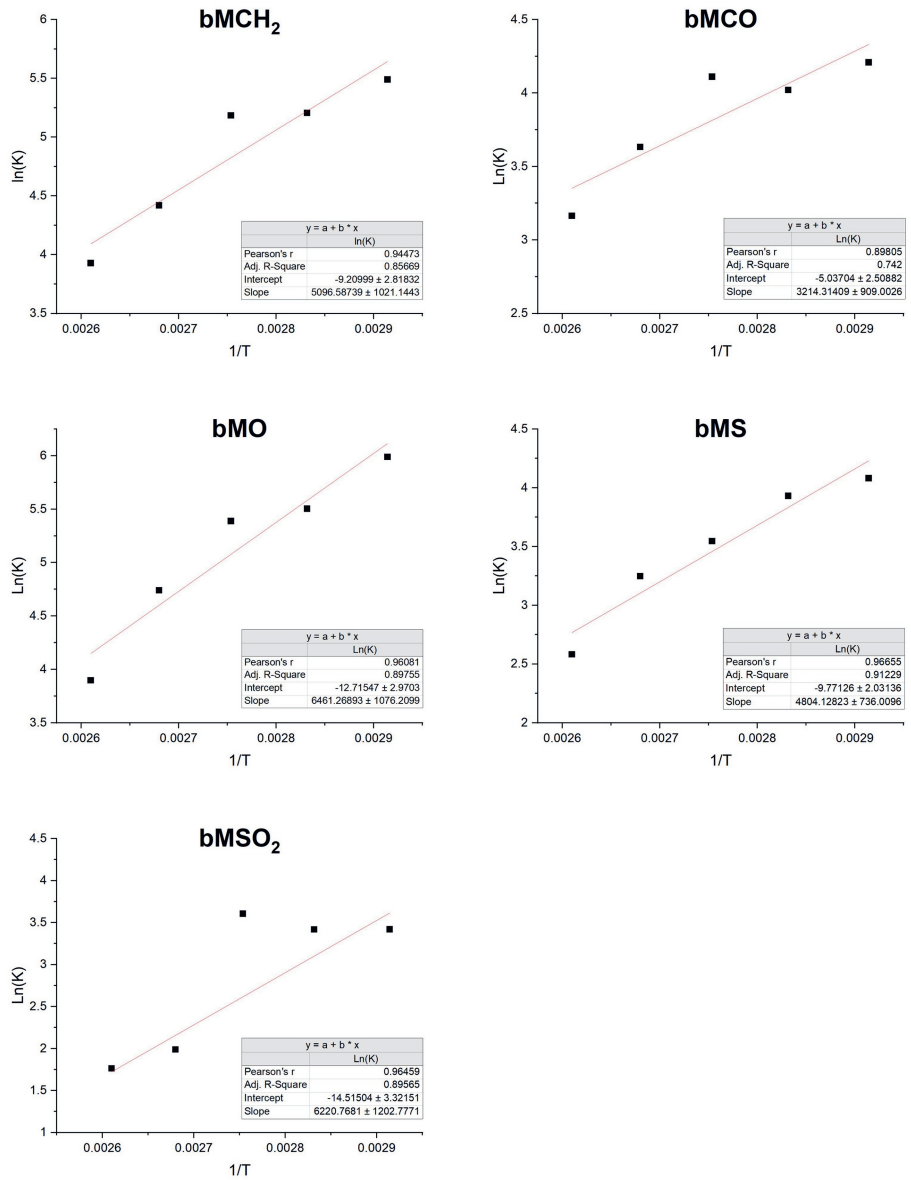

Figure 2.8: *Van't Hoff plots for the* ***FA4*** *networks obtained from IR data. Please note that the data point of 90 °C for the* ***bMSO$_2$*** *network was discarded, as it was classified as an outlier.*

When plotting the $\Delta_r H°$ and $\Delta_r S°$ obtained from the Van 't Hoff plots against the σ_p of the electronic groups in the linker series (**Figure 2.9**) we can observe that there appear to be differences for the different electronic

groups similar to what was observed in the previous **FA3-alkyl** networks. Increasing the σ_p of the substituent seems to result in a higher $\Delta_r H°$ and $\Delta_r S°$. A difference we see compared to previous results is that the **bMSO$_2$** network did not adhere to this perceived trend and instead is much lower than expected and much lower than determined in the **FA3-alkyl** network. More research should be performed to investigate the observed trends in equilibrium or kinetics and how they relate to the material properties of these networks.

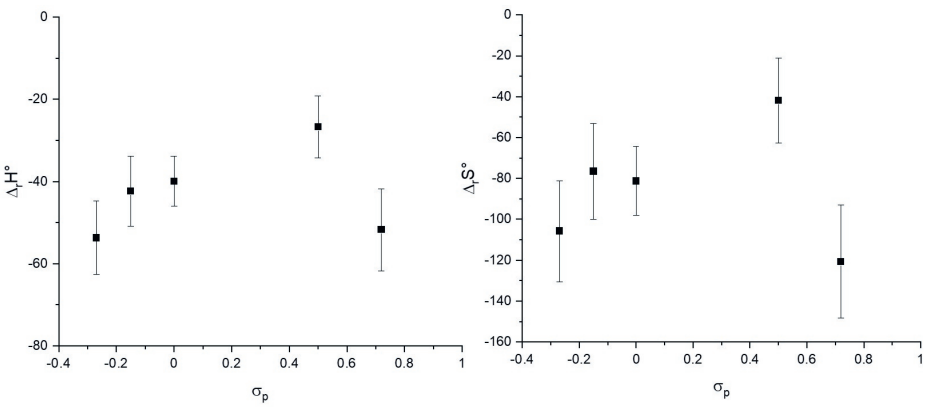

Figure 2.9: *Obtained reaction enthalpies (left) and entropies (right) from Van't Hoff plots for the various substituents.*

Intrigued by these differences in equilibrium conditions for the difference crosslinkers, the **FA4** networks were also investigated using rheology, to see if there would be an observable corresponding difference in their relaxation behaviour. By measuring the relaxation time at different temperatures, it was possible to construct an Arrhenius plot. This would allow for the determination of an activation energy for the net observed Diels-Alder reaction. The relaxation of the networks was measured at 70-110 °C with 10 °C intervals and 0.5% strain. The samples were equilibrated in an oven at the desired temperature for 2 days before measuring. The relaxation experiments were performed in a semi-random order, with the higher temperatures being measured first and lower temperatures last (90, 100, 110, 80, 70 °C). Curves were at least measured in duplicate, more if time allowed. This was done with the aim to reduce measurement error, which relaxation experiments can be susceptible to the application of a sudden strain. The averaged results can be seen in **Figure 2.10**. From this data it can be observed that there is an overall trend for faster relaxation with increasing temperature. However, the lower temperatures

seem to deviate from this trend. One possible explanation would be that the materials experienced damage due to (partial) thermal degradation. To test this, relaxation experiments were also performed at 105 °C. The data obtained at this temperature is also deviant (mostly slower) from the expected trend, thus hinting towards possible accumulated thermal damage for some of the materials. This made the analysis of this data more, if not too, complex.

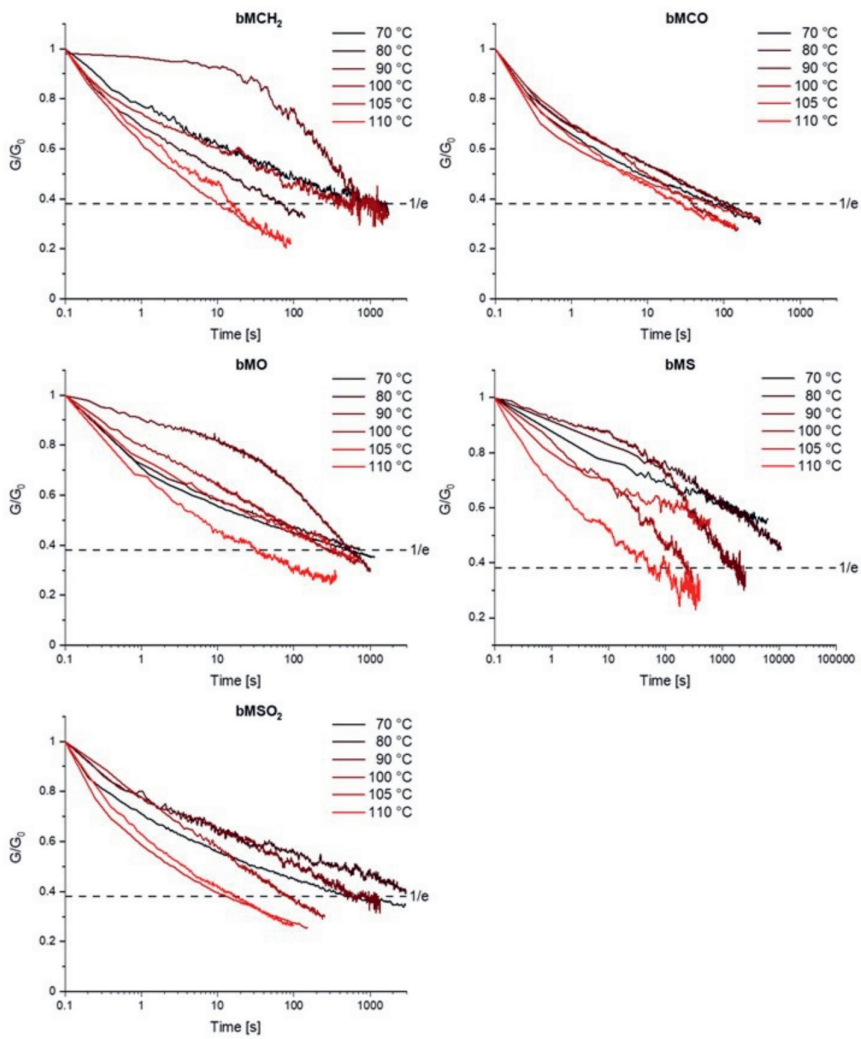

Figure 2.10: *Relaxation experiments with 0.5% strain at different temperatures for the five* ***FA4*** *network variants.*

Despite these limitations, we cautiously prepared the corresponding Arrhenius plots from the data (**Figure 2.11**). The general trend is that we observe longer relaxation times with decreasing temperatures, although the relaxation times at 70 °C seem to reach a plateau. This might be related to accumulated thermal damage, but it might also be related to the equilibrium of the Diels-Alder reaction having shifted fully towards the adduct formation resulting in the formation of a plateau. No Arrhenius plot could be constructed for the **bMCH$_2$** network, since the obtained data did not allow for any meaningful linear fit. Comparing the estimated activation energies obtained from the slopes and plotting these energies against the σ_p of the substituents does not result in an obvious trend. There does seem to be a difference in the estimated activation energy for the different networks, thus hinting towards there being an influence due to the substituent in question. However, there may be more factors influencing the relaxation behaviour, and thus the estimated activation energies, of these furan-maleimide networks. This makes it unlikely that the choice of electronic nature of the substituents of these maleimide linkers can be used to predict and tune the material behaviour solely based on the σ_p. While IR data showed a correlation between the $\Delta_r H°$ and $\Delta_r S°$ of the crosslinking reaction and the σ_p of the substituent, this did not seem to directly translate to a tunability in material properties.

A possible alternative to this study would be to investigate the effect of substituents on the furan ring for a more direct and likely profound influence on the Diels-Alder reaction. However, this would also increase the likelihood for non-linear relationships between k and σ values due to a stronger influence of resonance structures of the transition state on the reaction rate. Using substituted furan rings is still possible, but this approach might require corrections, such as switching to σ^+, due to the formation of a local positive charge in the transition state.[61] Another possibility that should be considered is that there might be more than one factor influencing the network, *e.g.*, the sterics and bond angles of the substituents in question. A SO_2 group is larger than a CH_2 group and would thus likely also impose a different geometry on the linker. While steric effects are considered negligible for small molecules in relation to their electronics,[67] it might be possible that the matrix in which the bis-maleimide linkers are confined can influence the geometry of the linker. This might then influence orbital overlap between the substituent in between the phenyl rings and -ene of the maleimide.

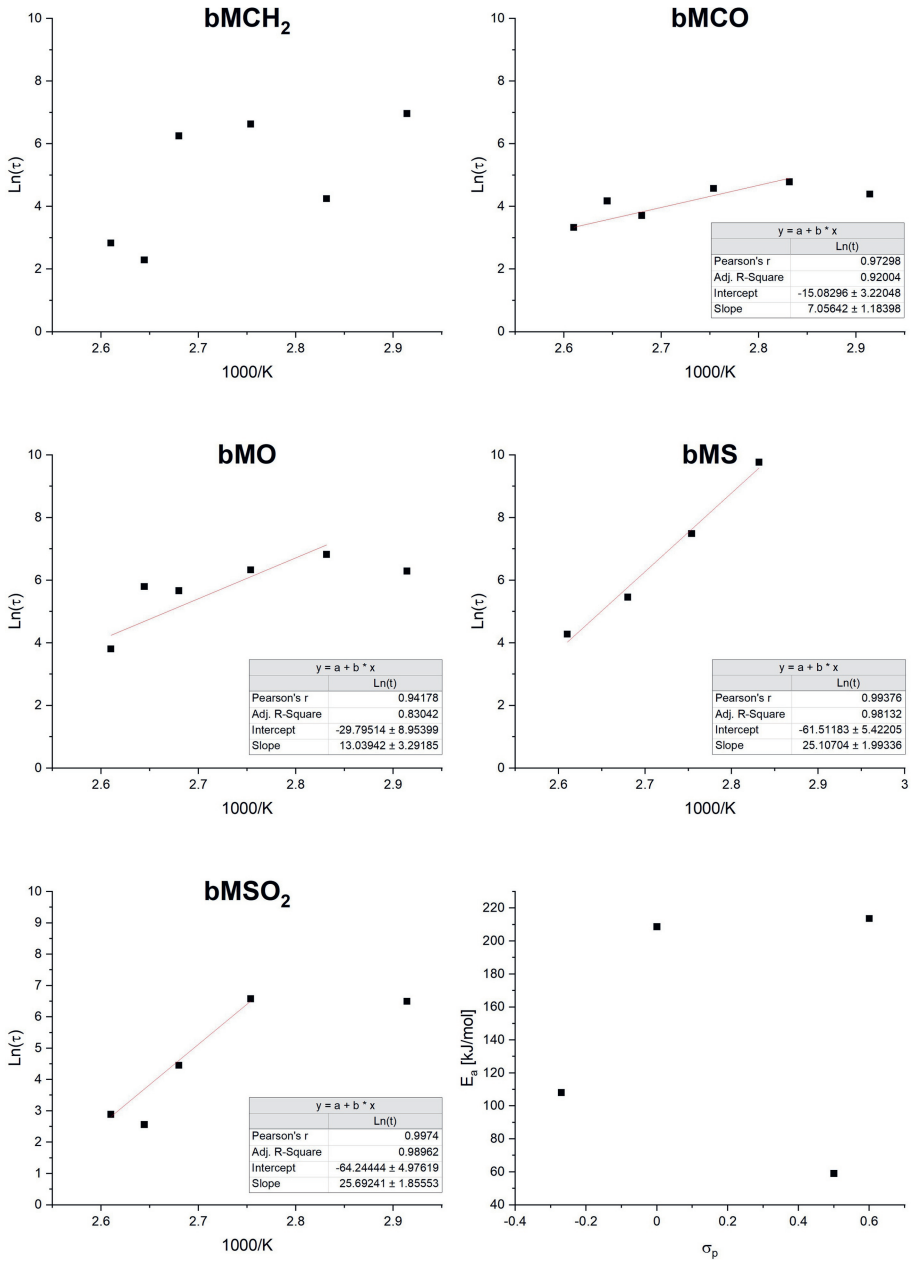

Figure 2.11: *Arrhenius plots and calculated activation energies from the relaxation data of the different network variants. The* ***bMCH₂*** *network was not included, for no activation energy could be calculated from its relaxation data.*

2.4 Conclusion

In this study several iterations of furan-maleimide networks were prepared to study the possibility of tuning material properties of such networks through the variation of electronic substituents in the maleimide linkers. Networks using five different maleimide linkers were made and compared. Van 't Hoff plots made using IR data recorded at different temperatures hinted towards a relationship between the σ_p of the substituents and the reaction enthalpy and entropy of the Diels-Alder reaction. However, activation energies estimated from rheological relaxation studies did not show a clear dependence on σ_p, suggesting other effects contributing significantly to the overall macroscopic stress relaxation. More research is thus required to further study the complex relation between substituents and material properties in furan-maleimide networks. A possibility would be to shift to substituted furans instead of substituted maleimides for more direct influence on the thermodynamics of the equilibrium reaction.

References

[1] E. Naderi Kalali, S. Lotfian, M. Entezar Shabestari, S. Khayatzadeh, C. Zhao, H. Yazdani Nezhad, *Curr. Opin. Green Sus. Chem.* **2023**, *40*, 100763, DOI 10.1016/j.cogsc.2023.100763.

[2] L. Cheng, X. Chen, J. Gu, N. Kobayashi, H. Yuan, Y. Chen, *Fund. Res.* **2024**, DOI 10.1016/j.fmre.2023.12.023.

[3] U. Salahuddin, J. Sun, C. Zhu, M. Wu, B. Zhao, P. Gao, *Adv. Sus. Sys.* **2023**, *7*, 2200471, DOI 10.1002/adsu.202200471.

[4] D. M. Mitrano, M. Wagner, *Nat. Rev. Mater.* **2021**, *7*, 71–73, DOI 10.1038/s41578-021-00406-9.

[5] J. Luo, Z. Demchuk, X. Zhao, T. Saito, M. Tian, P. Sokolov, A., P. Cao, *Matter* **2022**, *5*, 1391–1422, DOI 10.1016/j.matt.2022.04.007.

[6] N. Zheng, Y. Xu, Q. Zhao, T. Xie, *Chem. Rev.* **2021**, *121*, 1716–1745, DOI 10.1021/acs.chemrev.0c00938.

[7] C. Bowman, F. Du Prez, J. Kalow, *Poly. Chem.* **2020**, *11*, 5295–5296, DOI 10.1039/d0py90102d.

[8] W. Post, A. Susa, R. Blaauw, K. Molenveld, R. J. I. Knoop, *Polym. Rev.* **2020**, *60*, 359–388, DOI 10.1080/15583724.2019.1673406.

[9] G. M. Scheutz, J. J. Lessard, M. B. Sims, B. S. Sumerlin, *J. Am. Chem. Soc.* **2019**, *141*, 16181–16196, DOI 10.1021/jacs.9b07922.

[10] Y. H. Jin, Z. P. Lei, P. Taynton, S. F. Huang, W. Zhang, *Matter* **2019**, *1*, 1456–1493, DOI 10.1016/j.matt.2019.09.004.

[11] L. Imbernon, S. Norvez, *Eur. Polym. J.* **2016**, *82*, 347–376, DOI 10.1016/j.eurpolymj.2016.03.016.

[12] P. Wang, L. Yang, B. Dai, Z. H. Yang, S. Guo, G. Gao, L. G. Xu, M. Q. Sun, K. L. Yao, J. Q. Zhu, *Eur. Polym. J.* **2020**, *123*, 109382, DOI 10.1016/j.eurpolymj.2019.109382.

[13] S. K. Schoustra, T. Groeneveld, M. M. J. Smulders, *Polym. Chem.* **2021**, *12*, 1635–1642, DOI 10.1039/d0py01555e.

[14] L. D. Dugas, W. D. Walker, R. Shankar, K. S. Hoppmeyer, T. L. Thornell, S. E. Morgan, R. F. Storey, D. L. Patton, Y. C. Simon, *Macromol. Rapid. Commun.* **2022**, *43*, e2200249, DOI 10.1002/marc.202200249.

[15] P. R. Christensen, A. M. Scheuermann, K. E. Loeffler, B. A. Helms, *Nat. Chem.* **2019**, *11*, 442–448, DOI 10.1038/s41557-019-0249-2.

[16] X. Yu, J. Jia, S. Xu, K. U. Lao, M. J. Sanford, R. K. Ramakrishnan, S. I. Nazarenko, T. R. Hoye, G. W. Coates, J. DiStasio, R. A., *Nat. Commun.* **2018**, *9*, 2880, DOI 10.1038/s41467-018-05269-3.

[17] D. Montarnal, M. Capelot, F. Tournilhac, L. Leibler, *Science* **2011**, *334*, 965–8, DOI 10.1126/science.1212648.

[18] W. B. Kong, Y. Y. Yang, A. Q. Yuan, L. Jiang, X. W. Fu, Y. C. Wang, H. L. Xu, Z. M. Liu, J. X. Lei, *Energy* **2021**, *232*, 121070, DOI 10.1016/j.energy.2021.121070.

[19] A. Tsuruoka, A. Takahashi, D. Aoki, H. Otsuka, *Angew. Chem. Int. Ed.* **2020**, *59*, 4294–4298, DOI 10.1002/anie.201913430.

[20] J. A. Yoon, J. Kamada, K. Koynov, J. Mohin, R. Nicolaÿ, Y. Z. Zhang, A. C. Balazs, T. Kowalewski, K. Matyjaszewski, *Macromolecules* **2012**, *45*, 142–149, DOI 10.1021/ma2015134.

[21] N. Van Herck, D. Maes, K. Unal, M. Guerre, J. M. Winne, F. E. Du Prez, *Angew. Chem. Int. Ed.* **2020**, *59*, 3609–3617, DOI 10.1002/anie.201912902.

[22] X. Fu, A. Qin, Z. Tang, B., *J. Polym. Sci.* **2023**, *62*, 787–798, DOI 10.1002/pol.20230383.

[23] M. Gosecki, M. Gosecka, *Polymers (Basel)* **2022**, *14*, 842, DOI 10.3390/polym14040842.

[24] X. Zhang, S. Wang, Z. Jiang, Y. Li, X. Jing, *J. Am. Chem. Soc.* **2020**, *142*, 21852–21860, DOI 10.1021/jacs.0c10244.

[25] B. Marco-Dufort, M. W. Tibbitt, *Mater. Today Chem.* **2019**, *12*, 16–33, DOI 10.1016/j.mtchem.2018.12.001.

[26] E. E. L. Maassen, J. P. A. Heuts, R. P. Sijbesma, *Polym. Chem.* **2021**, *12*, 3640–3649, DOI 10.1039/d1py00292a.

[27] Y. Chao, A. Krishna, M. Subramaniam, D. D. Liang, S. P. Pujari, A. C. Sue, G. Li, F. M. Miloserdov, H. Zuilhof, *Angew. Chem. Int. Ed.* **2022**, *61*, e202207456, DOI 10.1002/anie.202207456.

[28] M. Thiessen, V. Abetz, *Polymers (Basel)* **2021**, *13*, 1189, DOI 10.3390/polym13081189.

[29] B. Wang, Z. Li, F. Liu, Y. Liu, *J. Macromol. Sci. - Pure Appl. Chem.* **2020**, *57*, 888–895, DOI 10.1080/10601325.2020.1807365.

[30] J. L. Ye, S. Q. Ma, B. B. Wang, Q. M. Chen, K. Huang, X. W. Xu, Q. Li, S. Wang, N. Lu, J. Zhu, *Green Chem.* **2021**, *23*, 1772–1781, DOI 10.1039/d0gc03946b.

[31] K. Ishida, V. Weibel, N. Yoshie, *Polymer* **2011**, *52*, 2877–2882, DOI 10.1016/j.polymer.2011.04.038.

[32] G. Griffini, B. Rigatelli, S. Turri, *Macromol. Mater. Eng.* **2023**, *308*, 2300133, DOI 10.1002/mame.202300133.

[33] P. van den Tempel, F. Picchioni, R. K. Bose, *Macromol. Rapid. Commun.* **2022**, *43*, e2200023, DOI 10.1002/marc.202200023.

[34] J. Wang, J. Li, J. Zhang, S. Liu, L. Wan, Z. Liu, F. Huang, *Polymers (Basel)* **2023**, *15*, 3470, DOI 10.3390/polym15163470.

[35] C. Zeng, H. Seino, J. Ren, K. Hatanaka, N. Yoshie, *Polymer* **2013**, *54*, 5351–5357, DOI 10.1016/j.polymer.2013.07.059.

[36] K. I. Galkin, I. V. Sandulenko, A. V. Polezhaev, *Processes* **2022**, *10*, 30, DOI 10.3390/pr10010030.

[37] V. K. Yadav, D. L. V. K. Prasad, A. Yadav, K. Yadav, *J. Phys. Org. Chem.* **2021**, *34*, e4131, DOI 10.1002/poc.4131.

[38] B. T. McReynolds, K. D. Mojtabai, N. Penners, G. Kim, S. Lindholm, Y. Lee, J. D. McCoy, S. Chowdhury, *Polymers* **2023**, *15*, 1106, DOI 10.3390/polym15051106.

[39] F. Orozco, Z. Niyazov, T. Garnier, N. Migliore, A. T. Zdvizhkov, P. Raffa, I. Moreno-Villoslada, R. K. Picchioni, F.and Bose, *Molecules* **2021**, *26*, 2230, DOI 10.3390/molecules26082230.

[40] K. J. Luo, L. B. Huang, Y. Wang, J. R. Yu, J. Zhu, Z. M. Hu, *Chinese J. Polym. Sci.* **2020**, *38*, 268–277, DOI 10.1007/s10118-019-2328-7.

[41] Q. Zhou, Z. Sang, K. K. Rajagopalan, Y. Sliozberg, F. Gardea, S. A. Sukhishvili, *Macromolecules* **2021**, *54*, 10510–10519, DOI 10.1021/acs.macromol.1c01662.

[42] J. D. Mayo, A. Adronov, *J. Polym. Sci. Part A: Polym. Chem.* **2013**, *51*, 5056–5066, DOI 10.1002/pola.26937.

[43] P. Raffa, A. Kassi, J. Gosschalk, N. Migliore, L. M. Polgar, F. Picchioni, *Macromo. Mater. Eng.* **2021**, *306*, 2000755, DOI 10.1002/mame.202000755.

[44] A. Safaei, S. Terryn, B. Vanderborght, G. Van Assche, J. Brancart, *Polymers* **2021**, *13*, 2522, DOI 10.3390/polym13152522.

[45] X. Kuang, G. M. Liu, X. Dong, D. J. Wang, *Mater. Chem. Front.* **2017**, *1*, 111–118, DOI 10.1039/c6qm00094k.

[46] J. Brancart, J. Van Damme, F. Du Prez, G. Van Assche, *Phys. Chem. Chem. Phys.* **2021**, *23*, 2252–2263, DOI 10.1039/d0cp05953f.

[47] R. Sustmann, *Tetrahedron Lett.* **1971**, *12*, 2721–2724, DOI 10.1016/s0040-4039(01)96962-x.

[48] J. P. Hernandez-Mancera, N. Rojas-Valencia, F. Nunez-Zarur, *J. Phys. Chem. A* **2022**, *126*, 6657–6667, DOI 10.1021/acs.jpca.2c04970.

[49] E. J. DeWitt, C. T. Lester, G. A. Ropp, *J. Am. Chem. Soc.* **1956**, *78*, 2101–2103, DOI 10.1021/ja01591a020.

[50] I. Benghiat, E. I. Becker, *J. Org. Chem.* **1958**, *23*, 885–890, DOI 10.1021/jo01100a031.

[51] C. Rücker, D. Lang, J. Sauer, H. Friege, R. Sustmann, *Chem. Ber.* **2006**, *113*, 1663–1690, DOI 10.1002/cber.19801130505.

[52] T. S. Khan, S. Gupta, M. Ahmad, M. I. Alam, M. A. Haider, *RSC Adv.* **2020**, *10*, 30656–30670, DOI 10.1039/d0ra04318d.

[53] V. Froidevaux, M. Borne, E. Laborbe, R. Auvergne, A. Gandini, B. Boutevin, *RSC Adv.* **2015**, *5*, 37742–37754, DOI 10.1039/c5ra01185j.

[54] R. C. Boutelle, B. H. Northrop, *J. Org. Chem.* **2011**, *76*, 7994–8002, DOI 10.1021/jo201606z.

[55] R. Sustmann, R. Schubert, *Angew. Chem. Int. Edit.* **2003**, *11*, 840–840, DOI 10.1002/anie.197208401.

[56] M. Mojica, F. Mendez, J. A. Alonso, *Molecules* **2016**, *21*, 200, DOI 10.3390/molecules21020200.

[57] E. Dumont, P. Chaquin, *J. Mol. Struc.-Theochem.* **2006**, *758*, 161–167, DOI 10.1016/j.theochem.2005.10.026.

[58] M. Carneiro de Oliveira, J.and Laborie, V. Roucoules, *Molecules* **2020**, *25*, 243, DOI 10.3390/molecules25020243.

[59] K. N. Houk, R. J. Loncharich, J. F. Blake, W. L. Jorgensen, *J. Am. Chem. Soc.* **1989**, *111*, 9172–9176, DOI 10.1021/ja00208a006.

[60] D. N. Matthews, E. I. Becker, *J. Org. Chem.* **1966**, *31*, 1135–1140, DOI 10.1021/jo01342a035.

[61] Y. Okamoto, H. C. Brown, *J. Org. Chem.* **1957**, *22*, 485–494, DOI 10.1021/jo01356a003.

[62] S. K. Schoustra, J. A. Dijksman, H. Zuilhof, M. M. J. Smulders, *Chem. Sci.* **2020**, *12*, 293–302, DOI 10.1039/d0sc05458e.

[63] B. J. Adzima, H. A. Aguirre, C. J. Kloxin, T. F. Scott, C. N. Bowman, *Macromolecules* **2008**, *41*, 9112–9117, DOI 10.1021/ma801863d.

[64] R. C. Cioc, M. Crockatt, J. C. van der Waal, P. C. A. Bruijnincx, *Angew. Chem. Int. Ed.* **2022**, *61*, e202114720, DOI 10.1002/anie.202114720.

[65] D. Wang, T.and Gao, H. Yin, J. Zhao, X. Wang, H. Niu, *Polymers* **2024**, *16*, 441, DOI 10.3390/polym16030441.

[66] A. Buonerba, R. Lapenta, S. Ortega S., C. Capacchione, S. Milione, A. Grassi, *ChemistrySelect* **2017**, *2*, 1605–1612, DOI 10.1002/slct.201602071.

[67] L. Rincon, R. Almeida, *J. Phys. Chem. A* **2012**, *116*, 7523–30, DOI 10.1021/jp300160g.

2.5 Appendix

An overview of the methodology is given below, while full details can be accessed from: https://doi.org/10.18174/661586

2.5.1 General synthesis of bismaleimide linkers (1-5)

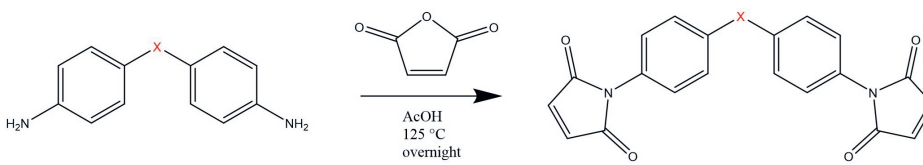

Scheme S1: *General synthesis of bismaleimide linkers.*

Maleic acid (1.5 g, 15.1 mmol) and 3.8 mmol bismaleimide precursor (see **Table S1**) were dissolved in 25 ml glacial acetic acid. This solution was then refluxed for 12 hours at 125 °C while stirring. The solution was subsequently cooled to room temperature and neutralised by addition of a saturated sodium carbonate solution (≈150-200 ml). The solution was then extracted with 5 × 50 ml ethyl acetate. The organic fractions were collected and washed with 5 × 50 ml of 1 M HCl. Afterwards the solvent was removed by rotary evaporation and the solids were dissolved in 60 ml acetone followed by a precipitation by addition of 100 ml ice cold water. The flask was then put in an ice bath for 30 min. Afterwards the solution was filtered and the precipitate was washed with ice cold water (≈200 ml). The solids were collected and dried overnight.
bMCO: ^{1}H NMR (400 MHz, $CDCl_3$) δ 7.94 (d, J = 8.7 Hz, 4H), 7.57 (d, J = 8.7 Hz, 4H), 6.92 (s, 4H).
^{13}C NMR (101 MHz, $CDCl_3$) δ 194.44, 168.96, 136.17, 135.13, 134.46, 130.89, 125.27, 77.33, 77.01, 76.70.
bMO: ^{1}H NMR (400 MHz, $CDCl_3$) δ 7.33 (d, J = 8.9 Hz, 4H), 7.13 (d, J = 8.9 Hz, 4H), 6.87 (s, 4H).
^{13}C NMR (101 MHz, $CDCl_3$) δ 169.54, 156.30, 134.24, 127.75, 126.56, 119.54, 77.33, 77.02, 76.70.

bMS: ^{1}H NMR (400 MHz, $CDCl_3$) δ 7.46 (d, J = 8.6 Hz, 4H), 7.33 (d, J = 8.7 Hz, 4H), 6.87 (s, 4H).
^{13}C NMR (101 MHz, $CDCl_3$) δ 169.25, 135.18, 134.31, 131.69, 130.37, 126.61, 77.33, 77.01, 76.69.
bMSO$_2$: ^{1}H NMR (400 MHz, $CDCl_3$) δ 8.06 (d, J = 8.8 Hz, 4H), 7.63 (d, J = 8.8 Hz, 4H), 6.90 (s, 4H).
^{13}C NMR (101 MHz, $CDCl_3$) δ 168.57, 139.88, 135.97, 134.51, 128.76, 125.78, 77.32, 77.01, 76.69.

Table S1: *Amounts and yields of bismaleimide linkers.*

Bismaleimide precursor	Name Product	g/mol precursor	g/mol product	g product	Yield (%)
4,4'-Diaminobenzophenone	**bMCO**	212.25	372.34	1.0	69
4,4'-Oxydianiline	**bMO**	200.24	360.33	1.1	71
4,4'-Diaminodiphenyl sulfide	**bMS**	216.30	376.39	0.9	65
4-Aminophenyl sulfone	**bMSO$_2$**	248.30	408.38	0.8	52

Table S2: *Dart-MS found m/z values for the synthesised bismaleimide linkers.*

Name Product	Adduct	m/z
bMCO	$[M+H]^+$	373.0821
bMO	$[M+NH_4]^+$	378.1084
bMS	$[M+NH_4]^+$	394.0856
bMSO$_2$	$[M+NH_4]^+$	426.0755

2.5.2 Synthesis of Pentaerythritol Tris(3-(furfurylthiol)-propionate) [PTF] (6) Adapted from Adzima *et al.* (2008)[1]

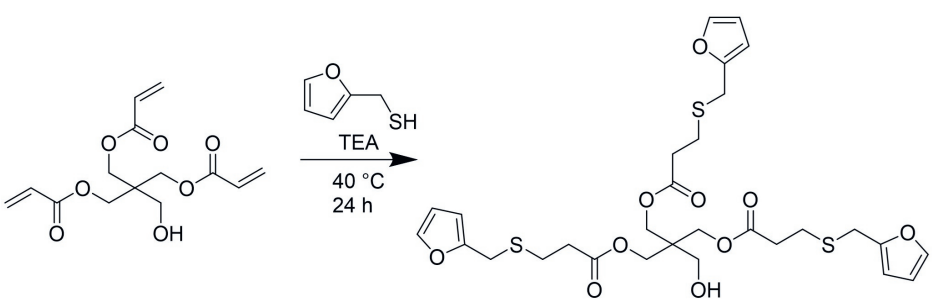

Scheme S2: *Synthesis of Pentaerythritol Tris(3-(furfurylthiol)-propionate).*

4.9 ml (19 mmol) pentaerythritol triacrylate was mixed with 6.4 ml (63 mmol) furfuryl mercaptan and 0.44 ml (3.15 mmol) triethylamine.

The reaction mixture was heated at 40 °C for 24 hours while stirring. After the reaction has completed, the remaining furfuryl mercaptan and triethylamine were removed under vacuum at 50 °C and finally under nitrogen flow in the fume hood. A viscous oil was obtained (10.9 g, 89.7%).

^{1}H NMR (400 MHz, $CDCl_3$) δ 7.32 – 7.25 (m, 3H), 6.24 (dt, J = 3.3, 1.6 Hz, 3H), 6.13 (d, J = 3.2 Hz, 3H), 4.13 – 4.01 (m, 5H), 3.97 (s, 2H), 3.66 (d, J = 2.6 Hz, 6H), 2.68 (td, J = 7.3, 1.6 Hz, 6H), 2.54 – 2.45 (m, 6H). ^{13}C NMR (101 MHz, $CDCl_3$) δ 171.80, 171.52, 171.30, 151.37, 142.36, 110.60, 110.58, 107.77, 77.48, 77.16, 76.84, 63.98, 62.36, 62.30, 42.07, 34.36, 28.41, 28.39, 26.62.

2.5.3 Synthesis of N,N'-(Octane-1,8-diyl)bis(furan-2-carboxamide) (7) Adapted from Mayo and Adronov (2013)[2]

All glassware used was dried in an oven at 120 °C before use.

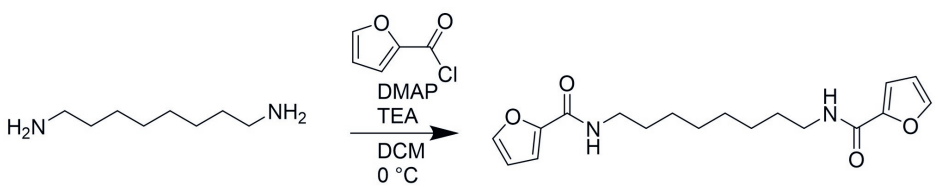

Scheme S3: *Synthesis of N,N'-(Octane-1,8-diyl)bis(furan-2-carboxamide).*

10.0 g (69.3 mmol) 1,8-octanediamine, 19.6 ml (141 mmol) triethylamine and 0.17 g (1.35 mmol) DMAP were dissolved in 200 ml anhydrous DCM under argon. This solution was cooled in an ice bath. A stock solution of 2-furoyl chloride was prepared by dissolving 14.4 ml (146 mmol) 2-furyol chloride in 50 ml anhydrous DCM under argon. The 2-furyol chloride solution was then added to the cooled 1,8-octadiamine solution via dropwise addition. After complete addition the reaction mixture was allowed to stir at room temperature for 1 hour after which the solvent was evaporated via rotary evaporation. The obtained solid was washed with ≈2 L of water via vacuum filtration. The solid was then dried overnight in a vacuum oven at 50 °C. A white powder was obtained (14.5 g, 65%).

^{1}H NMR (400 MHz, DMSO) δ 8.30 (t, J = 5.8 Hz, 2H), 7.80 (d, J = 1.7 Hz, 2H), 7.06 (d, J = 3.3 Hz, 2H), 6.60 (dd, J = 3.5, 1.7 Hz, 2H), 3.18 (q, J = 6.7 Hz, 4H), 1.49 (t, 4H), 1.27 (s, 8H).
^{13}C NMR (101 MHz, DMSO) δ 158.09, 148.61, 145.17, 113.40, 112.18, 40.68, 40.63, 40.47, 40.42, 40.26, 40.21, 40.06, 40.00, 39.80, 39.59, 39.38, 38.87, 29.63, 29.18, 26.86.

2.5.4 Synthesis of PPG-bis-furan (8)

All glassware used was dried in an oven at 120 °C before use.

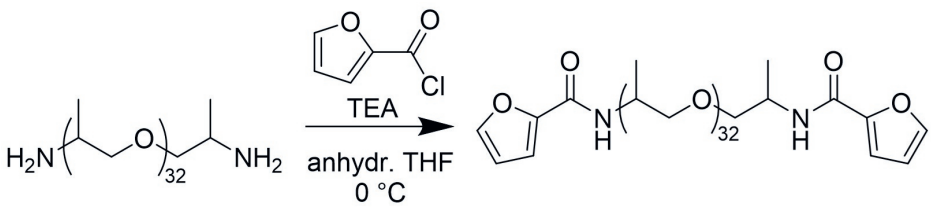

Scheme S4: *Synthesis of PPG-bis-furan.*

20.0 ml (10.0 mmol) poly(propylene glycol) bis(2-aminopropyl ether) Mn 2000 Da and 4.18 ml (30 mmol) triethylamine were dissolved in 50 ml anhydrous THF. This solution was then purged for 30 min with N_2 in an ice bath. After purging a N_2 filled balloon was added. The reaction mixture was cooled with an ice bath to 0 °C 6.0 ml (60.7 mmol) 2-furfuroyl chloride was dissolved in 2 ml anhydrous THF and added dropwise to the reaction mixture under stirring. After complete addition the reaction was allowed to stir for 1 hour at room temperature. The solvent was evaporated and the solid was redissolved in 30 ml H_2O:MeOH 1:1 and divided over 3 dialysis tubes. This was then dialysed (1 kDA cut-off) against H_2O:MeOH 1:1 for 2 days (medium was refreshed 3 times per day). Next the solvent was evaporated and the product was dried in a 70 °C oven till the weight stabilised, resulting in a brown/yellowish oil (16.4 g, 77.7% yield).

^{1}H NMR (400 MHz, MeOD) δ 7.68 (d, J = 1.9 Hz, 2H), 7.13 (t, J = 2.8 Hz, 2H), 6.60 (dd, J = 3.5, 1.8 Hz, 2H), 4.25 (dd, J = 6.7, 2.9 Hz, 2H), 3.93 – 3.70 (m, 3H), 3.70 – 3.36 (m, 102H), 1.26 (dd, J = 6.8, 4.0 Hz, 7H), 1.15 (dt, J = 5.9, 2.9 Hz, 99H).

^{13}C NMR (101 MHz, MeOD) δ 158.73, 158.67, 147.82, 144.78, 113.85, 113.81, 111.72, 111.68, 75.42, 75.37, 75.32, 75.29, 75.20, 75.16, 75.11, 75.09, 75.04, 75.01, 74.98, 74.95, 73.08, 73.04, 72.98, 72.80, 72.78, 72.72, 72.70, 71.66, 71.59, 71.57, 48.42, 48.21, 48.00, 47.79, 47.57, 47.36, 47.15, 45.29, 45.15, 17.59, 17.42, 17.36, 17.32, 17.22, 16.59, 16.57, 16.52, 16.47, 16.45, 16.42, 16.39, 16.31, 16.26, 16.23.

2.5.5 Synthesis of furfuryl glycidyl ether (adapted from Ye et al.)[3]

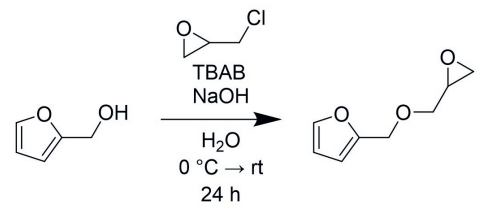

Scheme S5: *Synthesis of furfuryl glycidyl ether.*

15 g NaOH was dissolved in 22.5 ml DI water in a 250 ml round bottom flask. The flask was then cooled to 0 °C in an ice bath. 150 mg (0.465 mmol) TBAB was added to the reaction mixture. After the TBAB had fully dissolved, 90 g (0.98 mmol) epichlorohydrin was added. Then 15 g (0.15 mmol) furfuryl alcohol was added to the mixture in a dropwise manner. The reaction was stirred on ice for another four hours, after which the reaction was continued at room temperature for another 20 hours. Ater the reaction was completed, the mixture was extracted using 2x 100 ml diethyl ether and 1 × 100 ml ethyl acetate. The organic layers were collected and washed with 3 × 100 ml DI water and 2 × 100 ml brine. After washing the organic layer was dried with $MgSO_4$. The solvent was removed and the remaining epichlorohydrin was evaporated using a rotorvap at 50 °C and 33 mbar for 5 hours. The last remaining epichlorohydrin was removed using a silica plug run with 50/50 ethyl acetate/petroleum ether 40/60. This resulted in a yellow oil. The yield was 16.7 g (72.2%).

^{1}H NMR (400 MHz, $CDCl_3$) δ 7.41 (s, 1H), 6.35 (d, J = 1.5 Hz, 2H), 4.59 – 4.46 (m, 2H), 3.76 (dd, J = 11.5, 3.1 Hz, 1H), 3.44 (dd, J = 11.5, 5.8 Hz, 1H), 3.16 (ddt, J = 5.9, 4.0, 2.9 Hz, 1H), 2.79 (dd, J = 5.0, 4.1 Hz, 1H), 2.61 (dd, J = 5.0, 2.7 Hz, 1H).

2.5.6 Synthesis of four-armed furan linker FA4 (9) (as reported by McReynolds et al.)[4]

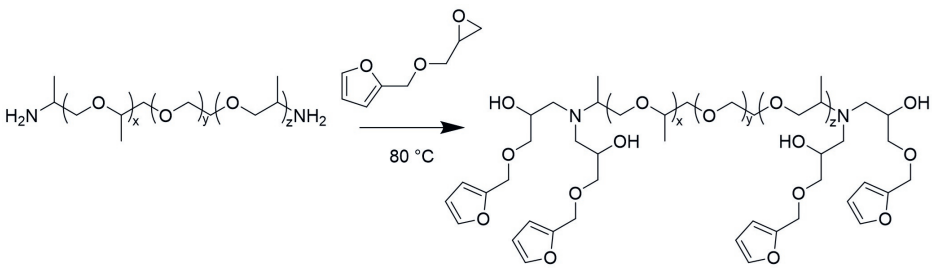

Scheme S6: *Synthesis of furan linker FA4.*

10.0 g (16.7 mmol) of Jeffamine ED-600 and 10.28 g (66.7 mmol) of furfuryl glycidyl ether were mixed in a round bottom flask and stirred at 80 °C for 48 h. The reaction mixture went from a deep yellow to a dark brown oil. Conversion was quantitative as determined by NMR.

^{1}H NMR (400 MHz, $CDCl_3$) δ 7.40 (d, J = 1.8 Hz, 2H), 6.37 – 6.29 (m, 3H), 4.56 – 4.46 (m, 3H), 3.85 – 3.75 (m, 1H), 3.74 (ddd, J = 14.0, 6.9, 3.0 Hz, 1H), 3.67 – 3.53 (m, 15H), 3.56 – 3.44 (m, 2H), 3.48 – 3.35 (m, 2H), 3.39 – 3.22 (m, 1H), 3.14 – 2.98 (m, 1H), 2.83 – 2.35 (m, 3H), 1.12 (td, J = 5.9, 2.8 Hz, 2H), 1.06 – 0.93 (m, 1H), 0.92 – 0.83 (m, 2H).
^{13}C NMR (101 MHz, $CDCl_3$) δ 151.85, 151.81, 151.79, 151.75, 151.73, 151.37, 142.93, 142.76, 142.75, 142.72, 110.29, 110.26, 110.24, 109.58, 109.37, 109.35, 109.31, 77.41, 77.29, 77.09, 76.77, 75.45, 75.32, 75.09, 74.96, 74.89, 74.66, 74.57, 74.40, 74.27, 73.50, 73.00, 72.56, 72.44, 72.34, 72.30, 72.25, 72.23, 72.20, 72.03, 72.00, 71.46, 71.28, 71.10, 70.70, 70.57, 70.53, 70.50, 70.47, 70.41, 70.34, 70.20, 70.10, 70.02, 69.96, 68.88, 68.79, 68.77, 68.16, 68.12, 67.18, 67.08, 66.95, 65.29, 65.19, 65.17, 65.05, 58.14, 57.80, 57.34, 57.31, 56.89, 56.19, 56.15, 55.81, 54.66, 54.59, 54.51, 53.79, 53.56, 53.49, 53.30, 53.23, 53.11, 52.98, 52.92, 52.76, 50.72, 44.30, 17.12, 17.05, 17.01, 16.96, 16.92, 16.85, 16.80, 16.66, 13.30, 13.14, 13.10, 10.94, 10.81, 9.68, 9.65, 9.61.

2.5.7 Preparation of FA3-alkyl/PPG networks

Materials were prepared by dissolving the bismaleimide, N,N'-(Octane-1,8-diyl)bis(furan-2-carboxamide) or PPG-bis-furan and Pentaerythritol Tris(3-(furfurylthiol)-propionate) in DCM:methanol 95:5 in a 1:1 molar equivalence of the reactive groups. The solution was then mixed and

evaporated. The resulting solid was powderised and pressed into shape with a circular 10 mm die and pressed for 20 seconds at 120 °C and 1 ton. The sample was then heated at 70 °C for at least 2 days.

2.5.8 Network deposition on KBr pellets (FA3-alkyl)

Stock solution of the different networks were prepared by dissolving low amounts of the (0.019 mmol) bMX linker, (0.0057 mmol) N,N'-(Octane-1,8-diyl)bis(furan-2-carboxamide) and (0.0089 mmol) Pentaerythritol Tris(3-(furfurylthiol)-propionate) in 0.1 ml DCM. After mixing 3 drops were deposited on a KBr pellet (400 mg) and dried in the fume hood at room temperature. After evaporation the samples were measured to obtain the starting intensity. The samples were then stored for at least 3 days each at 70, 80, 90 and 100 °C in a dry oven. All samples were prepared in triplicate. The IR absorbance was measured for each temperature and compared to the starting intensity. The maleimide peak at 690 cm^{-1} was integrated using an end point weighted baseline fit and compared for all samples.
The samples with **bMSO$_2$** were dissolved in 0.4 ml DCM due to solubility issues.
The samples with **bMCO** were dissolved in 0.6 ml DCM + 0.1 ml THF + 0.1 ml ACN due to solubility issues. The solution was extensively sonicated and vortexed before use.

2.5.9 Preparation of FA4 networks

352.8 mg (0.290 mmol) FA4 and (0.348 mmol) bMX linker were separately dissolved in 1 ml DMF. The molar ratio used was 0.6 maleimide/furan functional group. Both stock solutions were mixed and vortexed for 10 seconds. This solution was then cast in a plastic sample tube with a diameter of 1.5 cm. After drying in the oven at 70 °C a film was obtained. This film was then trimmed to a circle with a diameter of 1 cm for rheology.

2.5.10 FA4 network IR measurements

17.64 mg (0.0145 mmol) FA4 and 0.0174 mmol bMX linker were dissolved in 1 ml DCM. The solution was vortexed for 10 seconds. 1-2 drops of stock solution were deposited on a Teflon sheet. After evaporation of the solvent under air flow, the sample was transferred to the crystal of an ATR-IR that was already equilibrated to the set temperature. The sample was then measured every minute (16 scans, 4 cm^{-1} resolution).

2.5.11 References

[1] B. J. Adzima, H. A. Aguirre, C. J. Kloxin, T. F. Scott, C. N. Bowman, *Macromolecules* **2008**, *41*, 9112–9117, DOI 10.1021/ma801863d.

[2] J. D. Mayo, A. Adronov, *J. Polym. Sci. Part A: Polym. Chem.* **2013**, *51*, 5056–5066, DOI 10.1002/pola.26937.

[3] J. L. Ye, S. Q. Ma, B. B. Wang, Q. M. Chen, K. Huang, X. W. Xu, Q. Li, S. Wang, N. Lu, J. Zhu, *Green Chem.* **2021**, *23*, 1772–1781, DOI 10.1039/d0gc03946b.

[4] B. T. McReynolds, K. D. Mojtabai, N. Penners, G. Kim, S. Lindholm, Y. Lee, J. D. McCoy, S. Chowdhury, *Polymers* **2023**, *15*, 1106, DOI 10.3390/polym15051106.

Chapter 3

Covalent Adaptable Networks using Boronate Linkages by incorporating Tetraazaadamantanes

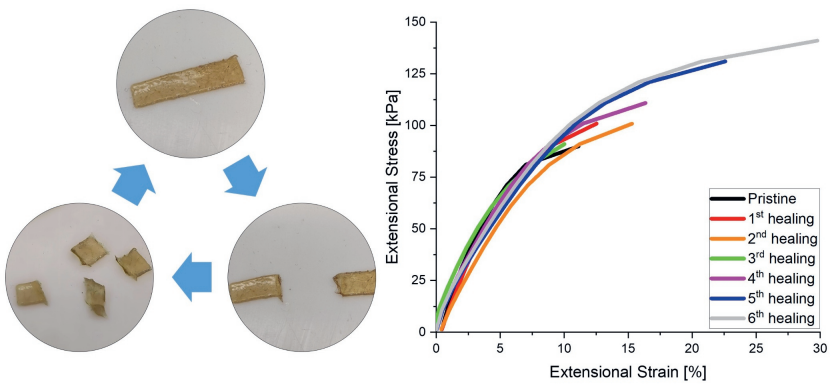

Simon van Hurne, Marijn Kisters, Maarten M. J. Smulders
This work was published as:
S. van Hurne, M. Kisters, and M. M. J. Smulders, *Frontiers in Chemistry*, **2023**. 11. https://doi.org/10.3389/fchem.2023.1148629

3.1 Abstract

Boronic esters prepared by condensation of boronic acids and diols have been widely used as dynamic covalent bonds in the synthesis of both discrete assemblies and polymer networks. In this study we investigate the potential of a new dynamic-covalent motif, derived from TetraAza-ADamantanes (TAADs), with their adamantane-like triol structure, in boronic ester-based covalent adaptable networks (CANs). The TAAD-boronic ester linkage has recently been reported as a more hydrolytically stable boronic ester variant, while still having a dynamic pH response: small-molecule studies found little exchange at neutral pH, while fast exchange occurred at pH 3.8. In this work, bi- and trifunctional TAAD linkers were synthesised and crosslinked with boronic acids to form rubber-like materials, with a Young's modulus of 1.75 MPa. The dynamic nature of the TAAD networks was confirmed by stress relaxation experiments, revealing Arrhenius-like behaviour, with a corresponding activation energy of 142 ± 10 kJ mol^{-1}. Increasing the crosslinking density of the material from 10% to 33% resulted in reduced relaxation times, as is consistent with a higher degree of crosslinking within the dynamic networks. In contrast to the reported accelerating effect of acid addition to small-molecule TAAD complexes, within the polymer network the addition of acid increased relaxation times. This suggests unanticipated interactions between the acid and the polymer that cannot occur in the corresponding small-molecules analogues. The obtained boronate-TAAD materials were thermally stable up to 150 °C. This thermal stability, in combination with the intrinsically dynamic bonds inside the polymer network, allowed these materials to be reprocessed and healed after damage by hot-pressing.

3.2 Introduction

The poor recyclability of most modern plastics, in particular of thermoset materials, has created a focus on making more sustainable and better recyclable materials. This recyclability issue can be tackled by incorporating dynamic covalent bonds[1] inside crosslinked polymer materials to create so-called covalent adaptable networks (CANs),[2–5] While dynamic-covalent bonds have proven very successful in the creation of dynamic combinatorial libraries,[6,7] discrete cage(-like) assemblies,[8] or covalent organic frameworks,[9] their use in polymer networks has only more recently been acknowledged.[10] Instead, polymer chemists previously focussed primarily on reversible, non-covalent interactions (notably hydrogen bonds).[11] However, by utilising dynamic covalent bonds, a more robust network can be created with crosslinks that can be made to exchange under specific conditions (*e.g.* by application of heat or light), thus allowing for reprocessing and recycling. The dynamicity of the introduced reversible crosslinks also means that the polymer material can undergo self-healing, which can extend the lifetime of the material.[12–14] Crucially, the use of dynamic bonds that are covalent in nature means that while these CANs can be recycled and/or demonstrate self-healing behaviour, at their operating temperature they still form a robust network –as a direct consequence of these covalent crosslinks– that impart mechanical strength to the material. Over the last few decades various dynamic bonds have been explored for use in CANs; these include the Diels-Alder reaction,[15,16] imines,[17,18] esters[19,20] and vinylogous urethanes.[21] Also, boronic esters[22,23] have received an increasing amount of interest, due to their dynamic reversible condensation reaction with diols and general biocompatibility.[24–26] Coupled with the affinity of boronic acids towards catechols[27] and sugars[28,29], this has led to various applications to include boronic acids in medical applications, such as drugs[30] and medical gels,[31–33] and biodegradable materials.[34,35] Boronic esters have also been used to form dynamic assemblies such as micelles[36,37] or cage structures.[38,39] Even a dynamically self-assembled nanoscale boronate ester ladder has been reported.[40]

Typically, bidentate boronic acid linkages are used via reactions with diols or poly-ols, which usually result in the formation of soft (hydro)gels.[41–44] However an interesting moiety[45] was found to be able to consistently give rigid tridentate complexes of boronic acids, due to its well defined adamantane-like structure and conformation. This

triol was named TetraAzaADamantane (TAAD) and is shown in **Figure 3.1**. TAAD can be obtained from the precursor tris-oxime named **TRISOXH$_3$**,[46] which is prepared in a one-pot synthesis, after which an acid is used to catalyse the conversion into the final adamantane-like conformation (see **Figure 3.1**).

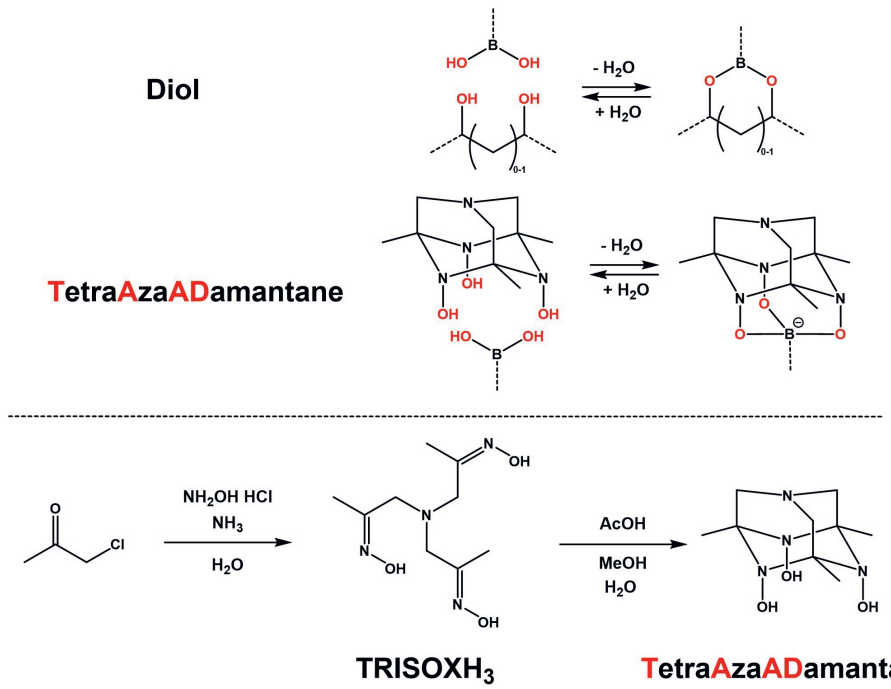

Figure 3.1: *Comparison between (conventional) bidentate complexation of a boronic acid with a diol, and novel tridentate complexation by Tetraazaadamantane. Below, the synthesis pathway of tris-oxime TRISOXH$_3$ and subsequent conversion into Tetraazaadamantane as reported.*[45]

This TAAD moiety was then further investigated.[46,47] It was found that the tridentate boronate complexation was stable at neutral to high pH with little dynamic exchange. However, around pH 3-4 dynamic exchange of the boronate groups was triggered, while at even lower pH complete disassembly of the boronate linkages was observed.[46] Coupled with a quick and simple synthesis, and the more rigid multicyclic TAAD structure, we envisioned that this dynamic response makes the TAAD moiety an interesting candidate for use in CANs to create novel boronic acid-based materials.

In this chapter, we investigate the potential of the TAAD moiety in dynamic CANs. To this end, bifunctional boronic acid linkers and bi- and trifunctional TAAD linkers were designed and synthesised, as shown in **Scheme 3.1**. These linkers were then reacted to form a crosslinked dynamic network. We found that the TAAD moieties can be successfully used for the formation of CANs. By using a small molecule network approach soft, rubber-like materials were prepared that were suitable for thermal reprocessing without the need for additional solvent and that could undergo stress relaxation.

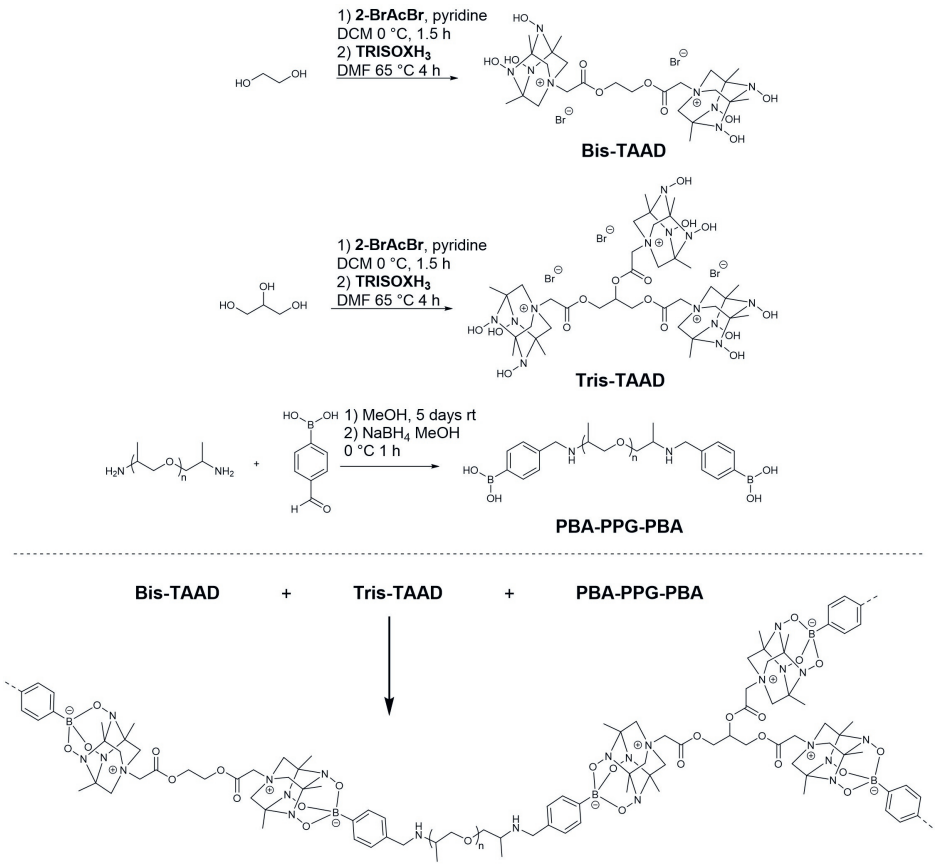

Scheme 3.1: *Synthesis and structure of the phenylboronic acid and TAAD linkers used in the boronate network (top), and synthesis of the TAAD-based polymer networks (bottom). For clarity, the counter anions have been omitted in the bottom figure.*

3.3 Results and Discussion

To incorporate TetraAzaADamantane (TAAD) groups in a boronate ester network, different linker molecules were synthesised. Both a linear bifunctional boronic acid and TAAD linker were prepared, as well as a trifunctional TAAD linker to enable crosslinking. For the linear boronic acid crosslinker it was chosen to react bis-amine terminated PPG2000 with 4-formylphenylboronic acid and subsequently reducing the formed imine bond.[48] For the bi- and trifunctional TAAD linkers **bis-TAAD** and **tris-TAAD**, ethylene glycol and glycerol, respectively, were reacted with bromoacetyl bromide. After a short work up, **TRISOXH$_3$** was attached via nitrogen quaternisation and converted to the desired TAAD-containing building blocks (see the link to the online **Supplementary Material** at the end of the chapter for full details of the synthetic procedures and characterisation).

To show the reversibility and exchange of the boronate-TAAD bond a small series of exchange studies was performed using differently substituted boronic acids, expanding on the existing exchange experiment involving only 4-bromophenyl-boronic acid.[46] A model TAAD molecule coupled to a phenylboronic acid, resembling the boronate-TAAD linkages used in the materials, was synthesised and exchanged with three different *para*-substituted phenylboronic acids (see **Supplementary Material**). This exchange was followed using ^{1}H-NMR, where the disappearance of the starting boronate-TAAD and the appearance of the exchanged product were correlated in time. All showed slow exchange over the course of 3 days, resulting in only 20% conversion. Subsequently, the pH was adjusted to 3.8 to enter the dynamic pH regime and the exchange reaction was followed for 5 hours. All three substituted phenylboronic acids showed an increase in exchange rate as expected (**Supplementary Figures S35-38**), reaching 40-60% conversion after only 5 hours. This shows that the boronate-TAAD linkages that are to be incorporated in the network can undergo exchange reactions.

Next, polymer materials were prepared by dissolving the **bis-TAAD**, **tris-TAAD**, and **PBA-PPG-PBA** in separate methanol stock solutions. These stock solutions were then combined using a stoichiometry TAAD : boronic acid of 1:1, and initially with 10% of the crosslinker **tris-TAAD**. The resulting mixture was vortexed, then cast in a silicone mould and left to dry in the fume hood for 2 days. Using this method,

a soft rubber-like material was obtained that was slightly yellowish in colour. Initial characterisation by thermal gravimetric analysis (TGA, **Supplementary Figure S65**) showed that the material was thermally stable up to 153 °C with only 5% weight loss. This thermal stability suggests that (re)processing of the material at elevated temperatures (*e.g.*, by hot-pressing) can be explored up to temperatures of approximately 150 °C. Below, we will further discuss the thermal (re)processing by hot-pressing.

The obtained polymer was then further characterised by rheometry. A frequency sweep of the material, as shown in **Figure 3.2A**, yielded a *storage modulus* (G') and *loss modulus* (G") between 0.1 and 1 MPa over the frequency domain of 0.01 to 100 rad/s. Extensional DMA showed that the material had a Young's modulus of 1.75 MPa, corresponding to a soft rubber. The temperature sweep from 4 °C to 170 °C (**Figure 3.2B**) of the formed network showed a typical rubbery plateau at a G_P of 1 MPa between 70 and 125 °C suggesting an entangled or crosslinked network, after which the material started to flow. The glassy state was not observed, but could likely be observed at lower temperatures.

A defining feature of CANs is their ability to undergo stress relaxation by dynamic bond exchange. The time for the material to relax imposed stress generally shortens with an increase in temperature, since the dynamic bond exchange becomes faster. This allows faster network rearrangement and thus faster stress relaxation. The Arrhenius equation can be applied to the dependence of the relaxation time (τ) with temperature), which will yield the activation energy E_a of relaxation process due to bond exchange. To this end, the relaxation behaviour of the boronate-TAAD network was investigated in the temperature range of 90 to 130 °C. The observed relaxation time τ decreased from 2478 seconds at 90 °C to 18 seconds at 130 °C, as can be seen in **Figure 3.2C**. From the corresponding Arrhenius plot (**Figure 3.2D**) for the boronate-TAAD exchange reaction an activation energy of 142 ± 10 kJ mol^{-1} could be determined, which is high compared to previously reported materials based on boronic esters[49–52] and more in the upper range of diethanolamine esters.[22,52] However, it is important to note that most reported boronic ester materials were prepared as a (hydro)gel, which can influence the determined activation energy. Remarkably, in contrast to the pH range of 3-4 necessary for dynamic exchange in the reactions,[46] this dynamic network manifested (stress) relaxation already at neutral pH.

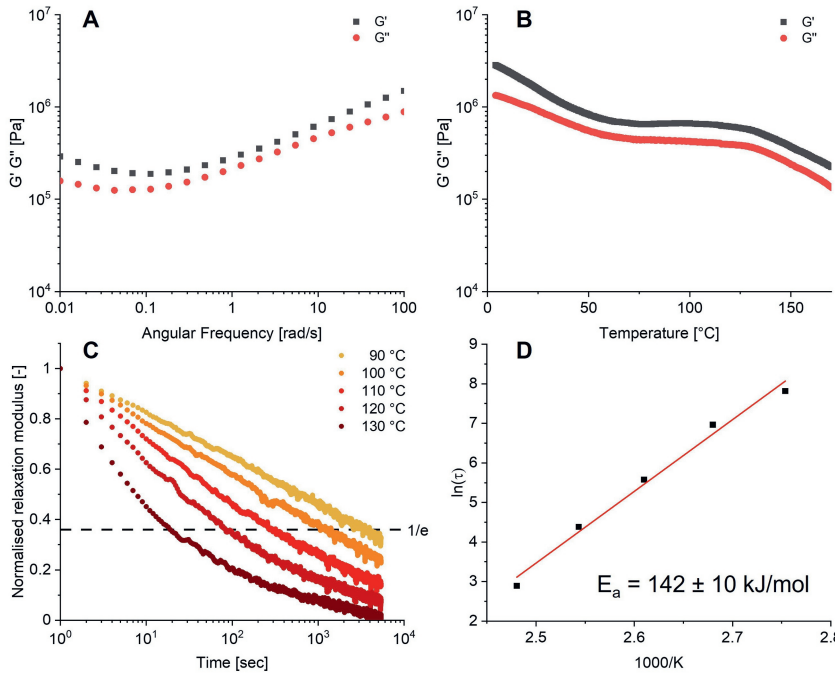

Figure 3.2: *(A) Frequency sweep at 0.5% strain, 25 °C. (B) Temperature sweep at 0.5% strain, 6.28 rad/s. (C) Relaxation series at 0.5% strain, 90–130 °C. (D) Arrhenius plot obtained from the relaxation data. All data were obtained from the 10% crosslinked material.*

Having established that a TAAD-based CAN could be prepared with a 10% crosslinker content, the effect of the crosslink density on the CAN's material properties was investigated. Additional CANs with 20% and 33% crosslinks were prepared and compared. Frequency sweeps (**Supplementary Figure S41, S42**) did not show a significant change to the moduli as *G*' and *G*" of the different materials were in the range of 0.1 to 1 MPa. Temperature sweeps (**Supplementary Figure S43, S44**) did show that increasing the crosslinking density shifted the onset of the rubbery plateau from around 50 °C to around 120—130 °C, which can be explained by considering the higher crosslink density. Next to this, the relaxation time (τ) of the material increased by one order of magnitude with increasing crosslink density from 10% to 33%, as can be seen in **Figure 3.3**. The added crosslinks reduce network mobility, thus slowing the material relaxation process.[53] This shows that it's possible to tune material properties by varying the crosslink density of these networks.

Since the boronate-TAAD network features pH-dependent bonds,[46] also the effect of acid addition to the material was investigated. Previously, researchers showed that addition of acid can accelerate the dynamic bond exchange processes inside a CAN.[54–56] In these reports, the pK_a of the added acid was found to correlate with the shortening of the material relaxation time. Combined with the reported findings[46] of the different pH regimes of the boronate-TAAD linkages, we anticipated that addition of acid in the material would have an effect by reducing the relaxation time of the material, via transesterification catalysis.

To investigate the effect of acid on this boronate-TAAD network a series of materials was prepared by mixing in different weight percentages of *p*-toluenesulfonic acid (PTSA), ranging from 0.25 wt% to 10 wt%. The relaxation behaviour of these materials was then measured and evaluated, as shown in **Figure 3.3**. The observed relaxation behaviour was more complex than initially anticipated: *i.e.*, the addition of acid did not simply lead to faster relaxation. In contrast, at low PTSA content (0.25–0.5 wt%) an increase in the relaxation time of the material compared to the material without PTSA was observed. These materials displayed a relaxation time that is about one order of magnitude longer than the original acid-free material. At moderate PTSA content (1–5 wt%) the relaxation time is still generally longer than without PTSA, but it started to decrease until at 5 wt% PTSA the material had a relaxation time similar to the control without PTSA. At high PTSA content (5–10 wt%) again an increase in relaxation time was observed. While the precise underlying mechanism of these trends remains unclear, one possible explanation might be that the PTSA is partially excluded from the network due to unfavourable interactions between the apolar aromatic ring of the acid and the polar building blocks, thus reducing its effectiveness as a catalyst while possibly introducing crystalline regions in the matrix. Another possible explanation could be an interaction with the secondary amines of the **PBA-PPG-PBA** linker. PTSA could protonate the secondary amines of this linker, resulting in the formation of charged nitrogen species similar to polyelectrolyte complexes, which often become stiff and brittle upon drying.[57,58] This unexpected acid response in the material relaxation shows that, although the characteristics of this boronate-TAAD network can be tuned through acid addition, predicting the resulting material behaviour might prove complex. Fortunately, since the control material was already quite dynamic even at neutral pH there was little need for additional acid

catalysis. More generally, it also serves as a reminder that translating molecular processes (*i.e.*, acid-catalysed transesterification) to the macroscopic material level, is not always straightforwardly possible, as other macroscopic phenomena, such as crystallisation, can affect the process.

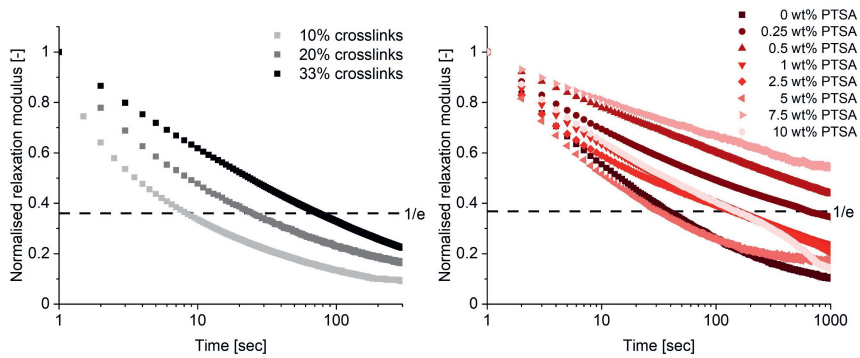

Figure 3.3: *Relaxation curves (at 0.1% strain, 25 °C) of materials with varying crosslink densities (left) and the effect of acid addition (at 0.1% strain, 25 °C) on the material properties (right).*

Another interesting observation could be seen in the temperature sweeps of these materials, where higher PTSA weight percentages resulted in the material melting at high temperatures, as shown by the loss factor steeply increasing (**Supplementary Figure S64**). This was not observed for the control material without PTSA.
The self-healing behaviour and recyclability of the material, as might be enabled by the dynamic bond exchange within the network, was also investigated using extensional DMA. The strain at which material breakage occurred was measured by linearly increasing the extensional stress of a CAN with 10% crosslinker. After breakage the material was cut in fine pieces and hot-pressed for 1 hour at 80 °C to allow the material to heal. As can be seen in **Figure 3.4**, the material is able to completely heal after multiple reprocessing cycles. The strengthening of the last few healing cycles seems to suggest that the network configuration is optimised during the applied thermal treatment.

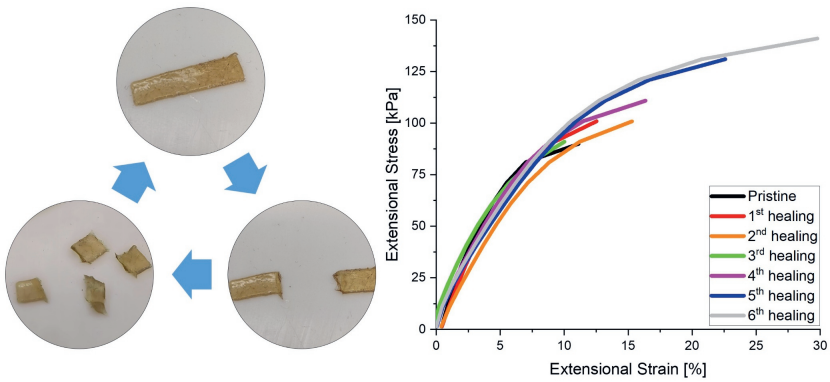

Figure 3.4: *Healing cycles performed by extensional DMA testing. Reprocessing was done by hot-pressing for 1 hour at 80 °C in a Teflon mould (10 × 5 × 1 mm). DMA was performed by linearly increasing the extensional stress till material breakage. After breakage the sample was cut into small pieces before reprocessing.*

3.4 Conclusion

In this study we synthesised and prepared a novel covalent adaptable network incorporating dynamic boronate-TAAD linkages using a small molecule network approach, resulting in a soft, rubber-like material. The material was thermally stable up to 150 °C as determined by TGA, thus allowing for hot-press moulding. In contrast to the behaviour of previously reported small-molecule boronate-TAAD complexes that could only undergo (fast) exchange under acidic conditions (pH 3.8), the corresponding CANs could already undergo (stress) relaxation under neutral conditions. Surprisingly, the addition of acid did not have a further accelerating effect on the exchange. The boronate-TAAD material showed complete self-healing after multiple thermal reprocessing cycles, and Arrhenius analysis gave a relatively high activation energy of 142 ± 10 kJ mol^{-1} for the crosslink relaxation process compared with regular boronic esters.
This first investigation into boronate-TAAD networks showed that the novel boronate-TAAD linkages can indeed be used to develop CANs. Coupled to the relatively simple synthesis of the TAAD moiety, this unique boronate-TAAD linkage offers an interesting alternative to the more commonly used boronic esters.

3.5 Supplementary information

The supplementary information is available at:
www.frontiersin.org/articles/10.3389/fchem.2023.1148629

References

[1] S. J. Rowan, S. J. Cantrill, G. R. Cousins, J. K. Sanders, J. F. Stoddart, *Angew. Chem. Int. Ed.* **2002**, *41*, 898–952, DOI 10.1002/1521-3773(20020315)41:6<898::AID-ANIE898>3.0.CO;2-E.

[2] N. Zheng, Y. Xu, Q. Zhao, T. Xie, *Chem. Rev.* **2021**, *121*, 1716–1745, DOI 10.1021/acs.chemrev.0c00938.

[3] C. Bowman, F. Du Prez, J. Kalow, *Polym. Chem.* **2020**, *11*, 5295–5296, DOI 10.1039/d0py90102d.

[4] J. M. Winne, L. Leibler, F. E. Du Prez, *Polym. Chem.* **2019**, *10*, 6091–6108, DOI 10.1039/c9py01260e.

[5] C. J. Kloxin, C. N. Bowman, *Chem. Soc. Rev.* **2013**, *42*, 7161–73, DOI 10.1039/c3cs60046g.

[6] S. Hamieh, V. Saggiomo, P. Nowak, E. Mattia, R. F. Ludlow, S. Otto, *Angew. Chem. Int. Ed.* **2013**, *52*, 12368–72, DOI 10.1002/anie.201305744.

[7] M. Mondal, A. K. Hirsch, *Chem. Soc. Rev.* **2015**, *44*, 2455–88, DOI 10.1039/c4cs00493k.

[8] M. Mastalerz, *Angew. Chem. Int. Ed.* **2010**, *49*, 5042–53, DOI 10.1002/anie.201000443.

[9] J. Hu, S. K. Gupta, J. Ozdemir, M. H. Beyzavi, *ACS Appl. Nano Mater.* **2020**, *3*, 6239–6269, DOI 10.1021/acsanm.0c01327.

[10] C. J. Kloxin, T. F. Scott, B. J. Adzima, C. N. Bowman, *Macromolecules* **2010**, *43*, 2643–2653, DOI 10.1021/ma902596s.

[11] L. Yang, X. Tan, Z. Wang, X. Zhang, *Chem. Rev.* **2015**, *115*, 7196–239, DOI 10.1021/cr500633b.

[12] M. Hayashi, *Polymers* **2020**, *12*, 1322, DOI 10.3390/polym12061322.

[13] D. A. Kissounko, P. Taynton, C. Kaffer, *Reinf. Plast.* **2018**, *62*, 162–166, DOI 10.1016/j.repl.2017.06.084.

[14] Z. P. Zhang, M. Z. Rong, M. Q. Zhang, *Prog. Polym. Sci.* **2018**, *80*, 39–93, DOI 10.1016/j.progpolymsci.2018.03.002.

[15] B. Briou, B. Ameduri, B. Boutevin, *Chem. Soc. Rev.* **2021**, *50*, 11055–11097, DOI 10.1039/d0cs01382j.

[16] V. Gaina, M. Nechifor, C. Gaina, O. Ursache, *Polym.-Plast. Tech. Mat.* **2021**, *60*, 253–270, DOI 10.1080/25740881.2020.1811315.

[17] P. Taynton, K. Yu, R. K. Shoemaker, Y. Jin, H. J. Qi, W. Zhang, *Adv. Mat.* **2014**, *26*, 3938–3942, DOI 10.1002/adma.201400317.

[18] S. K. Schoustra, J. A. Dijksman, H. Zuilhof, M. M. J. Smulders, *Chem. Sci.* **2020**, *12*, 293–302, DOI 10.1039/d0sc05458e.

[19] T. Liu, B. M. Zhao, J. W. Zhang, *Polymer* **2020**, *194*, 122392, DOI 10.1016/j.polymer.2020.122392.

[20] D. Montarnal, M. Capelot, F. Tournilhac, L. Leibler, *Science* **2011**, *334*, 965–8, DOI 10.1126/science.1212648.

[21] W. Denissen, G. Rivero, R. Nicolay, L. Leibler, J. M. Winne, F. E. Du Prez, *Adv. Funct. Mater.* **2015**, *25*, 2451–2457, DOI 10.1002/adfm.201404553.

[22] M. Gosecki, M. Gosecka, *Polymers* **2022**, *14*, 842, DOI 10.3390/polym14040842.

[23] A. P. Bapat, B. S. Sumerlin, A. Sutti, *Mater. Horiz.* **2020**, *7*, 694–714, DOI 10.1039/c9mh01223k.

[24] W. Yang, X. Gao, B. Wang, *Biological and medicinal applications of boronic acids*, John Wiley & Sons, Ltd, **2005**, p. 481, DOI 10.1002/3527606548.ch13.

[25] J. N. Cambre, B. S. Sumerlin, *Polymer* **2011**, *52*, 4631–4643, DOI 10.1016/j.polymer.2011.07.057.

[26] L. Banach, G. T. Williams, J. S. Fossey, *Adv. Ther.* **2021**, *4*, 2100118, DOI 10.1002/adtp.202100118.

[27] L. He, D. E. Fullenkamp, J. G. Rivera, P. B. Messersmith, *Chem. Commun.* **2011**, *47*, 7497–9, DOI 10.1039/c1cc11928a.

[28] H. Geethanjali, R. Melavanki, N. D., B. P., R. Kusanur, *J. Mol. Liq.* **2017**, *227*, 37–43, DOI 10.1016/j.molliq.2016.11.097.

[29] B. Cai, Y. Luo, Q. Guo, X. Zhang, Z. Wu, *Carbohydr. Res.* **2017**, *445*, 32–39, DOI 10.1016/j.carres.2017.04.006.

[30] J. Plescia, N. Moitessier, *Eur. J. Med. Chem.* **2020**, *195*, 112270, DOI 10.1016/j.ejmech.2020.112270.

[31] V. Yesilyurt, M. J. Webber, E. A. Appel, C. Godwin, R. Langer, D. G. Anderson, *Adv. Mater.* **2016**, *28*, 86–91, DOI 10.1002/adma.201502902.

[32] A. J. R. Amaral, V. M. Gaspar, J. F. Mano, *Polym. J.* **2020**, *52*, 997–1006, DOI 10.1038/s41428-020-0348-3.

[33] B. Marco-Dufort, M. W. Tibbitt, *Mater. Today Chem.* **2019**, *12*, 16–33, DOI 10.1016/j.mtchem.2018.12.001.

[34] L. Li, Z. Bai, P. A. Levkin, *Biomaterials* **2013**, *34*, 8504–10, DOI 10.1016/j.biomaterials.2013.07.053.

[35] A. Zych, J. Tellers, L. Bertolacci, L. Ceseracciu, L. Marini, G. Mancini, A. Athanassiou, *Acs Appl. Polym. Mater.* **2021**, *3*, 1135–1144, DOI 10.1021/acsapm.0c01335.

[36] Z. Zhao, X. Yao, Z. Zhang, L. Chen, C. He, X. Chen, *Macromol. Biosci.* **2014**, *14*, 1609–18, DOI 10.1002/mabi.201400251.

[37] X. Zhang, J. S. Gao, X. Y. Zhao, Z. T. Liu, Z. W. Liu, K. Wang, G. Li, J. Q. Jiang, *Chin. Chem. Lett.* **2020**, *31*, 1822–1826, DOI 10.1016/j.cclet.2020.03.018.

[38] H. Takata, K. Ono, N. Iwasawa, *Chem. Commun.* **2020**, *56*, 5613–5616, DOI 10.1039/d0cc01441a.

[39] E. Giraldi, R. Scopelliti, F. Fadaei-Tirani, K. Severin, *Inorg. Chem.* **2021**, *60*, 10873–10879, DOI 10.1021/acs.inorgchem.1c01719.

[40] V. Drogkaris, B. H. Northrop, *Org. Chem. Front.* **2020**, *7*, 1082–1094, DOI 10.1039/d0qo00083c.

[41] M. M. Perera, N. Ayres, *Polym. Chem.* **2020**, *11*, 1410–1423, DOI 10.1039/c9py01694e.

[42] W. Wang, R. Narain, H. Zeng, *Front. Chem.* **2018**, *6*, 497, DOI 10.3389/fchem.2018.00497.

[43] H. S. Yang, S. Cho, Y. Eom, S. A. Park, S. Y. Hwang, H. Jeon, D. X. Oh, J. Park, *Macromol. Res.* **2021**, *29*, 140–148, DOI 10.1007/s13233-021-9016-5.

[44] M. C. Roberts, M. C. Hanson, A. P. Massey, E. A. Karren, P. F. Kiser, *Adv. Mater.* **2007**, *19*, 2503–2507, DOI 10.1002/adma.200602649.

[45] A. N. Semakin, A. Y. Sukhorukov, A. V. Lesiv, S. L. Ioffe, K. A. Lyssenko, Y. V. Nelyubina, V. A. Tartakovsky, *Org. Lett.* **2009**, *11*, 4072–5, DOI 10.1021/ol9015157.

[46] I. S. Golovanov, G. S. Mazeina, Y. V. Nelyubina, R. A. Novikov, A. S. Mazur, S. N. Britvin, V. A. Tartakovsky, S. L. Ioffe, A. Y. Sukhorukov, *J. Org. Chem.* **2018**, *83*, 9756–9773, DOI 10.1021/acs.joc.8b01296.

[47] I. S. Golovanov, A. Y. Sukhorukov, Y. V. Nelyubina, Y. A. Khomutova, S. L. Ioffe, V. A. Tartakovsky, *J. Org. Chem.* **2015**, *80*, 6728–36, DOI 10.1021/acs.joc.5b00892.

[48] C. Y. Bao, Y. J. Jiang, H. Y. Zhang, X. Y. Lu, J. Q. Sun, *Adv. Funct. Mater.* **2018**, *28*, 1800560, DOI 10.1002/adfm.201800560.

[49] B. Kang, J. Kalow, *ACS macro lett.* **2022**, *11*, 394–401, DOI 10.1021/acsmacrolett.2c00056.

[50] M. Röttger, T. Domenech, R. van der Weegen, A. Breuillac, R. Nicolaÿ, L. Leibler, *Science* **2017**, *356*, 62–65, DOI 10.1126/science.aah5281.

[51] O. R. Cromwell, J. Chung, Z. Guan, *J. Am. Chem. Soc.* **2015**, *137*, 6492–5, DOI 10.1021/jacs.5b03551.

[52] X. Zhang, S. Wang, Z. Jiang, Y. Li, X. Jing, *J. Am. Chem. Soc.* **2020**, *142*, 21852–21860, DOI 10.1021/jacs.0c10244.

[53] R. Hajj, A. Duval, S. Dhers, L. Averous, *Macromolecules* **2020**, *53*, 3796–3805, DOI 10.1021/acs.macromol.0c00453.

[54] Y. Spiesschaert, C. Taplan, L. Stricker, M. Guerre, J. M. Winne, F. E. Du Prez, *Polym. Chem.* **2020**, *11*, 5377–5385, DOI 10.1039/d0py00114g.

[55] J. L. Self, N. D. Dolinski, M. S. Zayas, J. Read de Alaniz, C. M. Bates, *ACS Macro Lett.* **2018**, *7*, 817–821, DOI 10.1021/acsmacrolett.8b00370.

[56] W. Denissen, M. Droesbeke, R. Nicolay, L. Leibler, J. M. Winne, F. E. Du Prez, *Nat. Commun.* **2017**, *8*, 14857, DOI 10.1038/ncomms14857.

[57] H. M. Fares, Q. F. Wang, M. Yang, J. B. Schlenoff, *Macromolecules* **2019**, *52*, 610–619, DOI 10.1021/acs.macromol.8b01838.

[58] A. Krishna B, J. D. Willott, S. Lindhoud, W. M. de Vos, *Polymer* **2022**, *242*, 124583, DOI 10.1016/j.polymer.2022.124583.

Chapter 4

Tuning Material Properties of Covalent Adaptable Networks Containing Boronate-Tetraazaadamantane Bonds Through Systematic Variation in Electron Density of Ring Substituents

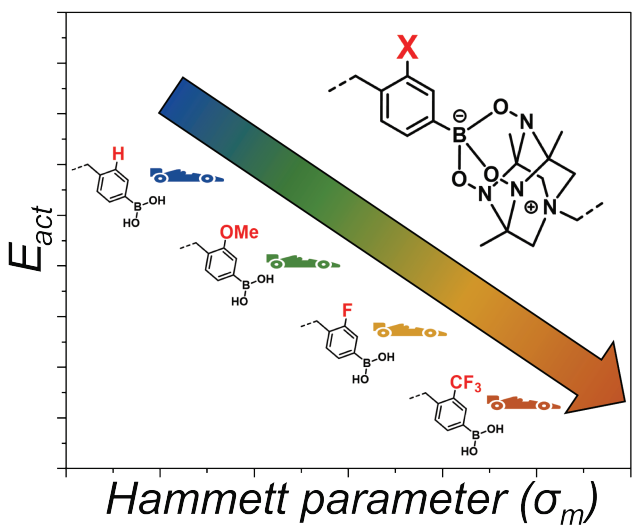

Simon van Hurne, Thomas J. M. Buijssen, Maarten M. J. Smulders
This work was published as:
S. van Hurne, T. J. M. Buijsen, and M. M. J. Smulders, *Journal of Polymer Science*, **2023**, 1. https://doi.org/10.1002/pol.20230446

4.1 Abstract

An outstanding challenge in modern society remains how to make crosslinked polymers (thermosets) more recyclable. A breakthrough solution to this challenge has been the introduction of dynamic covalent bonds in polymer networks, yielding covalent adaptable networks (CANs). Ongoing research is focused on finding new suitable dynamic covalent chemistries and on how to tune the material properties of CANs derived from these new chemistries. Here, we first compare two different dynamic boronic acid based covalent adaptable networks, namely a conventional boronate-diol and a novel boronate-Tetraazaadamantane system, which we presented in chapter 3. We show that incorporating boronate-Tetraazaadamantane bonds in networks results in stiffer materials, as seen in a slower relaxation and higher shear and storage moduli. This offers access to more mechanically robust boronate-based materials, compared to conventional boronate-based gels. Next, we investigate the effect of molecular tuning via the electron density of *meta*-positioned ring substituents on the macroscopic material properties for the boronate-Tetraazaadamantane network. By comparing relaxation experiments on materials with different substituents, we show that the macroscopic network relaxation can be tuned through the Hammett parameter of the meta-substituent and the activation energy of the boronate-Tetraazaadamantane exchange. This enables subtle control over the (dynamic) material properties of these novel, robust boronate-based networks.

4.2 Introduction

Polymer waste is becoming an increasingly larger problem in modern society.[1,2] Part of the solution lies in improving polymer waste stream management. However, not all polymers can currently be recycled. Those polymers are currently mainly disposed of in landfills or by incineration.[3–5] These non-recyclable polymers largely consist of thermosets. Thermosets, with their permanent covalent crosslinks, are polymers with excellent material properties. However, the same permanent crosslinks that give thermosets their excellent material properties also hinder their recyclability. A solution to this problem is to design recyclable thermoset-like materials by replacing the permanent crosslinks with dynamic covalent crosslinks, leading to materials

that have been called covalent adaptable networks (CANs).[6–8] Their crosslinks can be based on a variety of dynamic covalent bonds such as esters,[9,10] imines,[11,12] diketoenamines,[13,14] disulfides,[15,16] vinylogous urethanes,[17,18] acylsemicarbazides[19,20] and boronic esters.[21–24] Because these covalent bonds are dynamic, they can exchange when exposed to the appropriate stimulus, thus allowing polymer networks built using dynamic covalent bonds to be reprocessed, recycled or to display self-healing behaviour.[25–27] Here, we will focus on materials containing boronic esters because of their general biocompatibility[28–31] and their fast exchange reactions.[32,33]

In order for boronic ester-based CANs to become a more competitive option compared to conventional thermosets, more research is needed into the performance and tunability of these dynamic materials. While major advances have been realised in successfully integrating dynamic covalent bonds into polymer networks, these thus newly prepared covalent adaptable networks should have the correct material properties (*e.g.,* in terms of mechanical strength, creep-performance, solvent resistance, and/or (re-)processability) for them to become true substitutes for conventional thermosets (that currently lack the ability be reprocessed or recycled). Having a versatile toolbox with (molecular) handles to fine-tune the macroscopic material properties from the molecular level upwards would help design (boronic ester-based) CANs for specific applications. In recent years, the molecular tuning of CANs has proven to be a powerful strategy.[34–36] Many different (molecular) handles have been found that can used to control the macroscopic properties of boronic ester-containing materials, such as linker length,[37] internal catalysis,[38–41] crosslinking degree,[42] dual crosslinking[43,44] or the steric hindrance of reactive groups.[45]

Despite the great potential of fine-grained control as a result of a large range of possible substituents, the potential of molecular tuning in CANs by installing electron donating or withdrawing ring substituents, which can be quantified via the Hammett equation,[46–49] has received an increasing amount of attention. There have been studies into the electronic effect on the material properties for only a few CANs, specifically for imine,[50] thia-Micheal reactions,[51] thiol-yne[52] and thiol-ene.[53] For boronic esters structure-property relationship studies remain limited to small-scale molecule studies for structure variation in the boronic acid[54–57] and the structure of the diol,[58,59] or focus only on two different boronic acids, where the focus is generally not specifically on electronic effects.[60]

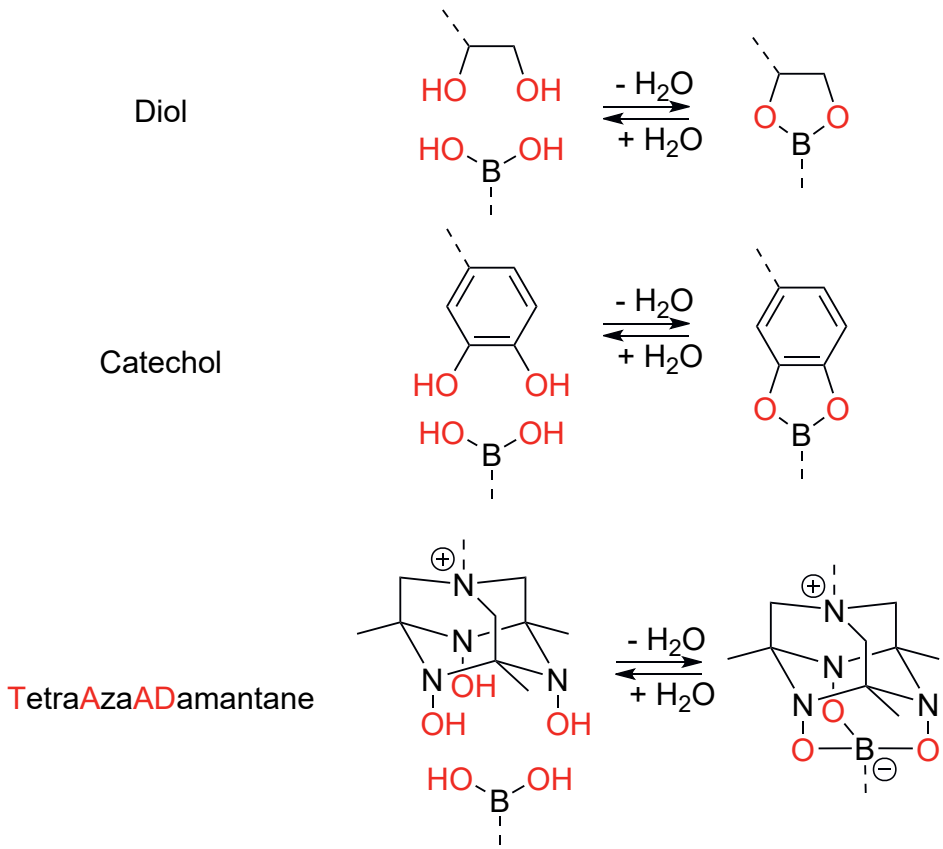

Scheme 4.1: *Formation of boronic esters using different diols or triols.*

Previously, Golovanov and Semankin *et al.* reported a new boronate-based dynamic covalent moiety, based on TetraAzaADamantane (TAAD), which is an adamantane containing four nitrogen atoms, three in the bottom ring and one on the top.[61–63] The three lower nitrogen atoms also have a hydroxyl group, thus making the TAAD a triol. The top nitrogen can be used to anchor the TAAD to a scaffold via nitrogen quaternisation as can be seen in **Scheme 4.1**. The TAAD moiety was shown to have strong binding to boronic acids, yet still retain a dynamic pH-sensitive equilibrium.[61] The strong, yet dynamic, binding of the TAAD moiety to boronic acids made it an interesting candidate for covalent adaptable network formation, which we showed to be possible in chapter 3.[64] The newly emerging boronate-TAAD networks gave rubbery materials, as opposed to the (hydro)gels that are generally obtained when working with boronic esters.

While we previously showed the promising use of TAAD moieties in CANs in chapter 3, no direct and systematic comparison between the novel boronate-TAAD system and its traditional boronate-diol counterpart was included in this study. For the comparison between the boronate-TAAD and boronate-diol networks two diol linkers, named **BDPE** and **TMPTPE**, and two TAAD linkers, named **bis-TAAD** and **tris-TAAD**, were prepared and crosslinked with a difunctional boronic acid PPG-based linker named **PPG-PBA-H** (**Figure 4.1**).

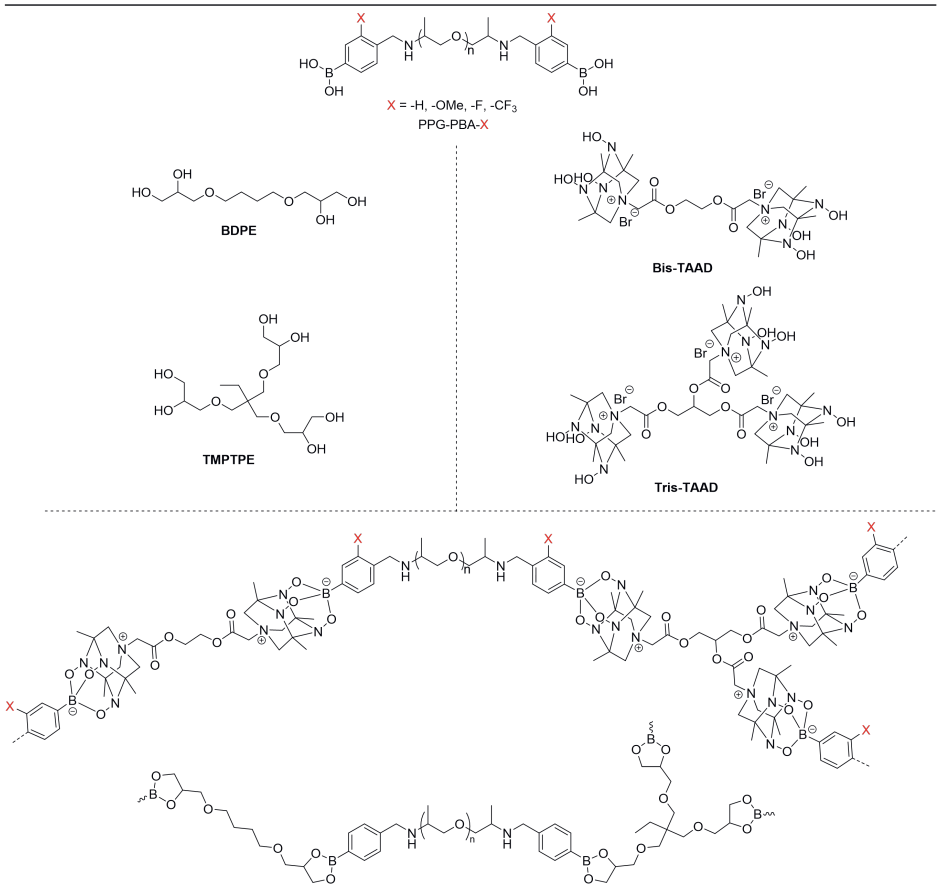

Figure 4.1: *The structure of the variable boronic acid linker* ***PPG-PBA-X****, the two diol linkers* ***BDPE*** *and* ***TMPTPE*** *(left) and the two TetraAzaADamantane (TAAD) linkers (right). The network structures for both the boronate-diol and boronate-TAAD is given below.*

In addition, we also investigated the possibility of using molecular tuning in boronate-TAAD networks through systematic variation in the electronic properties of substituents on the phenylboronic acid and studying its effect on the material properties of these CANs. To study this, variations of boronic linkers with differently *meta*-substituted phenylboronic acids were prepared and crosslinked. The resulting materials were then characterised using rheology, revealing a relation between their dynamic-mechanical properties (notably, the stress relaxation behaviour) and the nature of the substituent (as expressed by its Hammett parameter).

4.3 Results and Discussion

The diol linkers were prepared via epoxy ring opening from the corresponding epoxides. The boronic acid linker was prepared by reacting 4-formylphenylboronic acid with an amine-terminated PPG-2000 and subsequent reduction of the formed imine. The TAAD linkers were prepared as described as shown in **Scheme 3.1**.[64] Details on the synthesis and material preparation are given in the online **Supplementary Information** for which a link can be found at the end of the chapter.

Samples of both the boronate-diol and boronate-TAAD networks were prepared by making stock solutions of the different linkers in methanol, mixing them by vortexing and casting them in circular silicon molds (10 mm diameter, 1 mm height). Boronic acids and diol/TAAD were added stoichiometrically and 10 mol% crosslinker was added in all cases. An immediate observation made while casting both the boronate-diol and the boronate-TAAD materials in methanol was that network formation in the boronate-diol materials was hindered through the strong uptake of atmospheric water, thus resulting in the formation of a soft gel instead of a proper elastomer. In contrast, the boronate-TAAD networks were hardly impacted by the uptake of atmospheric water and were able to form bench-stable elastomers. However, since water also affects the network properties this would result in an unfair comparison of the two systems. For this reason, all samples were prepared under nitrogen atmosphere to prevent the uptake of water and allow for a proper comparison of the two systems.

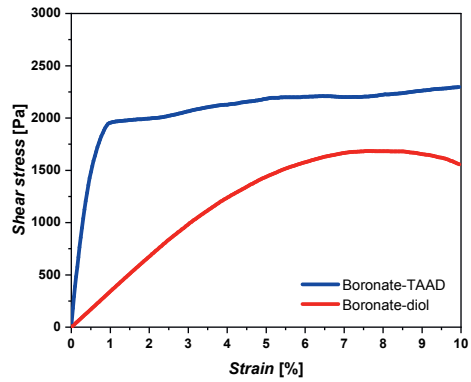

Figure 4.2: *Shear stress as function of applied strain for a boronate-diol and a boronate-TAAD 10% crosslinked network at 25 °C. The shear modulus of the boronate-diol network was 0.3 kPa; the shear modulus of the boronate-TAAD network was 3.5 kPa.*

First the shear stress over strain behaviour of the two networks was compared. In **Figure 4.2** it can be seen that the boronate-diol network shows a more gradual increase of shear stress compared to the relatively sharp increase of the boronate-TAAD network resulting in a significantly higher shear modulus for the boronate-TAAD networks (0.3 kPa for the boronate-diol networks; 3.5 kPa for the boronate-TAAD networks). Second, the obtained yield plateau is slightly higher for the boronate-TAAD network.

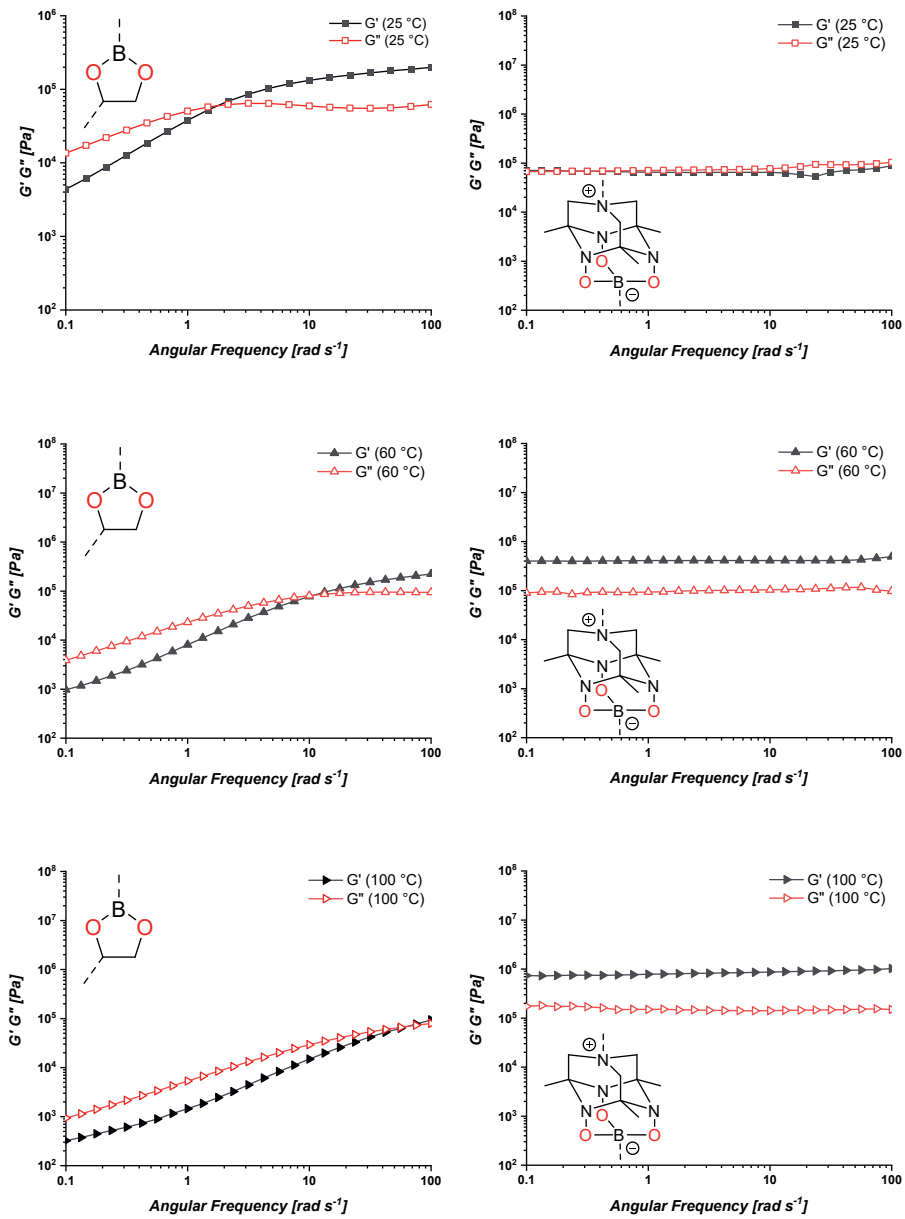

Figure 4.3: *Frequency sweeps at different temperatures of a 10% crosslinked boronate-diol network (left) and a 10% crosslinked boronate-TAAD network (right).*

Also, frequency sweeps were performed to gain further insight into the network properties. In **Figure 4.3** frequency sweeps for both networks are shown. The first observation was that the moduli of the boronate-TAAD network were higher than the moduli of the boronate-diol network, suggesting the formation of a stronger network. Secondly, the moduli of the boronate-TAAD network remained largely constant over the applied frequency range, in contrast to the boronate-diol network, which shifted over an order of magnitude. Thirdly, the boronate-diol network showed cross over points for the storage modulus (*G'*) and the loss modulus (*G"*) indicating a transition of a more solid-like material to a more viscous-like material. This cross over point also shifted to higher frequencies at higher temperatures. No cross over points were observed for the boronate-TAAD network. In all, these measurements confirm –in a quantitative manner– the increased mechanical stability that can be achieved by replacing the traditional boronate-diol crosslinks with the boronate-TAAD crosslinks within the covalent adaptable network structure.

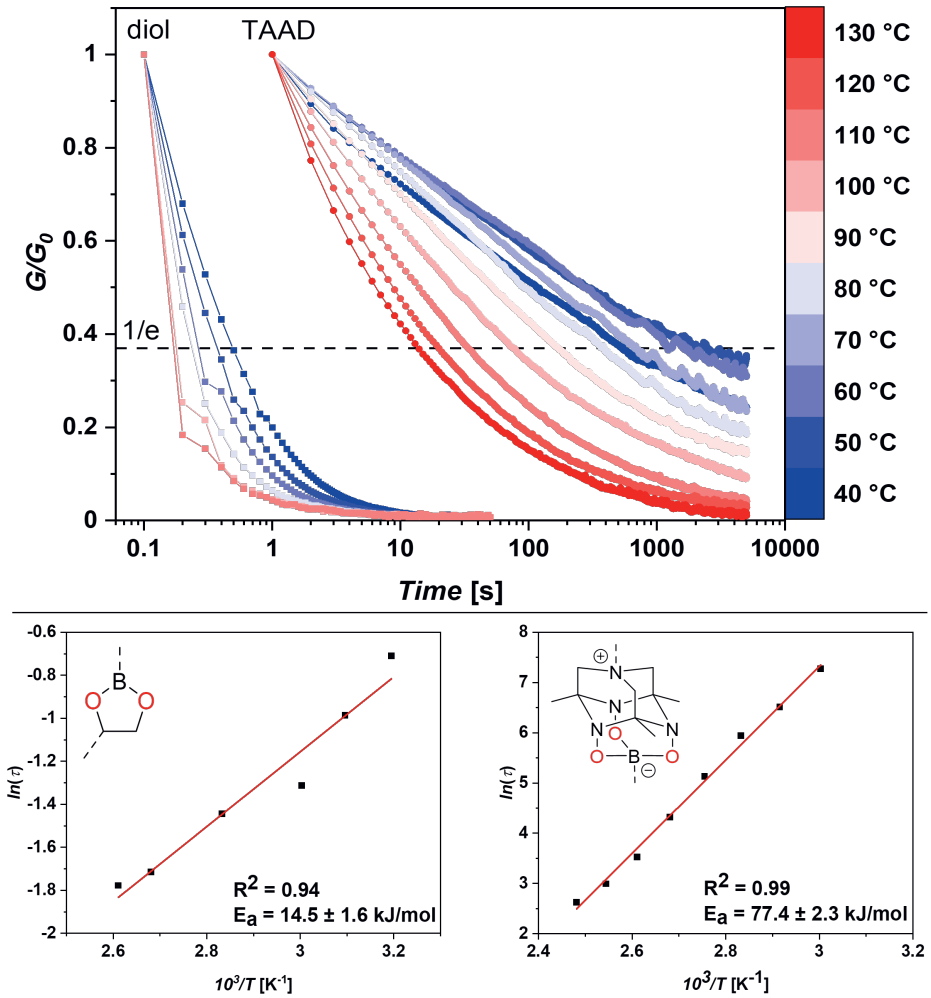

Figure 4.4: *Comparison of relaxation behaviour (0.5% strain) at different temperatures between dynamic 10% crosslinked boronic diol networks and 10% crosslinked boronate-TAAD networks (top) with their respective Arrhenius plot and activation energy (bottom).*

The stress relaxation of the two networks was also vastly different as can be seen in **Figure 4.4**. Boronate-diol networks, when subjected to a 0.5% strain, showed complete relaxation in approximately 10 seconds at room temperature. In stark contrast to this, for boronate-TAAD networks complete relaxation, at equal strain, was only reached around 20 minutes at 130 °C. In these relaxation experiments all materials showed a temperature dependency on their relaxation behaviour. By assuming a Maxwell model for the stress relaxation, we could obtain the relaxation time (τ) of the material at the time point at which the normalised relaxation curve crosses $^1/_e$ ($\approx$ 0.37). By plotting the relaxation times against the inverse of the temperature, Arrhenius plots can be constructed for the different two materials. From the slope of these Arrhenius plots we can then calculate the activation energy (E_a) of the dynamic exchange, with the help of the gas constant (R). This gave an activation energy of 14.5 ± 1.6 kJ mol^{-1} for the boronate-diol network, which is in accordance with existing literature,[24,32,39,41] versus an activation energy of 77.3 ± 2.3 kJ mol^{-1} for the boronate-TAAD network. The higher activation energy of the boronate-TAAD exchange compared to the boronate-diol network reduces the dynamicity of the network and thus results in sturdier materials, while still keeping the network dynamic enough to relax stress over time.

Finally, the networks were also compared in terms of temperature stability by subjecting the samples to TGA measurements. **Supplementary Figures S79** and **S80** show that both the boronate-TAAD and the boronate-diol network are stable till 150 °C as displayed by the $T_{95\%}$ of 170 °C and 330 °C, respectively. Though the boronate-diol network does show higher thermal stability. we would like to stress that TGA only measures the weight at different temperatures and does not probe the network composition or properties at these temperatures. The comparison of material properties of the boronate-diol with the boronate-TAAD networks, revealed that the latter displayed superior mechanical properties (as seen in the stress-strain data, the frequency sweeps and the stress relaxation experiments). At the same time, the boronate-TAAD network is dynamic enough to undergo stress relaxation at a temperature far below its thermal stability limit. Also, the boronate-TAAD network was far less impacted by atmospheric water, thus making these networks easier to work with. For these reasons the boronate-TAAD networks were chosen for the molecular tunability experiments.

To study the effect of different ring substituents a series of PPG-PBA linkers was synthesised by replacing the 4-formylphenylboronic acid with a substituted derivative (see **Supplementary Information**). For this study only the meta position relative to the boronic acid was varied. This resulted in four PPG-PBA variants containing a –H, –OMe, –F or a $–CF_3$ as *meta*-substituent, giving networks as seen in **Figure 4.1**.

After preparing all the different 10% crosslinked variant networks it was observed that the colour of the different variants was different, ranging from yellow to brownish/red. Investigating the shearing behaviour of these different materials, no clear correlation between the observed shear moduli and the substituents (data shown in **Supplementary Figures S84–S88**) could be established. The shear moduli of the networks with –H, –OMe and –F substituent showed a trend of lower shear moduli with increasing electron withdrawing ring substituent, however materials made with **PPG-PBA-CF_3** showed shear moduli similar to networks with **PPG-PBA-H**. Of course, there could be other effects, such as sterics combined with the apparent size of the substituent,[65–69] influencing the shear moduli, but this will require further research.

Table 4.1: *Observed shear moduli for the different* ***PPG-PBA-X*** *networks*

PPG-PBA-X	*Shear Modulus* [kPa]
–H	3.5 ± 0.1
–OMe	3.1 ± 0.1
–F	2.3 ± 0.1
–CF_3	3.5 ± 0.2

From frequency sweeps, (**Supplementary Figures S89–S93**) it was found that all materials displayed a stable storage modulus in the range of 10^5–10^6 Pa with no crossover points.

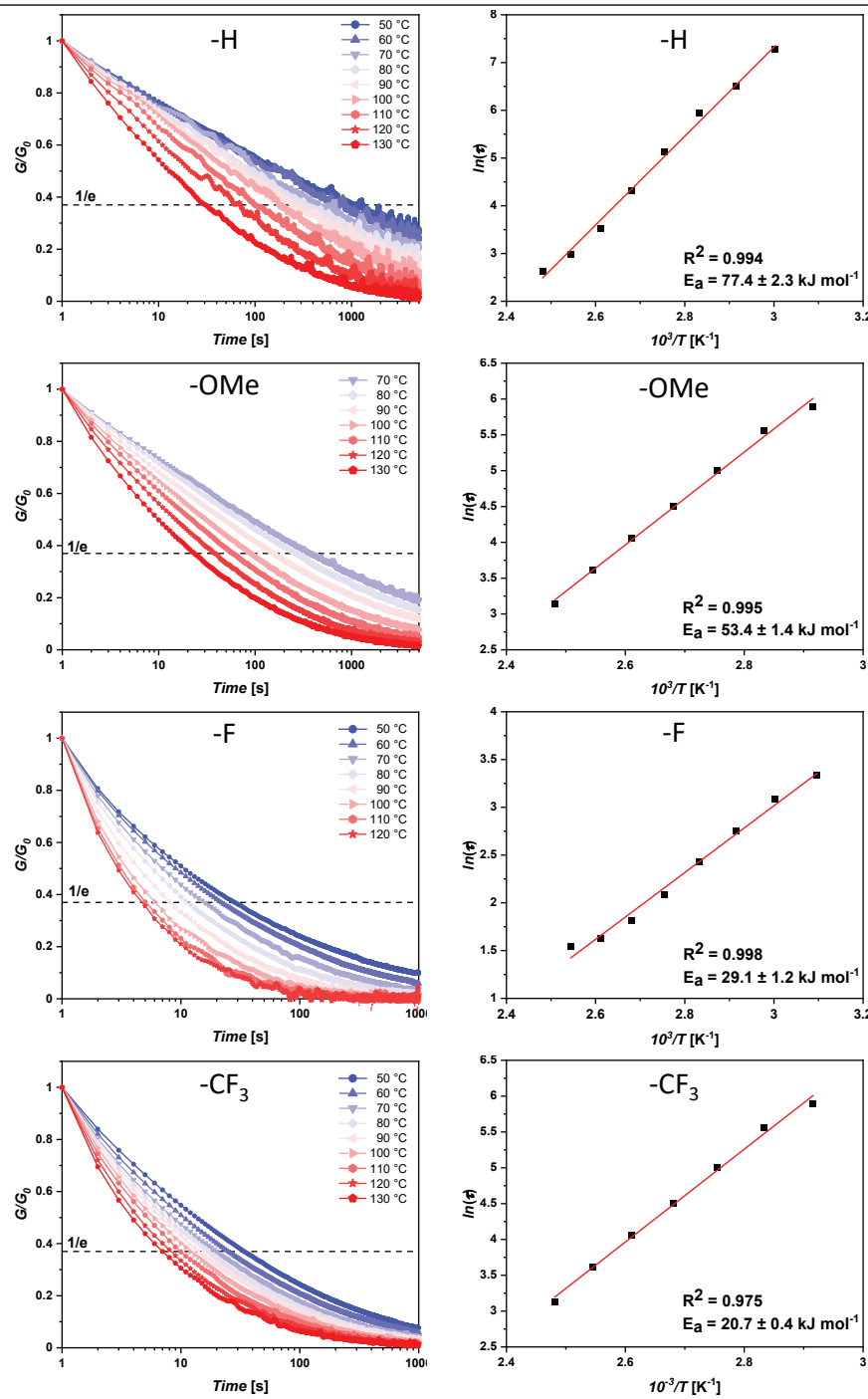

Figure 4.5: *Representative relaxation curves at varying temperatures (0.5% strain) for the networks made using different* ***PPG-PBA-X*** *linkers (10% crosslinking) and their resulting Arrhenius plot. Duplo measurements can be found in the* ***Supplementary Information*** *(**S94-S97**).*

Also, the relaxation behaviour at different temperatures for the **PPG-PBA-X** material series was investigated, as shown in **Figure 4.5** (duplo measurements are shown in **Supplementary Figures S94–S97**). Here, we see that the different materials all show a different temperature dependence on the relaxation time. When comparing the calculated activation energies for the different **PPG-PBA-X** materials, we can see significant differences in the obtained values. These activation energies range from 77.3 ± 4.3 kJ mol^{-1} for the **PPG-PBA-H** network to 20.6 ± 0.8 kJ mol^{-1} for the **PPG-PBA-CF$_3$** network. These activation energies can then be plotted against the Hammett constant (σ_m) of the ring substituent and fitted with a (weighted) linear fit, resulting in **Figure 4.6**. The linear fit shows a good correlation with the activation energies obtained from the network relaxation. This shows that the macroscopic relaxation of the network can be tuned by varying only a few atoms in the molecular structure of the building blocks through the electronic properties of the ring substituents. Considering that these two substituents are part of a large, polymeric building block (with molecular weight of ≈2500 g mol^{-1}), this Hammett-based effect seems rather pronounced, and is in contrast with earlier work[51,52] that introduced varying substituents on small-molecule, non-polymeric building blocks. Having a direct, and highly tuneable molecular handle to control the activation energy for exchange, will enable further control over the dynamic function (*e.g.,* self-healing, reprocessing and recycling) of covalent adaptable networks.

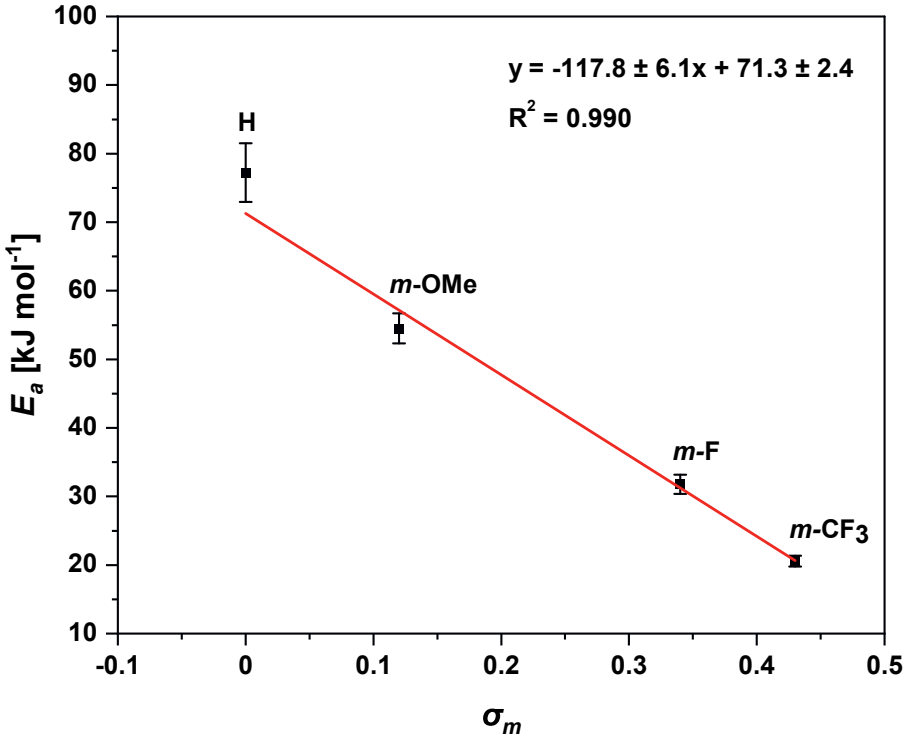

Figure 4.6: *Activation energy E_a for the dynamic boronate-TAAD exchange in the networks (10% crosslinked) using different* ***PPG-PBA-X*** *linkers against their substituent Hammett constant (σ_m). Obtained activation energies were fitted using a weighted linear fit.*

4.4 Conclusion

In this study we showed that dynamic boronic networks can show quite different material properties depending on the dynamic boronic linkage used. A systematic, quantitative comparison allowed us to conclude that the boronate-TAAD networks outperformed the classical boronate-diol networks, giving stronger materials as shown in frequency sweeps, shear experiments and temperature sweeps. From there, the tunability of the boronate-TAAD networks was investigated, where we found that (*meta*-positioned) ring substituents on the boronic acid can be used to tune the macroscopic material relaxation through the electronic substituents by changing the activation energy of the bond exchange. The activation energy of the bond exchange could be changed over almost a full order of magnitude. Also, the shear modulus of the different variants seems to

show a trend with decreasing shear modulus for increasing electron withdrawing character of the ring substituent, but further research on other contributing factors is necessary. We foresee that our tunable TAAD-based dynamic bonds can be extended to other polymer networks to help design new covalent adaptable networks that combine robustness with tuneability. Further control over mechanical performance can be obtained by studying the effect of the soft segments within the network; *e.g.,* by replacing PPG by another polymer.

4.5 Supplementary information

The supplementary information is available at:
https://onlinelibrary.wiley.com/doi/10.1002/pol.20230446

References

[1] A. Rahimi, J. M. Garcia, *Nat. Rev. Chem.* **2017**, *1*, 0046, DOI 10.1038/s41570-017-0046.

[2] M. R. Johansen, T. B. Christensen, T. M. Ramos, K. Syberg, *J. Environ. Manage.* **2022**, *302*, 113975, DOI 10.1016/j.jenvman.2021.113975.

[3] J. P. Lange, *ACS Sustain. Chem. Eng.* **2021**, *9*, 15722–15738, DOI 10.1021/acssuschemeng.1c05013.

[4] L. Imbernon, S. Norvez, *Eur. Polym. J.* **2016**, *82*, 347–376, DOI 10.1016/j.eurpolymj.2016.03.016.

[5] S. M. Al-Salem, P. Lettieri, J. Baeyens, *Waste Manag.* **2009**, *29*, 2625–43, DOI 10.1016/j.wasman.2009.06.004.

[6] W. Post, A. Susa, R. Blaauw, K. Molenveld, R. J. I. Knoop, *Polym. Rev.* **2020**, *60*, 359–388, DOI 10.1080/15583724.2019.1673406.

[7] G. M. Scheutz, J. J. Lessard, M. B. Sims, B. S. Sumerlin, *J. Am. Chem. Soc.* **2019**, *141*, 16181–16196, DOI 10.1021/jacs.9b07922.

[8] Y. H. Jin, Z. P. Lei, P. Taynton, S. F. Huang, W. Zhang, *Matter* **2019**, *1*, 1456–1493, DOI 10.1016/j.matt.2019.09.004.

[9] F. Fu, M. Huang, W. Zhang, Y. Zhao, X. Liu, *Sci. Rep.* **2018**, *8*, 10325, DOI 10.1038/s41598-018-27942-9.

[10] Z. Pei, Y. Yang, Q. Chen, E. M. Terentjev, Y. Wei, Y. Ji, *Nat. Mater.* **2014**, *13*, 36–41, DOI 10.1038/nmat3812.

[11] S. K. Schoustra, T. Groeneveld, M. M. J. Smulders, *Polym. Chem.* **2021**, *12*, 1635–1642, DOI 10.1039/d0py01555e.

[12] J. J. Lessard, G. M. Scheutz, R. W. Hughes, B. S. Sumerlin, *ACS Appl. Polym. Mater.* **2020**, *2*, 3044–3048, DOI 10.1021/acsapm.0c00523.

[13] L. D. Dugas, W. D. Walker, R. Shankar, K. S. Hoppmeyer, T. L. Thornell, S. E. Morgan, R. F. Storey, D. L. Patton, Y. C. Simon, *Macromol. Rapid Commun.* **2022**, *43*, 2200249, DOI 10.1002/marc.202200249.

[14] P. R. Christensen, A. M. Scheuermann, K. E. Loeffler, B. A. Helms, *Nat. Chem.* **2019**, *11*, 442–448, DOI 10.1038/s41557-019-0249-2.

[15] W. B. Kong, Y. Y. Yang, A. Q. Yuan, L. Jiang, X. W. Fu, Y. C. Wang, H. L. Xu, Z. M. Liu, J. X. Lei, *Energy* **2021**, *232*, 121070, DOI 10.1016/j.energy.2021.121070.

[16] L. Imbernon, E. K. Oikonomou, S. Norvez, L. Leibler, *Polym. Chem.* **2015**, *6*, 4271–4278, DOI 10.1039/c5py00459d.

[17] J. J. Lessard, L. F. Garcia, C. P. Easterling, M. B. Sims, K. C. Bentz, S. Arencibia, D. A. Savin, B. S. Sumerlin, *Macromolecules* **2019**, *52*, 2105–2111, DOI 10.1021/acs.macromol.8b02477.

[18] W. Denissen, M. Droesbeke, R. Nicolay, L. Leibler, J. M. Winne, F. E. Du Prez, *Nat. Commun.* **2017**, *8*, 14857, DOI 10.1038/ncomms14857.

[19] D. Fu, W. Pu, J. Escorihuela, X. Wang, Z. Wang, S. Chen, S. Sun, S. Wang, H. Zuilhof, H. Xia, *Macromolecules* **2020**, *53*, 7914–7924, DOI 10.1021/acs.macromol.0c01667.

[20] S. Wang, D. Fu, X. Wang, W. Pu, A. Martone, X. Lu, M. Lavorgna, Z. Wang, E. Amendola, H. Xia, *J. Mater. Chem. A* **2021**, *9*, 4055–4065, DOI 10.1039/D0TA11251H.

[21] P. Commins, M. B. Al-Handawi, D. P. Karothu, G. Raj, P. Naumov, *Chem. Sci.* **2020**, *11*, 2606–2613, DOI 10.1039/c9sc05640h.

[22] C. K. Chu, A. J. Joseph, M. D. Limjoco, J. Yang, S. Bose, L. S. Thapa, R. Langer, D. G. Anderson, *J. Am. Chem. Soc.* **2020**, *142*, 19715–19721, DOI 10.1021/jacs.0c09691.

[23] A. P. Bapat, B. S. Sumerlin, A. Sutti, *Mater. Horiz.* **2020**, *7*, 694–714, DOI 10.1039/c9mh01223k.

[24] M. Röttger, T. Domenech, R. van der Weegen, A. Breuillac, R. Nicolaÿ, L. Leibler, *Science* **2017**, *356*, 62–65, DOI 10.1126/science.aah5281.

[25] A. Khan, N. Ahmed, M. Rabnawaz, *Polymers* **2020**, *12*, 2027.

[26] R. J. Sheridan, C. N. Bowman, *Polym. Chem.* **2013**, *4*, 4974–4979, DOI 10.1039/C2PY20960H.

[27] M. M. Perera, N. Ayres, *Polym. Chem.* **2020**, *11*, 1410–1423, DOI 10.1039/c9py01694e.

[28] V. Yesilyurt, M. J. Webber, E. A. Appel, C. Godwin, R. Langer, D. G. Anderson, *Adv. Mater.* **2016**, *28*, 86–91, DOI 10.1002/adma.201502902.

[29] W. L. Brooks, B. S. Sumerlin, *Chem. Rev.* **2016**, *116*, 1375–97, DOI 10.1021/acs.chemrev.5b00300.

[30] D. G. Hall, *Boronic acids: preparation, applications in organic synthesis and medicine*, John Wiley & Sons, **2006**.

[31] J. Plescia, N. Moitessier, *Eur. J. Med. Chem.* **2020**, *195*, 112270, DOI 10.1016/j.ejmech.2020.112270.

[32] M. Gosecki, M. Gosecka, *Polymers* **2022**, *14*, 842, DOI 10.3390/polym14040842.

[33] X. T. Zhang, Y. H. Zhao, S. J. Wang, X. L. Jing, *Mater. Chem. Front.* **2021**, *5*, 5534–5548, DOI 10.1039/d1qm00514f.

[34] V. Zhang, B. Kang, J. V. Accardo, J. A. Kalow, *J. Am. Chem. Soc.* **2022**, *144*, 22358–22377, DOI 10.1021/jacs.2c08104.

[35] L. Cheng, X. Zhao, J. Zhao, S. Liu, W. Yu, *Macromolecules* **2022**, *55*, 6598–6608, DOI 10.1021/acs.macromol.2c01057.

[36] S. V. Wanasinghe, O. J. Dodo, D. Konkolewicz, *Angew. Chem. Int. Ed.* **2022**, *61*, e202206938, DOI https://doi.org/10.1002/anie.202206938.

[37] T. T. Duncan, R. G. Weiss, *Colloid Polym. Sci.* **2018**, *296*, 1047–1056, DOI 10.1007/s00396-018-4326-7.

[38] M. Piest, X. L. Zhang, J. Trinidad, J. F. J. Engbersen, *Soft Matter* **2011**, *7*, 11111–11118, DOI 10.1039/c1sm06230a.

[39] B. Kang, J. Kalow, *ACS Macro Lett.* **2022**, *11*, 394–401, DOI 10.1021/acsmacrolett.2c00056.

[40] F. Cuminet, S. Caillol, E. Dantras, E. Leclerc, V. Ladmiral, *Macromolecules* **2021**, *54*, 3927–3961, DOI 10.1021/acs.macromol.0c02706.

[41] O. R. Cromwell, J. Chung, Z. Guan, *J. Am. Chem. Soc.* **2015**, *137*, 6492–5, DOI 10.1021/jacs.5b03551.

[42] Y. Yang, F. S. Du, Z. C. Li, *Polym. Chem.* **2020**, *11*, 1860–1870, DOI 10.1039/c9py01546a.

[43] L. Hammer, N. J. Van Zee, R. Nicolaÿ, *Polymers* **2021**, *13*, 396.

[44] M. A. Lucherelli, A. Duval, L. Averous, *ACS Sustain. Chem. Eng.* **2023**, *11*, 2334–2344, DOI 10.1021/acssuschemeng.2c05956.

[45] F. Chen, F. Gao, X. Guo, L. Shen, Y. Lin, *Macromolecules* **2022**, *55*, 10124–10133, DOI 10.1021/acs.macromol.2c01378.

[46] D. Schultz, J. R. Nitschke, *J. Am. Chem. Soc.* **2006**, *128*, 9887–9892, DOI 10.1021/ja061841u.

[47] I. Fernández, G. Frenking, *J. Org. Chem.* **2006**, *71*, 2251–2256.

[48] C. Hansch, A. Leo, R. W. Taft, *Chem. Rev.* **1991**, *91*, 165–195, DOI 10.1021/cr00002a004.

[49] C. D. Johnson, C. D. Johnson, *The Hammett Equation*, CUP Archive, **1973**.

[50] S. K. Schoustra, J. A. Dijksman, H. Zuilhof, M. M. J. Smulders, *Chem. Sci.* **2020**, *12*, 293–302, DOI 10.1039/d0sc05458e.

[51] K. M. Herbert, P. T. Getty, N. D. Dolinski, J. E. Hertzog, D. de Jong, J. H. Lettow, J. Romulus, J. W. Onorato, E. M. Foster, S. J. Rowan, *Chem. Sci.* **2020**, *11*, 5028–5036, DOI 10.1039/D0SC00605J.

[52] N. Van Herck, D. Maes, K. Unal, M. Guerre, J. M. Winne, F. E. Du Prez, *Angew. Chem. Int. Ed.* **2020**, *59*, 3609–3617, DOI 10.1002/anie.201912902.

[53] B. M. El-Zaatari, J. S. A. Ishibashi, J. A. Kalow, *Polym. Chem.* **2020**, *11*, 5339–5345, DOI 10.1039/D0PY00233J.

[54] W. L. A. Brooks, C. C. Deng, B. S. Sumerlin, *ACS Omega* **2018**, *3*, 17863–17870, DOI 10.1021/acsomega.8b02999.

[55] H. Geethanjali, R. Melavanki, N. D., B. P., R. Kusanur, *J. Mol. Liq.* **2017**, *227*, 37–43, DOI 10.1016/j.molliq.2016.11.097.

[56] S. Soundararajan, M. Badawi, C. M. Kohlrust, J. H. Hageman, *Anal. Biochem.* **1989**, *178*, 125–34, DOI 10.1016/0003-2697(89)90367-9.

[57] J. Jian, R. Hammink, C. J. McKenzie, F. M. Bickelhaupt, J. Poater, J. Mecinovic, *Chemistry* **2022**, *28*, e202104044, DOI 10.1002/chem.202104044.

[58] C. D. Roy, H. C. Brown, *J. Organomet. Chem.* **2007**, *692*, 784–790, DOI 10.1016/j.jorganchem.2006.10.013.

[59] K. Kur, M. Przybyt, E. Miller, *J. Lumin.* **2017**, *183*, 486–493, DOI 10.1016/j.jlumin.2016.11.062.

[60] V. Yesilyurt, A. M. Ayoob, E. A. Appel, J. T. Borenstein, R. Langer, D. G. Anderson, *Adv. Mater.* **2017**, *29*, 1605947, DOI 10.1002/adma.201605947.

[61] I. S. Golovanov, G. S. Mazeina, Y. V. Nelyubina, R. A. Novikov, A. S. Mazur, S. N. Britvin, V. A. Tartakovsky, S. L. Ioffe, A. Y. Sukhorukov, *J. Org. Chem.* **2018**, *83*, 9756–9773, DOI 10.1021/acs.joc.8b01296.

[62] I. S. Golovanov, A. Y. Sukhorukov, Y. V. Nelyubina, Y. A. Khomutova, S. L. Ioffe, V. A. Tartakovsky, *J. Org. Chem.* **2015**, *80*, 6728–36, DOI 10.1021/acs.joc.5b00892.

[63] A. N. Semakin, A. Y. Sukhorukov, A. V. Lesiv, S. L. Ioffe, K. A. Lyssenko, Y. V. Nelyubina, V. A. Tartakovsky, *Org. Lett.* **2009**, *11*, 4072–5, DOI 10.1021/ol9015157.

[64] S. van Hurne, M. Kisters, M. M. J. Smulders, *Front. Chem.* **2023**, *11*, 1148629, DOI 10.3389/fchem.2023.1148629.

[65] N. J. DeWeerd, E. V. Bukovsky, K. P. Castro, I. V. Kuvychko, A. A. Popov, S. H. Strauss, O. V. Boltalina, *J. Fluor. Chem.* **2019**, *221*, 1–7, DOI 10.1016/j.jfluchem.2019.02.010.

[66] M. Albrecht, H. Yi, O. Koksal, G. Raabe, F. Pan, A. Valkonen, K. Rissanen, *Chem. Eur. J.* **2016**, *22*, 6956–63, DOI 10.1002/chem.201600249.

[67] T. Nagai, G. Nishioka, M. Koyama, A. Ando, T. Miki, I. Kumadaki, *Chem. Pharm. Bull.* **1991**, *39*, 233–235, DOI 10.1248/cpb.39.233.

[68] H. Oberhammer, *J. Fluor. Chem.* **1983**, *23*, 147–162, DOI 10.1016/S0022-1139(00)84976-3.

[69] V. Belot, D. Farran, M. Jean, M. Albalat, N. Vanthuyne, C. Roussel, *J. Org. Chem.* **2017**, *82*, 10188–10200, DOI 10.1021/acs.joc.7b01698.

Chapter 5

Recyclable Covalent Adaptable Polystyrene-Networks using Boronates and Tetraazaadamantanes

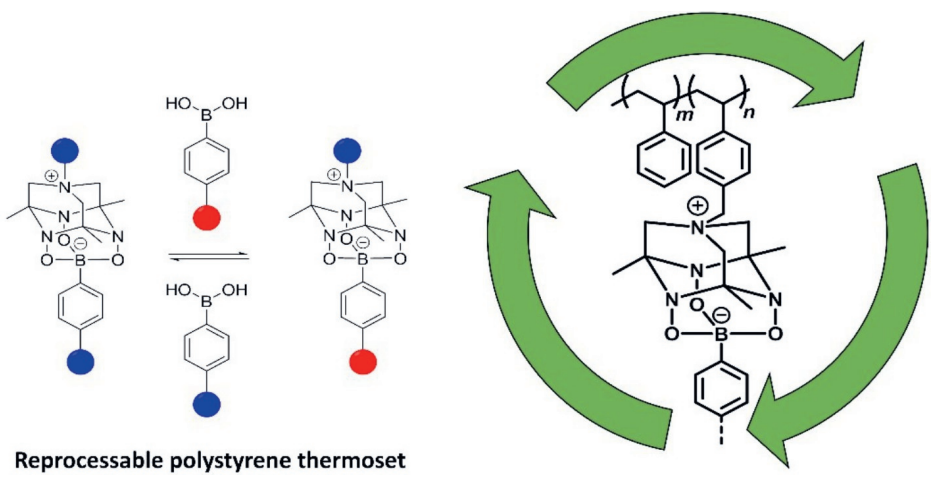

Simon van Hurne, Sagar K. Raut, Maarten M. J. Smulders
This work was published as:
S. van Hurne, S. K. Raut, M. M. J. Smulders, *ACS Applied Polymer Materials*, **2024**, *6*, 13, 7918–7925, https://doi.org/10.1021/acsapm.4c01633

5.1 Abstract

With an ever-increasing annual production of polymers and the accumulation of polymer waste leading to progressively adverse environmental consequences, it has become important that all polymers can be efficiently recycled at the end of their life cycle. Especially thermosets are intrinsically difficult to recycle, because of their permanent covalent crosslinks. A possible solution is to switch from using thermosets to covalent adaptable networks, sparking the rapid development of new dynamic covalent chemistries and derived new polymer materials. Next to the development of these new polymer materials, there is also an evident advantage of merging the virtues of covalent adaptable networks with the proven material properties of widely used commodity plastics, by introducing dynamic covalent bonds in these –originally– thermoplastic materials to obtain recyclable thermosets. Here we report the synthesis and characterisation of a polystyrene polymer, functionalised with tetraazaadamantanes and crosslinked with dynamic covalent boronic esters. The material properties were characterised for different degrees of crosslinking. The materials showed good solvent resistance with a high remaining insoluble fraction. In line with the typical behaviour of traditional covalent adaptable networks, the newly prepared polystyrene-based boronate-tetraazaadamantane materials were able to undergo stress relaxation. The material relaxation was also shown to be tuneable by mixing in an acid catalyst. Lastly, the materials could be recycled at least two times.

5.2 Introduction

In modern times polymers have become crucial materials for society, because of their versatile use and low production costs.[1] Because of this, the annual polymer production continues to rise every year. This increasing polymer production is also leading to increasing polymer waste being produced each year. When that polymer waste ends up in the environment, it leads to negative environmental impact. This makes the recycling of polymers of increasing importance.[2,3] However, the degree to which a polymer can be recycled strongly depends on its structure. Thermoplastics, generally composed of linear polymer chains, can be recycled relatively easily. Their more robust thermoset counterparts, on the other hand, are inherently highly difficult or even impossible to recycle due to their permanent crosslinks.[4–7]

Over the last few decades covalent adaptable networks (CANs) have grown in interest as a means of tackling the build-up of polymer waste,[8–11] while at the same time imbuing new (dynamic) properties in polymeric materials.[12,13] CANs are networks that are covalently crosslinked using reversible covalent bonds. The exchange between those reversible covalent bonds gives CANs access to the strength of permanently crosslinked thermosets, while at the same time retaining the reprocessability of non-crosslinked thermoplastics.[14,15] One of the most interesting new properties that CANs have is their ability to heal after damage. This can significantly extend the useful lifetime of such a material, thus reducing the need for new replacements.

CANs operate on the principle of dynamic covalent chemistry,[16,17] where covalent bonds can exchange over time, as opposed to supramolecular chemistry,[18] where non-covalent bonds can exchange. Examples of dynamic covalent bonds used in CANs are those resulting from the Diels-Alder reaction,[19,20] *N*,*S*-acetals,[21] or nucleophilic transalkylation reactions,[22] as well as imines,[23–25] disulfides,[26–28] esters,[29,30] vinylogous urethanes,[31,32] diketoamines,[33,34] acylsemicarbazides[35,36] and boronic esters.[37–40] In this study we chose to use the well-known boronic ester bond, on which we reported previously in chapters 3 and 4,[41,42] for the formation of dynamically crosslinked networks.[43,44]

Boronic esters-containing networks can be prepared via a condensation reaction between bifunctional boronic acids and poly-ols, such as a sugar or polyvinyl alcohol.[45,46] Generally, these boronic networks form (hydro)gels and thus have low structural integrity and are prone to tearing. However, they exhibit low toxicity due to the biocompatibility of boronic acids, allowing for potential usage in biomedical applications.[47–49]

An elegant possibility to improve the properties of the conventional boronic ester bond is to replace the typical diols with the strong and rigid triol binding of the TetraAzaADamantanes (TAADs).[50–52] In chapters 3 and 4 we discussed the possibility of introducing such TAAD moiety in CANs with boronic acids by using a small linker, resulting in the formation of boronate-TAAD soft rubbers.[41,42] These rubbers displayed a high healing capacity. However, the resulting soft rubbers might not be suitable to more structural end product applications. This prompted us to look towards introducing boronate-TAAD linkages in established commodity polymers. The process of turning established thermoplastics into dynamically crosslinked CANs can help facilitate the transition towards circular plastics, since industry is already familiar in the handling of those materials.[53–56] As commodity plastic we chose polystyrene, since it is a well-

known and widely used plastic, which application ranges widely from food packaging to *e.g.*, components in the automotive industry. In this, our aim was not to make conventional polystyrene recyclable, but to make recyclable thermosets (crosslinked polymers) from an established industrially relevant polymer (polystyrene) backbone. Several groups have investigated dynamically crosslinked networks containing styrene moieties. Most of these used styrene-butadiene rubber (SBR) with roughly only 15-19% styrene in the main polymer chain as a platform for crosslinking.[57–60] In contrast, there are only a few studies that focused on a higher styrene content in their polymers.[25,61–63] While this did result in recyclable crosslinked polystyrene materials, most of these examples still relied on mixing in non-styrenic monomers, or used environmentally unfriendly components (*e.g.*, diisocyanates or copper(I)), which could impact the ultimate applicability of such new materials.

Building on this early work, our aim was to maintain the polystyrene character of the final polymer (network) to a high degree, while at the same time incorporate the dynamic bonds (and corresponding dynamic network properties) inside the polymer, to ultimately arrive at polystyrene-based CANs. The former objective was realised by synthesising (and later functionalising) a polymer whose backbone is fully composed of styrene monomers, while the latter objective was achieved by integration of the boronate-TAAD linkages (**Figure 5.1**).

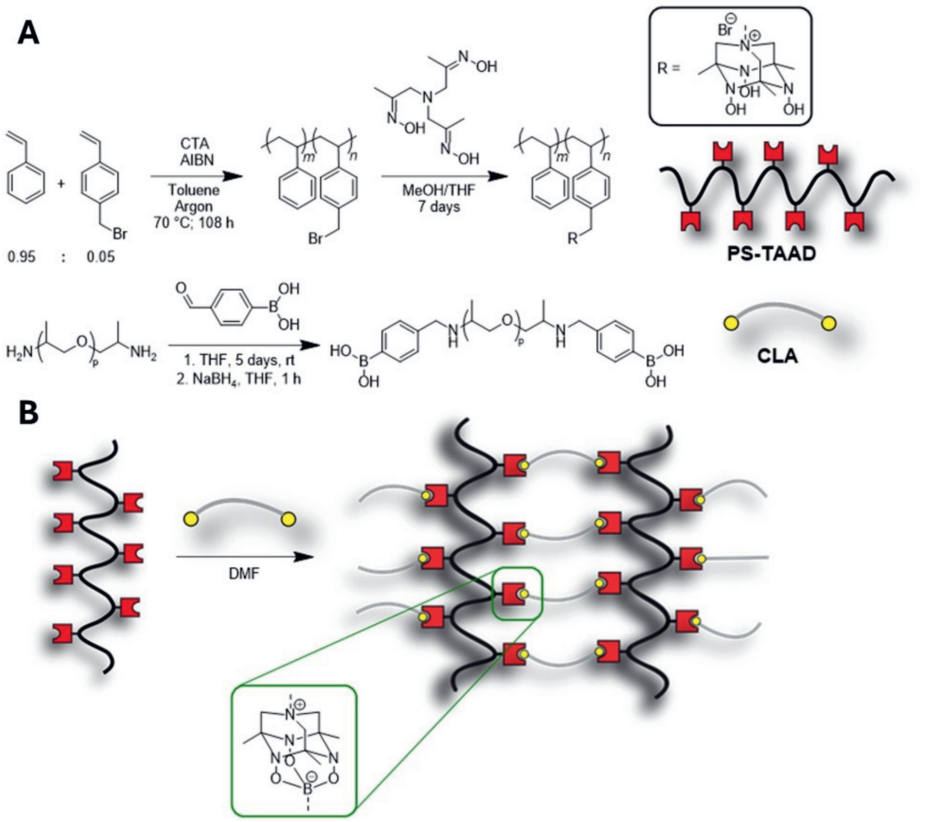

Figure 5.1: *(A) The synthesis of the polystyrene modified with tetraazaadamantanes, named* ***PS-TAAD****, and the polypropylene glycol end-capped with phenylboronic acid, named crosslinking agent (CLA). (B) A schematic representation of the crosslinked network.*

5.3 Results and discussion

In order to introduce dynamic covalent bonds in polystyrene, firstly 4-vinylbenzyl bromide was copolymerised with styrene (in a molar ratio of 5 to 95, respectively), to create a pre-polymer of poly(styrene-co-4-vinylbenzyl bromide) using a RAFT polymerisation under argon at 70 °C (**Figure 5.1**). The 4-vinylbenzyl bromide monomer was prepared by halide exchange from 4-vinylbenzyl chloride with 98% yield. The remaining 2% 4-vinylbenzylchloride present in the feed was included in the molar ratio of the monomers. (See **Supplementary Information** or Appendix section 5.1 for full synthetic details and characterisation). The poly(styrene-co-4-vinylbenzyl bromide) was characterised by GPC

and NMR. The copolymer had a M_n of 86 kDa (as determined by GPC, calibrated against polystyrene) and 5% incorporated benzyl bromide (as determined by NMR, see **Supplementary Information Figure S3 and Table S1**. Subsequently, the introduced benzyl bromide was then used for the attachment of the TetraAzaADamantane (TAAD) moieties via nitrogen quaternisation (**Figure 5.1**). The incorporation of the TAAD moiety was determined by using NMR, by comparing the integral value of the TAAD -CH_3 groups to that of the benzyl groups of the polymer backbone. This revealed a quantitative conversion of the bromide end groups into the TAAD moieties. Any remaining 4-vinylbenzylchloride would also have been converted during the functionalisation, albeit at a slower rate. The functionalised polymer was not soluble in toluene, chloroform, THF or acetone, thus confirming that the quaternisation was successful (and –unfortunately– hampering characterisation by GPC). Gratifyingly, the increase in molecular weight (and concomitant change in polarity) could be observed by (uncalibrated) DOSY (see **Supplementary Information Figures S4** and **S6**), as indicated by a decrease in diffusion coefficient of the polymer. Given the large difference in polarity of the two polymers, we refrained from directly comparing the molecular weight by converting the observed diffusion coefficient into a hydrodynamic volume and corresponding molecular weight. Instead, we determined the molecular weight by NMR based on the degree of TAAD functionalisation (determined by NMR, see **Supplementary Information Figure S5**), since no change in the length of the polymer was expected. We calculated the increase in molecular weight from the bromide-containing polystyrene polymer (with known molecular weight of 86 kDa), which resulted in a functionalised polymer named **PS-TAAD** with a M_n of 96 kDa, with 5% TAAD incorporation. For comparison, a shorter **PS-TAAD**, with a M_n of only 8.5 kDa, was also prepared and tested (See **Supplementary Information** for synthetic details and characterisation). However, samples prepared with this shorter **PS-TAAD** were found to have reprocessing issues and thus this study focused primarily on the longer **PS-TAAD**. Finally, the bifunctional boronic acid crosslinking agent (CLA) was prepared by reacting 4-formylphenylboronic acid onto amine-terminated PPG and reducing the formed imine with $NaBH_4$, (following the procedure described in chapters 3 and 4).[41,42]

Once the two components were synthesised, they were mixed in different molar ratios relative to the functional groups to prepare a series of materials with different degree of crosslinking: 25%, 50%, 75% and 100%, (to clarify, in case of the 50% sample this meant that within the material

there was one boronic acid group per two TAAD moieties). The materials were prepared by dissolving the **PS-TAAD** in DMF and the CLA in methanol and mixing the two components by vortexing, before casting them in a silicone mold (see also the **Supplementary Information** for further details on material preparation). The solvent was removed by drying the samples for two days in an oven at 70 °C, followed by a night in a vacuum oven at 50 °C. This resulted in the formation of yellow-brownish materials. The materials were characterised using a swelling and insoluble fractions experiment, DSC, TGA, rheology and DMA.

To determine if the formed materials all really form a crosslinked network, the different materials were subjected to a solubility (swelling) study, in which the materials were soaked in an excess of solvent overnight to determine the swelling behaviour and the remaining weight percentage after drying in a vacuum oven (**Figure 5.2**). The solvents were chosen to cover a broad range of different well known and commonly used laboratory solvents.

The first observation that can be made is that the crosslinked polymer materials do not dissolve in any of the selected solvents with a remaining solid content of >90 wt% for almost all samples. Polystyrene itself dissolves well in DCM, THF and to a degree in DMF. The fact that these materials do not dissolve in these solvents is direct experimental evidence that our crosslinking reaction was effective. DCM, THF and DMF resulted in a larger swelling compared to acetone, water and methanol, which is understandable considering that they are good at dissolving polystyrene. What can also be observed is that the swelling ratio and the remaining solid fraction remain largely consistent for a given solvent when varying the crosslinking degree. When comparing the 100% crosslinked material with the long and the short **PS-TAAD**, the 10-fold difference in M_n does not make a big difference (**Supplementary Figure S31**). The most notable difference is that the shorter polymer swells slightly more in water than the higher molecular weight polymers. This is in line with expectations, since the longer styrene chain imparts a more hydrophobic character to the material. The 25% crosslinked sample did show much more swelling in DMF compared to the other solvents or crosslinking degrees. This increased swelling ratio might be due to the reduced number of crosslinks creating a looser network that can thus swell more easily, but in that case also an increased swelling ratio for the other solvents might have been expected as well. Alternatively, the delicate handling required to deal with these fragile solvent-swollen samples (with associated difficulty of fully removing excess solvent) could account for the high swelling ratio.

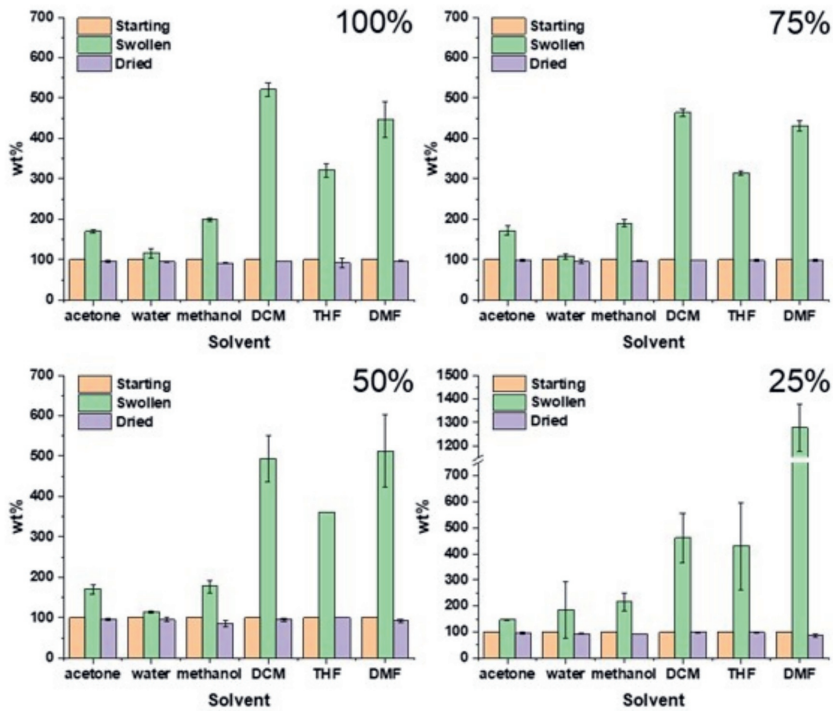

Figure 5.2: *Solvent study of the different degrees of crosslinking. Both the swelling and the remaining fraction are denoted as a weight percentage (wt%), normalised to the starting weight. All measurements were performed in duplicate.*

When looking at the thermal properties of the new materials, DSC revealed that the boronate-TAAD materials have a T_g of approximately 83 °C, which is slightly lower than the T_g of a polystyrene homopolymer of around 100 °C (**Supplementary Information Figure S23**).[64] TGA showed that the materials follow a three-step thermal decomposition (**Supplementary Information Figures S24—-S27**). The first, smaller, step is around 183 °C, followed by the second, step around 335 °C and the final, large, step around 435 °C. The decomposition step around 180 °C is likely due to the decomposition of the TAAD moiety (from earlier work described in chapters 3 and 4[41,42] using MeOH as solvent instead of DMF, we could infer that this step is not related to residual DMF). From the TGA data we can conclude that these materials are stable to elevated temperatures and eligible for hot-press molding.
Next, the dynamic-mechanical material properties were investigated using rheology. Frequency sweeps of the polymer networks with different

crosslinking degrees, as shown in **Figure 5.3A**, showed that all four materials had a storage modulus (G') around 10^5–10^6 Pa at 100 °C. The loss moduli (G") was lower than the storage modulus for all cases, thus showing that the materials respond more like solids. No crossovers for the G' and G" could be observed within the measurement window. This contrasts with the frequency sweep obtained from neat polystyrene (97 kDa), which did reveal a crossover frequency (**Supplementary Information Figure S37A**). It was expected that the degree of crosslinking would positively correlate with G', but this does not seem to be the case. To explain this observation, we propose that a combination of various factors, including –but not necessarily limited to– the variable degree of crosslinking, a plasticizing effect of the increasing amount of PPG,[65–67] and/or a possible phase separation between the more hydrophilic PPG polymer and the hydrophobic PS backbone, may jointly have resulted in the absent correlation between G' and degree of crosslinking. In **Figure 5.3B** the results of the shear measurements can be seen. All samples were found to yield around 1% strain at a temperature of 100 °C. It was expected that the degree of crosslinking would correlate with an increasing shear modulus, however, again we see that the CLA not only acts as a crosslinker, but also as a plasticiser. Both the crosslinking and the plasticiser have a significant impact on the shearing behaviour, be it with different contributions.

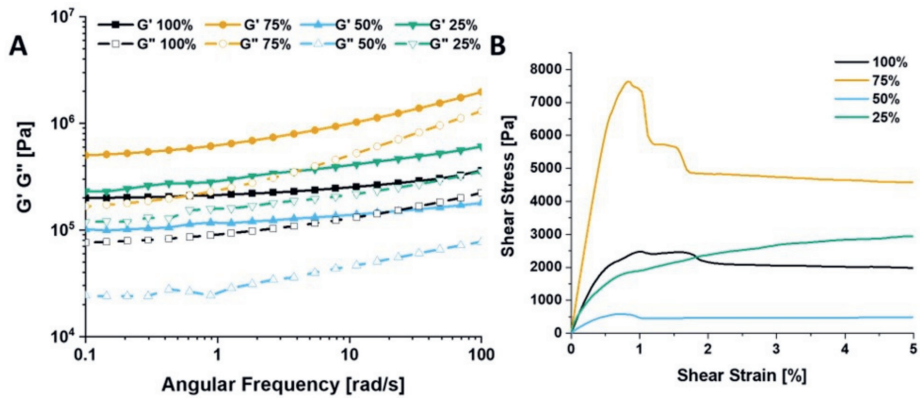

Figure 5.3: *(A) Frequency sweep data of the materials with different crosslinking degrees at 100 °C with 0.1% strain from 100 rad/s to 0.1 rad/s. The solid lines with filled symbols are the storage moduli; the dashed lines with the empty symbols are the loss moduli. (B) Shear measurements of the materials with the different crosslinking degrees at 100 °C. The full measurements till 10% strain can be found in the* ***Supplementary Information Figures S15****,* ***S16****,* ***S17*** *and* ***S18****.*

The relaxation behaviour of the materials at 120 °C was also studied and is shown in **Figure 5.4A**. The most notable result is the fact that these covalently crosslinked materials are able to relax stress, thus showing that they did indeed form CANs, since non-dynamic covalently crosslinked networks are not able to efficiently relax stress. Looking at the relaxation data of these materials, a trend can be seen where higher degrees of crosslinking correspond with longer relaxation. A notable exception can be seen in the 75% crosslinked material, which for unknown reasons relaxes significantly faster compared to the other crosslinking degrees. Unmodified polystyrene (M_n 97 kDa) was added as a reference and has the fastest relaxation of this series, as was expected since it is a similar polymer but without any crosslinking.

When comparing the relaxation time of the 100% crosslinked materials with the long and the short **PS-TAAD** (Supplementary Figure S33), the short polymer has a longer relaxation time. This is likely due to the short polystyrene chain being less flexible than the longer chain and thus showing a slower relaxation.

Since boronate esters are sensitive to pH, we also studied the response of different amounts of acid mixed into the material. For this we chose *para*-toluenesulfonic acid (PTSA). **Figure 5.4B** shows the relaxation behaviour of the 100% crosslinked materials with different wt% of PTSA mixed in ranging from 0% to 10%. It was hypothesised that additional acid would decrease the relaxation time of the material either directly through catalysis of the exchange reaction or indirectly by shifting the equilibrium more towards free hydroxyl groups, which could then increase the exchange rate. This is also what we observed, as the relaxation time got shorter with increasing PTSA content. Increasing the PTSA wt% from 5 to 10 wt% did not result in faster relaxation, suggesting a limit to the effect that PTSA has on the network relaxation. This effect was also shown to work in materials prepared using the short **PS-TAAD** polymer, where the relaxation time decreased with increasing PTSA content (Supplementary Figure S36). This is in contrast to the observed relaxation behaviour of similar networks with boronate-TAAD linkages prepared from small linkers as shown in chapter 3.[42] In those networks no simple trend was observed concerning the amount of acid added and the relaxation behaviour of the material. As the materials in this study contain largely the same functional groups it supports the hypothesis that matrix effects might have played a role in the effectiveness of the mixed in acid, as was also put forward in chapter 3.[42] Unfortunately, the fragility of the polystyrene backbone in combination with the bulky, polar TAAD

side groups disrupted the temperature dependency of the network stress relaxation and thus the construction of an Arrhenius plot even with acid mixed in, thus no activation energy could be determined for these materials.[68]

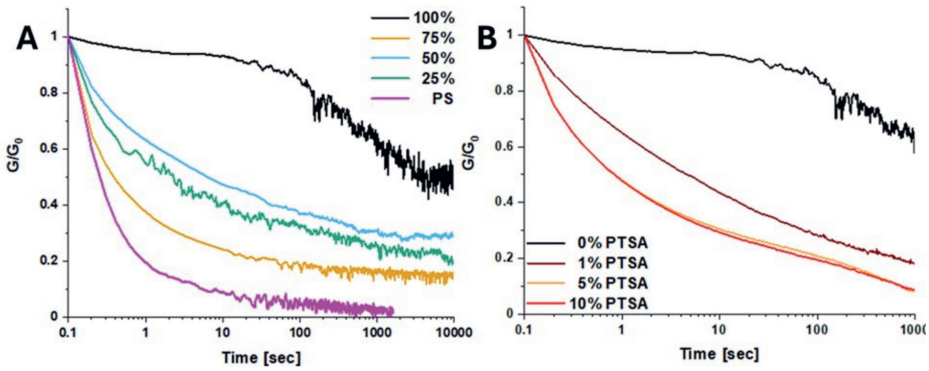

Figure 5.4: *(A) Relaxation measurements of the materials with the different crosslinking degrees at 120 °C with a strain of 1%. (B) Relaxation measurements at 120 °C with 1% strain for a 100% crosslinked material with different wt% of para-toluenesulfonic acid mixed in.*

Lastly, the reprocessability of the materials was tested using extensional DMA at room temperature. The samples were cut in half and reprocessed in a Teflon hot-press mold (20 × 5 × 1 mm) for 2 h at 145 °C and 5 ton. The samples were reprocessed a total of two cycles, as shown in **Figure 5.5**. The samples with 25% crosslinking were too brittle at room temperature to be clamped effectively. This could be due to these samples having the least amount of plasticiser and thus retaining mostly the characteristics of a brittle crosslinked polystyrene material. The data shows that even after reprocessing the materials behave quite similar to the pristine material for all three tested crosslinking degrees with an average Young's modulus over all reprocessing steps of 6.2 ± 0.1, 7.8 ± 0.1, and 8.8 ± 0.1 MPa for the 100%, 75% and 50%, respectively. The 100% crosslinked material does become more extensible in the second reprocessing cycle, far more than is seen for the other crosslinking degrees, however the maximum stress remains largely the same. This does suggest that the network structure has been affected by the reprocessing steps. This could be due to some accumulative damage to the TAAD moieties at the elevated reprocessing temperatures, thus resulting in a lower effective crosslinking density after repeated reprocessing cycles. Another possibility would be that the network gets less entangled through polymer alignment during the reprocessing steps. The 100% crosslinked material

with the short **PS-TAAD** polymer was also prepared and tested, however its increased stiffness and slower relaxation made it difficult to efficiently reprocess these materials, although it was possible to reprocess the materials for at least one cycle (**Supplementary Information Figure S34**).

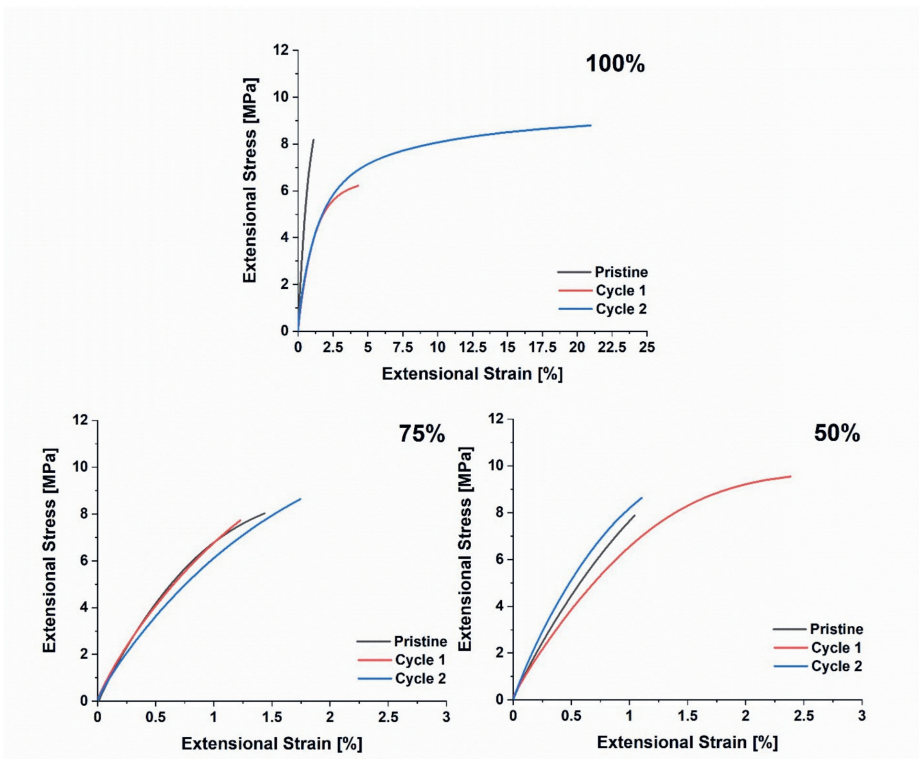

Figure 5.5: *Extensional DMA measurements on the pristine and recycled materials with different crosslinking degrees. The materials with 25% crosslinking were too brittle to be measured and as such are not included. After breakage, the materials were reprocessed by heating the materials in a hot-press at 145 °C for 2 h at 5 ton pressure in a Teflon mold.*

5.4 Conclusions

We successfully prepared and characterised a covalently crosslinked, yet recyclable, polystyrene-based thermoset using RAFT polymerisation. To do so, we prepared a dynamic-covalently crosslinked polymer entirely composed of polystyrene in its backbone and integrated the dynamic-covalent boronate-TAAD chemistry to accomplish dynamic crosslinks. The material was able to relax stress with and without the use of a catalyst. The

material properties could be tuned through both the degree of crosslinking and the addition of acid catalyst. The materials were demonstrated to be reprocessable over at least two cycles using hot-pressing. We believe this work demonstrates that dynamic covalent bonds can transform tried-and-tested commodity polymers (polystyrene in our case) into recyclable and adaptable thermosets with dynamic properties. In this regard, our approach offers a promising platform for polymer waste reduction and for enhancing the circularity of polymers, while also promoting the growing field of covalent adaptable networks.

References

[1] A. L. Andrady, M. A. Neal, *Philos. Trans. R. Soc. Lond. B Biol. Sci.* **2009**, *364*, 1977–84, DOI 10.1098/rstb.2008.0304.

[2] R. C. Thompson, C. J. Moore, F. S. vom Saal, S. H. Swan, *Philos. Trans. R. Soc. Lond. B Biol. Sci.* **2009**, *364*, 2153–66, DOI 10.1098/rstb.2009.0053.

[3] M. R. Johansen, T. B. Christensen, T. M. Ramos, K. Syberg, *J. Environ. Manag.* **2022**, *302*, 113975, DOI 10.1016/j.jenvman.2021.113975.

[4] J. P. Lange, *ACS Sus. Chem. Eng.* **2021**, *9*, 15722–15738, DOI 10.1021/acssuschemeng.1c05013.

[5] A. Rahimi, J. M. García, *Nat. Rev. Chem.* **2017**, *1*, 0046, DOI 10.1038/s41570-017-0046.

[6] L. Imbernon, S. Norvez, *Eur. Polym. J.* **2016**, *82*, 347–376, DOI 10.1016/j.eurpolymj.2016.03.016.

[7] S. M. Al-Salem, P. Lettieri, J. Baeyens, *Waste Manag.* **2009**, *29*, 2625–43, DOI 10.1016/j.wasman.2009.06.004.

[8] Y. Zhang, A. A. Broekhuis, F. Picchioni, *Macromolecules* **2009**, *42*, 1906–1912, DOI 10.1021/ma8027672.

[9] Y. H. Jin, Z. P. Lei, P. Taynton, S. F. Huang, W. Zhang, *Matter* **2019**, *1*, 1456–1493, DOI 10.1016/j.matt.2019.09.004.

[10] G. M. Scheutz, J. J. Lessard, M. B. Sims, B. S. Sumerlin, *J. Am. Chem. Soc.* **2019**, *141*, 16181–16196, DOI 10.1021/jacs.9b07922.

[11] W. Post, A. Susa, R. Blaauw, K. Molenveld, R. J. I. Knoop, *Polym. Rev.* **2020**, *60*, 359–388, DOI 10.1080/15583724.2019.1673406.

[12] J. Luo, Z. Demchuk, X. Zhao, T. Saito, M. Tian, A. P. Sokolov, P.-F. Cao, *Matter* **2022**, *5*, 1391–1422, DOI 10.1016/j.matt.2022.04.007.

[13] N. Zheng, Y. Xu, Q. Zhao, T. Xie, *Chem. Rev.* **2021**, *121*, 1716–1745, DOI 10.1021/acs.chemrev.0c00938.

[14] C. J. Kloxin, C. N. Bowman, *Chem. Soc. Rev.* **2013**, *42*, 7161–73, DOI 10.1039/c3cs60046g.

[15] C. Bowman, F. Du Prez, J. Kalow, *Polym. Chem.* **2020**, *11*, 5295–5296, DOI 10.1039/d0py90102d.

[16] S. Huang, X. Kong, Y. S. Xiong, X. R. Zhang, H. Chen, W. Q. Jiang, Y. Z. Niu, W. L. Xu, C. G. Ren, *Eur. Polym. J.* **2020**, *141*, 110094, DOI 10.1016/j.eurpolymj.2020.110094.

[17] J. M. Winne, L. Leibler, F. E. Du Prez, *Polym. Chem.* **2019**, *10*, 6091–6108, DOI 10.1039/c9py01260e.

[18] L. Yang, X. Tan, Z. Wang, X. Zhang, *Chem. Rev.* **2015**, *115*, 7196–239, DOI 10.1021/cr500633b.

[19] F. Orozco, J. Li, U. Ezekiel, Z. Niyazov, L. Floyd, G. M. R. Lima, J. G. M. Winkelman, I. Moreno-Villoslada, F. Picchioni, R. K. Bose, *Eur. Polym. J.* **2020**, *135*, 109882, DOI 10.1016/j.eurpolymj.2020.109882.

[20] P. Raffa, A. Kassi, J. Gosschalk, N. Migliore, L. M. Polgar, F. Picchioni, *Macromol. Mater. Eng.* **2021**, *306*, 2000755, DOI 10.1002/mame.202000755.

[21] T. Habets, G. Seychal, M. Caliari, J.-M. Raquez, H. Sardon, B. Grignard, C. Detrembleur, *J. Am. Chem. Soc.* **2023**, *145*, 25450–25462, DOI 10.1021/jacs.3c10080.

[22] E. E. L. Maassen, J. P. A. Heuts, R. P. Sijbesma, *Polym. Chem.* **2021**, *12*, 3640–3649, DOI 10.1039/d1py00292a.

[23] S. K. Schoustra, T. Groeneveld, M. M. J. Smulders, *Polym. Chem.* **2021**, *12*, 1635–1642, DOI 10.1039/d0py01555e.

[24] R. L. Snyder, C. A. L. Lidston, G. X. De Hoe, M. J. S. Parvulescu, M. A. Hillmyer, G. W. Coates, *Polym. Chem.* **2020**, *11*, 5346–5355, DOI 10.1039/c9py01957j.

[25] J. J. Lessard, G. M. Scheutz, R. W. Hughes, B. S. Sumerlin, *Acs Appl. Polym. Mater.* **2020**, *2*, 3044–3048, DOI 10.1021/acsapm.0c00523.

[26] L. Imbernon, E. K. Oikonomou, S. Norvez, L. Leibler, *Polym. Chem.* **2015**, *6*, 4271–4278, DOI 10.1039/c5py00459d.

[27] A. Tsuruoka, A. Takahashi, D. Aoki, H. Otsuka, *Angew. Chem. Int. Ed.* **2020**, *59*, 4294–4298, DOI 10.1002/anie.201913430.

[28] G. Vozzolo, M. Ximenis, D. Mantione, M. Fernández, H. Sardon, *ACS Macro Lett.* **2023**, *12*, 1536–1542, DOI 10.1021/acsmacrolett.3c00544.

[29] Z. Pei, Y. Yang, Q. Chen, E. M. Terentjev, Y. Wei, Y. Ji, *Nat. Mater.* **2014**, *13*, 36–41, DOI 10.1038/nmat3812.

[30] M. Hayashi, *Acs Appl. Polym. Mater.* **2020**, *2*, 5365–5370, DOI 10.1021/acsapm.0c01099.

[31] J. J. Lessard, L. F. Garcia, C. P. Easterling, M. B. Sims, K. C. Bentz, S. Arencibia, D. A. Savin, B. S. Sumerlin, *Macromolecules* **2019**, *52*, 2105–2111, DOI 10.1021/acs.macromol.8b02477.

[32] W. Denissen, M. Droesbeke, R. Nicolay, L. Leibler, J. M. Winne, F. E. Du Prez, *Nat. Commun.* **2017**, *8*, 14857, DOI 10.1038/ncomms14857.

[33] L. D. Dugas, W. D. Walker, R. Shankar, K. S. Hoppmeyer, T. L. Thornell, S. E. Morgan, R. F. Storey, D. L. Patton, Y. C. Simon, *Macromol. Rapid. Commun.* **2022**, *43*, e2200249, DOI 10.1002/marc.202200249.

[34] P. R. Christensen, A. M. Scheuermann, K. E. Loeffler, B. A. Helms, *Nat. Chem.* **2019**, *11*, 442–448, DOI 10.1038/s41557-019-0249-2.

[35] D. H. Fu, W. L. Pu, J. Escorihuela, X. R. Wang, Z. H. Wang, S. Y. Chen, S. J. Sun, S. Wang, H. Zuilhof, H. S. Xia, *Macromolecules* **2020**, *53*, 7914–7924, DOI 10.1021/acs.macromol.0c01667.

[36] S. Wang, D. H. Fu, X. R. Wang, W. L. Pu, A. Martone, X. L. Lu, M. Lavorgna, Z. H. Wang, E. Amendola, H. S. Xia, *J. Mater. Chem. A* **2021**, *9*, 4055–4065, DOI 10.1039/d0ta11251h.

[37] A. P. Bapat, B. S. Sumerlin, A. Sutti, *Mater. Horiz.* **2020**, *7*, 694–714, DOI 10.1039/c9mh01223k.

[38] X. Zhang, S. Wang, Z. Jiang, Y. Li, X. Jing, *J. Am. Chem. Soc.* **2020**, *142*, 21852–21860, DOI 10.1021/jacs.0c10244.

[39] B. Marco-Dufort, M. W. Tibbitt, *Mater. Today Chem.* **2019**, *12*, 16–33, DOI 10.1016/j.mtchem.2018.12.001.

[40] M. Rottger, T. Domenech, R. van der Weegen, A. Breuillac, R. Nicolay, L. Leibler, *Science* **2017**, *356*, 62–65, DOI 10.1126/science.aah5281.

[41] S. van Hurne, T. J. M. Buijsen, M. M. J. Smulders, *J. Polym. Sci.* **2023**, *62*, 891–899, DOI 10.1002/pol.20230446.

[42] S. van Hurne, M. Kisters, M. M. J. Smulders, *Front. Chem.* **2023**, *11*, 1148629, DOI 10.3389/fchem.2023.1148629.

[43] S. Cho, S. Y. Hwang, D. X. Oh, J. Park, *J. Mater. Chem. A* **2021**, *9*, 14630, DOI 10.1039/d1ta02308j.

[44] W. A. Ogden, Z. Guan, *J. Am. Chem. Soc.* **2018**, *140*, 6217–6220, DOI 10.1021/jacs.8b03257.

[45] G. Springsteen, B. H. Wang, *Tetrahedron* **2002**, *58*, 5291–5300, DOI 10.1016/S0040-4020(02)00489-1.

[46] J. Yan, G. Springsteen, S. Deeter, B. Wang, *Tetrahedron* **2004**, *60*, 11205–11209, DOI 10.1016/j.tet.2004.08.051.

[47] J. Plescia, N. Moitessier, *Eu. J. Med. Chem.* **2020**, *195*, 112270, DOI 10.1016/j.ejmech.2020.112270.

[48] W. L. Brooks, B. S. Sumerlin, *Chem. Rev.* **2016**, *116*, 1375–97, DOI 10.1021/acs.chemrev.5b00300.

[49] J. N. Cambre, B. S. Sumerlin, *Polymer* **2011**, *52*, 4631–4643, DOI 10.1016/j.polymer.2011.07.057.

[50] S. Okamoto, S. Onoue, M. Kobayashi, A. Sudo, *J. Polym. Sci. Part A: Polym. Chem.* **2014**, *52*, 3498–3505, DOI 10.1002/pola.27414.

[51] I. S. Golovanov, G. S. Mazeina, Y. V. Nelyubina, R. A. Novikov, A. S. Mazur, S. N. Britvin, V. A. Tartakovsky, S. L. Ioffe, A. Y. Sukhorukov, *J. Org. Chem.* **2018**, *83*, 9756–9773, DOI 10.1021/acs.joc.8b01296.

[52] A. N. Semakin, A. Y. Sukhorukov, A. V. Lesiv, S. L. Ioffe, K. A. Lyssenko, Y. V. Nelyubina, V. A. Tartakovsky, *Org. Lett.* **2009**, *11*, 4072–5, DOI 10.1021/ol9015157.

[53] L. Yue, H. Guo, A. Kennedy, A. Patel, X. Gong, T. Ju, T. Gray, I. Manas-Zloczower, *ACS Macro Lett.* **2020**, *9*, 836–842, DOI 10.1021/acsmacrolett.0c00299.

[54] Z. Wang, Y. Gu, M. Ma, Y. Liu, M. Chen, *Macromolecules* **2021**, *54*, 1760–1766, DOI 10.1021/acs.macromol.0c02870.

[55] R. G. Ricarte, F. Tournilhac, M. Cloître, L. Leibler, *Macromolecules* **2020**, *53*, 1852–1866, DOI 10.1021/acs.macromol.9b02415.

[56] Z. Wang, Y. Gu, M. Ma, M. Chen, *Macromolecules* **2020**, *53*, 956–964, DOI 10.1021/acs.macromol.9b02325.

[57] X. Kuang, G. M. Liu, X. Dong, D. J. Wang, *Mater. Chem. Front.* **2017**, *1*, 111–118, DOI 10.1039/c6qm00094k.

[58] L. Wang, Y. Liu, N. Hao, Y. Qiao, W. Zeng, L. Wei, A. Du, *Polymer* **2023**, *265*, 125595, DOI 10.1016/j.polymer.2022.125595.

[59] L. Wang, Y. J. Liu, Y. Y. Wei, W. T. Zeng, Z. W. Cui, A. H. Du, *Eur. Polym. J.* **2023**, *193*, 112101, DOI 10.1016/j.eurpolymj.2023.112101.

[60] Y. Liu, Z. Tang, Y. Chen, C. Zhang, B. Guo, *ACS Appl. Mater. Interfaces* **2018**, *10*, 2992–3001, DOI 10.1021/acsami.7b17465.

[61] A. Jourdain, R. Asbai, A. Omaima, M. M. Chehimi, E. Drockenmuller, D. Montarnal, *Macromolecules* **2020**, *53*, 1884–1900, DOI 10.1021/acs.macromol.9b02204.

[62] Y. Xiong, L. L. Liu, C. Y. Hu, J. X. Yang, Y. W. Huang, *Macromol. Chem. Phys.* **2023**, *224*, 2300042, DOI 10.1002/macp.202300042.

[63] S. J. Wang, B. Wang, X. T. Zhang, L. Wang, W. Fan, H. Y. Li, C. Bian, X. L. Jing, *Appl. Surf. Sci.* **2021**, *570*, 151157, DOI 10.1016/j.apsusc.2021.151157.

[64] P. Claudy, J. M. Letoffe, Y. Camberlain, J. P. Pascault, *Polym. Bull.* **1983**, *9*, 208–215, DOI 10.1007/Bf00283709.

[65] F. M. Vanin, P. J. A. Sobral, F. C. Menegalli, R. A. Carvalho, A. M. Q. B. Habitante, *Food Hydrocoll.* **2005**, *19*, 899–907, DOI 10.1016/j.foodhyd.2004.12.003.

[66] Z. Kulinski, E. Piorkowska, K. Gadzinowska, M. Stasiak, *Biomacromolecules* **2006**, *7*, 2128–35, DOI 10.1021/bm060089m.

[67] D. Xie, Y. Zhao, Y. Li, A. M. LaChance, J. Lai, L. Sun, J. Chen, *Materials (Basel)* **2019**, *12*, 3519, DOI 10.3390/ma12213519.

[68] V. N. Novikov, A. P. Sokolov, *Entropy (Basel)* **2022**, *24*, DOI 10.3390/e24081101.

5.5 Appendix

An overview of the methodology is given below, while full details can be accessed from: https://doi.org/10.1021/acsapm.4c01633

5.5.1 Synthesis of $TRISOXH_3$ (as reported by Golovanov *et al.* 2018)[1]

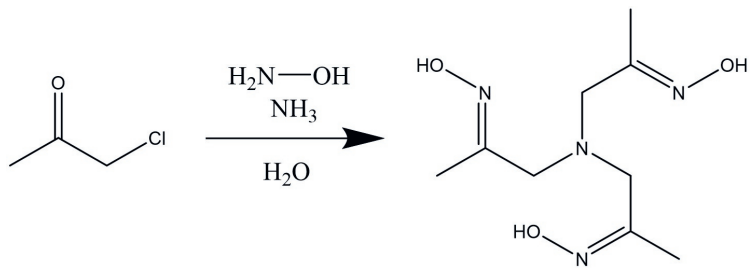

Scheme S1: *Synthesis of $TRISOXH_3$.*

In a 250-ml round bottom flask 10.2 g (146.8 mmol) of hydroxylamine hydrochloride was dissolved in 60 ml water. 60 ml of a 25% ammonium hydroxide solution in water was added. The flask was put in a water bath to provide passive cooling. Then 11.8 ml (146.8 mmol) chloroacetone was added via syringe. The reaction was stirred for 1 hour, after which the white precipitate was filtered off and washed with plenty of water and finally with diethyl ether. The white powder was then dried overnight at 50 °C in a vacuum oven. This resulted in a fine white powder (3.38 g; 29.7%).
^{1}H NMR (400 MHz, DMSO-d_6) δ 10.57 (s, 3H), 2.90 (s, 6H), 1.74 (s, 9H).

5.5.2 Synthesis of 4-vinylbenzyl bromide (as reported by Chakma *et al.* 2019)[2]

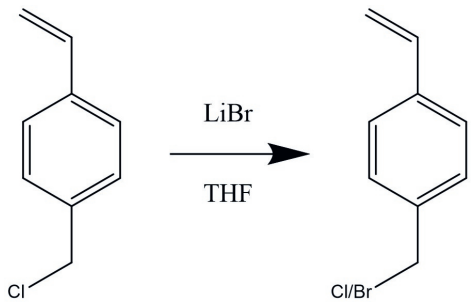

Scheme S2: *Synthesis of 4-vinylbenzyl bromide.*

In an oven heated 100-ml round bottom flask 10 g (115.1 mmol) of lithium bromide was dissolved in 50 ml anhydrous THF. To this solution 3.7 ml (26.3 mmol) of 4-vinylbenzyl chloride was added. This mixture was purged with N_2 for 30 min while in an ice bath. The solution was allowed to stir at room temperature for 24 hours. The solvent was evaporated and the residue was taken up in 30 ml water. The new yellow solution was extracted with 30 ml diethyl ether, which was then washed 4 times with 30 ml brine. After washing the organic layer was dried with magnesium sulfate and evaporated to yield a light-yellow oil. This oil was then resubmitted to the same procedure in the place of the 4-vinylbenzyl chloride to increase the bromide conversion. After three cycles in total, a yellow oil was obtained (2.84 g; 61.4%). The ratio bromide/chloride was determined via ^{1}H-NMR and was found to be 0.98.
^{1}H NMR (400 MHz, $CDCl_3$) δ 7.38 (m, 4H), 6.71 (dd, J = 17.6, 10.9 Hz, 1H), 5.77 (dd, J = 17.6, 0.9 Hz, 1H), 5.29 (dd, J = 10.9, 0.9 Hz, 1H), 4.59 (s, 0H CH_2Cl), 4.50 (s, 2H CH_2Br).

5.5.3 Polymerisation of styrene and 4-vinylbenzyl bromide

10.8 ml (93.9 mmol) of styrene (after inhibitor removal via basic aluminum oxide column) and 1.0 g (5.2 mmol) of 4-vinylbenzyl bromide were dissolved in 5 ml anhydrous toluene in a 50-ml round bottom flask. 0.020 ml (0.0033 mmol) of 0.2 M AIBN in toluene and 7.2 mg (0.0198 mmol) of 4-cyano-4-[(dodecylsulfanylthiocarbonyl)sulfanyl]pentanoic acid were added. The flask was then sealed with a septum and parafilm. The mixture was then cooled in an ice bath and purged with N_2 for 30 minutes. After purging, an argon balloon was added and the reaction mixture was

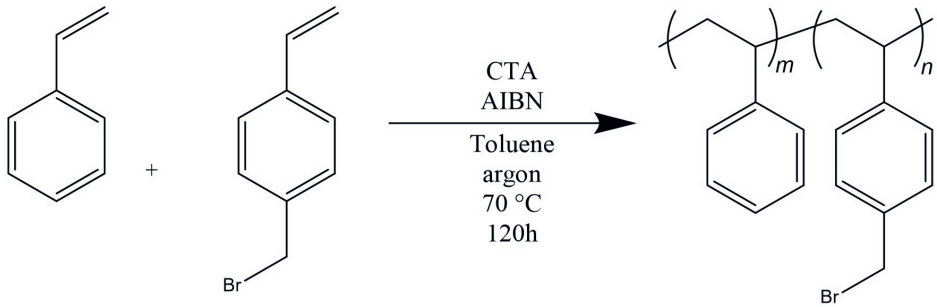

Scheme S3: *RAFT polymerisation of styrene and 4-vinylbenzyl bromide.*

heated at 70 °C for 120 hours. The reaction was quenched by introduction of oxygen and the viscous liquid was diluted with 5 ml THF. The polymer was then precipitated into ice cold methanol 2 times and finally dialysed against DCM overnight (cut-off 1 kDa). After solvent evaporation the polymer was dried in a vacuum oven overnight at 50 °C, resulting in 4.7 g product. ^{1}H NMR (400 MHz, $CDCl_3$) δ 7.66 – 6.20 (75H), 4.42 (s, 2H), 2.10-1.60 (13H), 1.43 (s, 29H).

Table S1: *Characterisation of polystyrene-co-4-vinylbenzyl bromide. Note that the used 4-vinylbenzyl bromide still contained 3.5% 4-vinylbenzyl chloride. The reported monomers incorporated are for both the bromide and the chloride monomer combined.*

M_n (g/mol)	86200
M_w (g/mol)	128200
Dispersity	1.5
Chain length	791
4-vinylbenzyl bromide/chloride in chain	5.3%
4-vinyl benzyl/chain	42

5.5.4 TAAD functionalisation of polystyrene-co-4-vinylbenzyl bromide via nitrogen quaternisation (based on Golovanov *et al.*)[1]

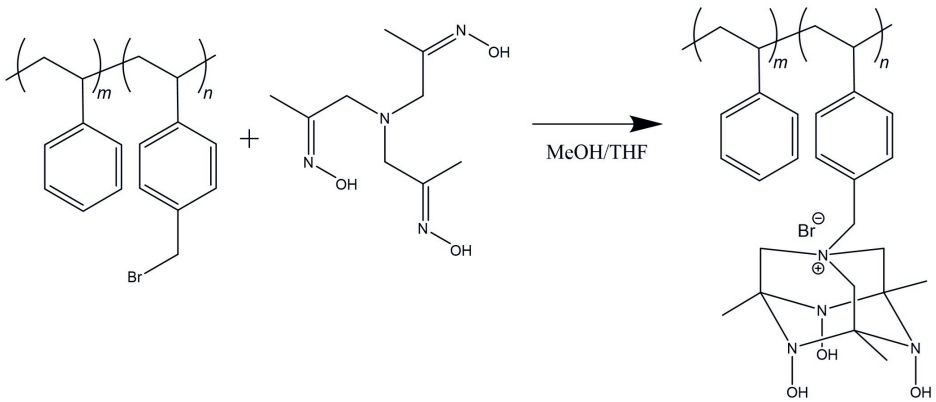

Scheme S4: *Functionalisation of polystyrene-co-4-vinylbenzyl bromide with $TRISOXH_3$ via nitrogen quaternisation to produce a TAAD-functionalised polystyrene named* ***PS-TAAD****.*

4.5 g (0.052 mmol) of polystyrene-co-4-vinylbenzyl bromide and 0.76 g (3.3 mmol) of $TRISOXH_3$ were dissolved in 115 ml THF/MeOH 60/40. The reaction was then stirred for 7 days at room temperature. The volume was reduced and the product was precipitated in diethyl ether 2 times. The product was then collected via vacuum filtration and dried in a vacuum oven at 50 °C overnight. This resulted in a white powder (3.72 g, ≈100% functionalisation as determined by NMR).
^{1}H NMR (400 MHz, DMSO-d_6) δ 8.55 (m, 3H), 6-7.5 (74H), 4.46 (s, 2H), 2.12 - 0.71 (49H).

5.5.5 Synthesis of bisboronic acid crosslinker CLA (adapted from Boa *et al.* 2018)[3]

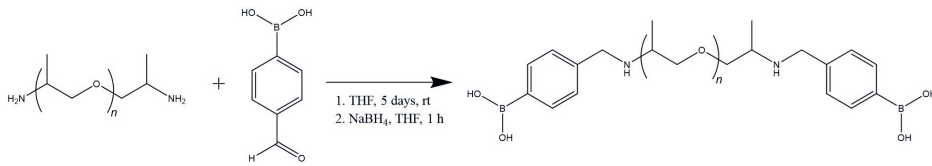

Scheme S5: *Synthesis of boronic acid linker CLA.*

13.0 ml (6.5 mmol) poly(propylene glycol) bis(2-aminopropyl ether) M_n 2000 and 3.76 g (16.3 mmol) 4-formylphenylboronic acid were dissolved in 40 ml anhydrous THF under nitrogen and stirred for 5 days. The solution was then cooled in an ice batch. Then 0.81 g (21.4 mmol) $NaBH_4$ was added slowly. The solution was stirred for 1 hour at room temperature, after which it was dialysed (1 kDA cut-off) against H_2O/MeOH (50/50) for 2 days. After evaporation of the solvent a yellow/greenish sticky plaque was obtained (14.4 g; 86.4%)

^{1}H NMR (400 MHz, MeOD) δ 7.47 (d, J = 7.4 Hz, 4H), 7.14 (d, J = 7.7 Hz, 4H), 3.83 (dq, J = 24.3, 12.4, 11.9 Hz, 3H), 3.59 – 3.22 (m, 106H), 1.04 (dd, J = 6.5, 3.1 Hz, 105H).

^{13}C NMR (101 MHz, MeOD) δ 208.93, 163.45, 133.51, 133.18, 132.93, 132.45, 129.58, 128.21, 126.92, 126.60, 125.43, 75.54, 75.50, 75.42, 75.40, 75.31, 75.28, 75.17, 75.15, 75.08, 75.03, 74.98, 74.95, 73.30, 72.99, 72.93, 72.72, 72.69, 72.62, 72.57, 66.52, 64.27, 56.29, 56.08, 55.86, 52.30, 52.03, 51.89, 50.05, 49.96, 49.85, 48.49, 48.28, 48.06, 47.85, 47.64, 47.42, 47.21, 47.00, 46.44, 39.10, 35.57, 30.29, 28.78, 28.58, 28.39, 17.38, 17.16, 17.02, 16.35, 16.30, 16.25, 16.01, 15.84, 15.77, 14.53.

5.5.6 Material preparation

General protocol

100 mg (0.001 mmol polymer; 0.044 mmol TAAD) **PS-TAAD** was dissolved in 0.2 ml DMF. Then 49.9/37.4/24.9/12.5 mg (0.022/0.017/0.011/0.006 mmol; respectively for 100%/75%/50%/25%) CLA was dissolved separately in 0.1 ml methanol. The solutions were mixed and vortexed for 10 seconds, after which it was quickly transferred divided over 2 silicon molds (r = 10 mm, h = 1 mm) via syringe.
Note: after mixing the stock solutions, crosslinking will immediately start. Make sure you have the vortex, syringe and mold at hand when you begin. After 20-30 seconds it will be difficult for the material to exit the syringe. The solutions were mixed and vortexed for 10 seconds, after which it was quickly transferred to a silicon mold (r = 10 mm, h = 1 mm) via syringe.

Protocol for PTSA containing samples

50 mg (0.0005 mmol polymer; 0.022 mmol TAAD) **PS-TAAD** was dissolved in 0.1 ml DMF. Then 24.9 mg (0.011) CLA was dissolved separately in 0.1 ml methanol. Also 0.8/3.9/8.3 mg (for 1%, 5% and 10%) PTSA was dissolved separately in 0.1 ml methanol.

5.5.7 Solvent study

The solvent study was performed by putting ≈5 mg material in 10 ml solvent and letting it swell overnight. The material was then carefully removed from the solvent, excess solvent was removed with a tissue. Then the material was placed on a weighted glass Petri dish and the swollen weight was measured. The material was then dried overnight in a vacuum oven at 50 °C after which the material was weighted again to determine the remaining fraction.

5.5.8 References

[1] I. S. Golovanov, G. S. Mazeina, Y. V. Nelyubina, R. A. Novikov, A. S. Mazur, S. N. Britvin, V. A. Tartakovsky, S. L. Ioffe, A. Y. Sukhorukov, *J. Org. Chem.* **2018**, *83*, 9756–9773, DOI 10.1021/acs.joc.8b01296.

[2] P. Chakma, Z. A. Digby, M. P. Shulman, L. R. Kuhn, C. N. Morley, J. L. Sparks, D. Konkolewicz, *ACS Macro. Lett.* **2019**, *8*, 95–100, DOI 10.1021/acsmacrolett.8b00819.

[3] C. Y. Bao, Y. J. Jiang, H. Y. Zhang, X. Y. Lu, J. Q. Sun, *Adv. Funct. Mater.* **2018**, *28*, 1800560, DOI 10.1002/adfm.201800560.

Chapter 6

General Discussion

6.1 Introduction

The general aim of this thesis was to bring new (boronate ester-based) dynamic bonds into covalent adaptable networks (CANs), and to study how the macroscopic material properties of these CANs can be tuned by molecular-level control over their constituents. Chapter 2 focused on furan-maleimide networks with differently substituted maleimide linkers to study if and how the variation of electronic properties of substituents can be used to tune material properties. Chapter 3 introduced a novel family of CANs by introducing the boronate-TAAD motif in dynamic networks. Chapter 4 built on the knowledge obtained in chapter 3 and investigated the structure-property relationships in dynamic boronate-TAAD networks by evaluating the effect of different electronic groups on (macroscopic) material properties. Chapter 5 used the boronate-TAAD motif to convert thermoplastic polystyrene to a CAN, to showcase how this dynamic motif can be used to create new CANs from polymers with established beneficial properties using polystyrene as a model system.
Besides the subjects discussed in the research chapters of this thesis, there are still many interesting topics left for future research projects. Here some prospects will be discussed. In addition, the wider context of the research is discussed.

6.2 Reflections

The work presented in this thesis aimed to advance the field of covalent adaptable networks. Although chapter 2 requires further studies to understand the exact details of the relationship between the electronic substituents of the monomers and the macroscopic material properties, the study does present strong indications as to what conclusions could be

expected from further research on this topic. The work hints that the material properties of these furan-maleimide networks cannot be directly tuned through electronic substituents even though the molecular dynamics of the dynamic furan-maleimide bond can.

Chapter 3 provides a more direct contribution by introducing a new type of dynamic motif to the field of CANs, namely the boronate-TAAD-based moiety. This dynamic motif had made a brief appearance as a COF-like in the study by Golovanov *et al.*,[1] however the properties of the motif had not been studied and evaluated as a CAN. This chapter firmly adds the boronate-TAAD motif to the already extensive list of possible CANs. More diverse CANs will allow material scientists to better select the precise CAN they need for a specific application. This is then further explored in chapter 4 where a boronate-TAAD CAN is compared to the conventional boronic ester CANs. This comparison shows the possible differences, both positives and negatives, in performance between the two similar CANs. This can help others to make more informed decisions when selecting which type of CANs to use for certain applications.

Chapter 5 deals with the conversion of widely-used linear polymers into CANs as a method to generate recyclable, crosslinked networks with properties more closely related to the linear polymers of which the network is based upon. Generally, these linear polymers have desirable properties *e.g.*, low-cost and ease-of-use, which can be at least partially imparted on the new CAN using these conversions while also adding the mechanical benefits of covalent crosslinks between the polymers. The possibility of using the addition of acid to the network in order to tune the properties of these new boronate-TAAD CANs is also explored in chapters 3 and 5. While this was already explored in other CANs,[2–4] the work in these two chapters show that the acid-controlled tuning of boronate-TAAD CAN properties can also be achieved, depending on the polymer matrix of the CAN. It remains a topic of discussion whether the tuning of material properties through the use of external catalysts as additives is a desired method.[5] The catalyst is not connected to the polymer network and can, and eventually likely: will, thus leach from the CAN.[6] The leached additives can then have negative environmental consequences.[7] In addition, the remaining polymer network will no longer be dynamic (*e.g.*, it will stop being recyclable and/or self-healing) after the catalyst has leached out. This can be largely negated by switching to internal catalysis in which the catalytic moiety is covalently incorporated in the polymer

network.[8] Combining these chapters, a new promising dynamic-covalent bond has been added to the toolbox of CANs: the boronate-TAAD CANs. The introduction of these CANs and the subsequent exploration of their properties adds to the collective knowledge necessary for the (eventual) industrial and societal transition towards a circular polymer economy.

6.3 Future research prospects

6.3.1 Tetraazaadamantane derivatisation

The research described in this thesis focussed on the use of the archetypical, original TAAD group, as reported first by the group of Sukhorukov.[9] Apart from this initial work, the same group showed that different variants of the TAAD moiety could be synthesised by utilising different starting compounds.[1,9,10] However, this work mostly focused on the synthesis of asymmetrical TAAD variants that feature different R groups as side groups appended to the lower ring of the TAAD moiety.[9,11] This derivatisation was of interest as the TAAD moiety has a structure similar to hexamethylenetetramine (hexamine/urotropine), which has found broad applicability in organic, medicinal and material chemistry due to it being a versatile coordination ligand.[12–15] Most derivatives of hexamethylenetetramine are thermodynamically unstable, in contrast to the stable derivatives of the TAAD moiety.[9] Being able to replace one or two of the hydroxyl groups of the original TAAD group, as depicted in **Figure 6.1**, would also be interesting, for it would allow the introduction of functional groups that could change the dynamic motif from a boronate to a boronic ester. The boronic-TAAD motif is then expected to have a lower binding affinity to the selectively capped TAAD, since it would involve bidentate instead of tridentate binding, which would make the boronic-TAAD more dynamic than the boronate-TAAD. These motifs could then be combined in a network to tune the dynamic material properties of the resulting CAN in terms of network relaxation and creep based on the ratio between the more stable boronate-TAAD and the more dynamic boronic-TAAD.[16] The bidentate or tridentate binding of the boronic- or boronate-TAAD could be experimentally confirmed using the fluorescent biphenylboronic acid probe developed by Oesch *et al.*, which red shifts upon tridentate binding of the boronic acid and not upon bidentate binding.[17]

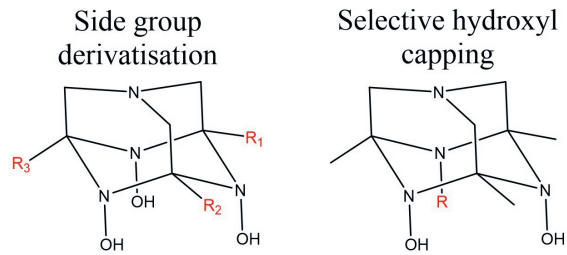

Figure 6.1: *General structure of the side chain derivatives of TAAD developed by Semakin et al. (2009)[9] (left) and the new proposed derivative with only two hydroxyl groups (right).*

Several routes have been proposed to selective modify the hydroxyl groups of TAAD derivatives, such as a selective reaction with isocyanates using dibutyltin dilaurate (DBTDL),[18] selective protection of two hydroxyl groups with 1,3-dichloro-1,1,3,3-tetraisopropyldisiloxane ($TIPDSiCl_2$) and subsequent capping of the final hydroxyl using acetyl chloride or iodomethane,[19] or oxime exchange to generate derivatives of $TRISOXH_3$ (tri-functional oxime precursor of TAAD).[20] Unfortunately, preliminary work I performed using these proposed routes did not yield controlled, selective capping of the hydroxyl groups. Most experiments gave a mixture of TAAD with all three hydroxyls capped, a large amount of unreacted TAAD and trace amounts of once or twice capped TAAD products when tested by TLC.

The group of Sukhorukov, facing similar difficulties with the derivatisation of the hydroxyl groups of the TAAD moiety, went back to their original synthesis of asymmetric TAAD moieties and managed to prepare a TAAD derivative with only two hydroxyl groups, with the third group being replaced with a hydrazine as shown in **Scheme 6.1**. This does open up new possibilities as a terminal hydrazine group can be an interesting functional group for boronic acids, and is known to interact with amine functionalities. In fact, an amine in close proximity to a boronic ester can speed up the exchange rate by over several orders of magnitude.[21] However, dehydration of hydrazones can lead to irreversible binding of the boronic acid.[22,23]

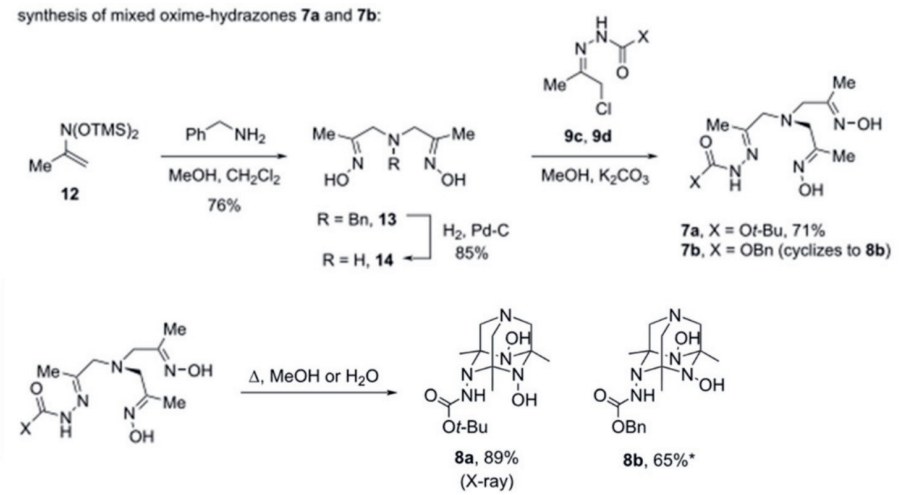

Scheme 6.1: *Synthesis of hydrazine-TAAD variants by Semakin et al. (2022).*[24]

6.3.2 Tuning boronic acid-based CANs through (an)ionic interactions

Kang *et al.* showed that the relaxation time and the storage modulus of boronic acid-based CANs can be tuned via the addition of a selection of salts.[25] However, the study only encompassed a limited selection of salts with different cation and anion combinations. This makes it difficult to differentiate the possible effect cations or anions, or both, have on the dynamics of the boronic ester motif. Boronic acids are also known to have interactions with anions, including but not limited to fluoride, cyanide and metal ions (through second-sphere coordination).[26–29] Not only can it be interesting to study how the properties of boronic acid-based CANs could be tuned through interactions between boronic acids and fluoride or cyanide, these interactions could also be interesting for the development of boronic acid-based CANs as sensors for fluoride or cyanide. An effort was made to prepare dynamically crosslinked hydrogels using boronic esters that could be used to study these interactions. This was done by functionalising poly(allylamine hydrochloride) (PAH) with boronic acids (**Scheme 6.2**) through EDC/NHS coupling, as has been used for the preparation of ionic membranes.[30,31] This resulted in functionalised PAH with four different boronic acids (9-13% functionalisation based on ^{1}H-NMR; -H, -F, -OMe, -NO_2 at the *meta* position relative to the boronic acid). This series of functionalised PAH with differently substi-

tuted boronic acids was also used to study the tunability of boronic ester-based CANs through electronic ring substituents, similar to the study on the tunability of boronate-TAAD networks in chapter 4. Unfortunately, the formed hydrogels were difficult to study and the characterisation of these gels proved irreproducible.

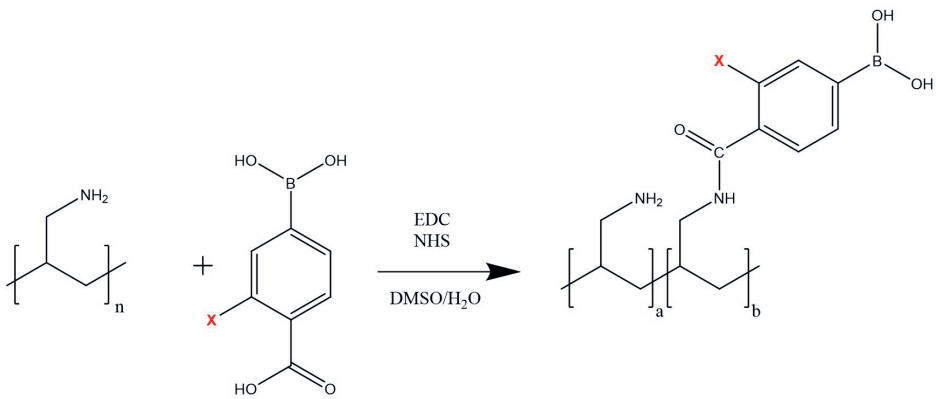

X = -H, -F, -OMe, NO_2, $-CF_3$

Scheme 6.2: *Synthesis of boronic acid functionalised poly(allylamine hydrochloride) variants.*

Using the knowledge on boronate-TAAD networks obtained in chapters 3, 4 and 5 it is now possible to prepare boronate-TAAD-based gels that can be used to study these interactions in detail. Especially chapter 5 already shows that these networks can be tuned through external catalysis, as shown through the incorporation of acid in the polystyrene-based network.

6.3.3 Boronic acid metal coordination

There is already evidence that the properties of covalent adaptable networks can be influenced by the incorporation of metal ions. For example, metal catalysis has been shown for epoxy networks[32] and metal coordination has been shown for oxime[33] and imine networks.[34] Boronic acids also show interactions with various transition metals though this generally leads to deborylation, most famous of all with palladium(II) in the Suzuki coupling,[35] but also nickel(II)[36,37] or copper(I or II).[38,39] Interestingly enough, phenylboronic acids do not seem to form dative bonds with some common transition metals and instead the interaction between the boronic acid and the metal seems to be through second-sphere coordination with water.[29] Borates by themselves do form complexes with

(transition) metals.[40,41] Unfortunately, there are not many reports on metal complexes involving boronic acids or boronates in general, with no known works involving the effects of metal complexation on boronic acid-based CANs. The review of Sene *et al.* from 2016 gives the most complete overview of the few studies available on the boronic acid-based metal complexes.[42] The work by Reinholdt *et al.* shows that boronic acids can form complexes with calcium, strontium (hydrate) and barium.[43] This suggests that boronic acids are capable to form complexes with various alkaline earth metals. It might be interesting to study if incorporating alkaline earth metals in polymer networks containing boronic acids results in the formation of a dynamic metal-coordinated network, similar to how transition metals have been used to construct (supramolecular) metal-coordinated networks.[44–47] Further research is needed to study if and how coordinating metal ions to boronic esters could be used to modulate the exchange dynamics of this dynamic motif in a CAN.
Another interesting work by Fan *et al.* shows phenylboronic acids coordinating to various lanthanides to make coordination polymers.[48] The possibility to incorporate lanthanides into CANs could prove interesting, especially for medical applications where lanthanides can be used as fluorescent and/or magnetic contrast agents.[49,50] Lanthanide complexes are also used for therapeutical applications, such as anticancer agents in chemotherapies.[51–53] Boronic acids have already been used in responsive hydrogels for drug release[54–57] and (fluorescence-based) imaging[58–60] purposes. Further research is needed to test if alkaline- or lanthanide-coordination complexes can be used in boronic acid-based CANs.

6.4 Current developments towards a circular polymer economy

6.4.1 Composites

One of the biggest issues at the moment in the field of CANs is the creep these materials tend to display. The dynamic bonds allow for exchange and thus flow of the material. This creep is undesired around temperatures where the material is to be used, since the material will simply deform over time under the effect of gravity or of an imposed load. By combining CANs with fibres to create composites, it is possible improve the mechanical strength and thus (largely) negate creep behaviour in a material.[61,62] The downside is that composites are more difficult to recycle, due to the introduction of the fibres. Still, this has great potential, not

only since reprocessable composites would be a big step towards creating a circular polymer economy, but it could also contribute to the green energy transition, *e.g.*, by allowing recycling of wind turbine blades, which typically are based on composites.[63]

Typically, the incorporated fibres are not part of the polymer network, such as is generally the case for carbon fibres,[64,65] however boronic acid-based CANs can covalently incorporate cellulose fibres, since those fibres contain hydroxyl groups that can be dynamically bound by the boronic acids. Shi *et al.* have already shown that incorporation of nanocellulose fibres can enhance the mechanical strength of boronic acid-based CANs.[66] Du *et al.* were able to show that incorporating small amounts of the stiffer nanocellulose crystals increases the storage modulus of those materials at least seven-fold compared to the control networks.[67] More work will need to be done to investigate how the incorporation of nanocellulose fibres or crystals affects the dynamics of the CAN and if these networks can remain easily reprocessable at the higher stiffness after the creation of the composite.

6.4.2 Supramolecular networks

CANs are not the only materials by which a circular polymer economy might be realised. One other class of materials that is currently being explored are the supramolecular polymer networks.[68,69] These networks utilise dynamic non-covalent interactions to form networks with exchanging crosslinks in contrast to the dynamic covalent bonds in CANs. Since non-covalent interactions tend to be less strong than covalent bonds, these networks generally try to make up for this difference in bond strength by combining a multitude of non-covalent bonds in non-covalent motifs,[70] such as the UPy motif which uses multiple hydrogen bonds to form a supramolecular crosslink.[71] Other non-covalent interactions used in these non-covalent networks include metal-ligand interactions,[44,72] host-guest chemistry,[73,74] Van der Waals forces[75] and π-π interactions.[76] Sometimes the properties of supramolecular networks are enhanced through the introduction of some (dynamic) covalent backbone.[77] The opposite is used as well to increase the stress dissipation of covalently crosslinked networks by introducing sacrificial non-covalent interactions.[78] These hybrid networks CANs with some incorporated supramolecular bonds have the potential to be more mechanically robust materials that still can be reprocessed quite easily and display self-healing behaviour, although this topic needs further exploration.[79,80]

6.4.3 Reversible-deactivation radical (de)polymerisation

The discovery of controlled depolymerisation of polymers synthesised using RAFT agents[81] or ATRP[82] is a potentially powerful method for achieving a circular polymer economy. There has even been the first experimental success on the depolymerisation of gels.[83] This method has a lot of potential since no major changes have to be made to the molecular structure of existing polymers, as would be the case for switching to CANs or supramolecular networks. This has a high probability to preserve the existing polymer characteristics. However, this method is dependent on two things. The first is that the production process of existing polymers has to be switched to RAFT polymerisations. This might make commodity polymers more expensive, since a RAFT agent has to be added for the polymerisation. The polymerisation itself will also likely require more time as RAFT is a controlled polymerisation technique and thus slows down the polymerisation reaction to achieve control. The second requirement is that the depolymerisation can only occur if the RAFT moiety is still part of the polymer. If the RAFT moiety is removed by choice or by gradual degradation, then the polymer can no longer be depolymerised. Depolymerisation using ATRP is also viable and has mostly caught up to the RAFT depolymerisation.[84,85]

Reversible-deactivation radical depolymerisation could be easily implemented by using a polymer backbone, prepared using RAFT or ATRP, as the scaffold to attach the dynamic functional group on. An example of what such a network might look like can be found in chapter 5, where RAFT was used to prepare polystyrene polymers, which were then crosslinked using dynamic boronate-TAAD chemistry. During normal operations, the CAN would display dynamic bond exchange while being mechanically reinforced by the polymer backbone.[86] The CAN could then be reprocessed using the dynamic bonds, or completely recycled back to its monomers by opening the dynamic bonds and performing the depolymerisation.

6.5 Closing remarks

As shown in this chapter, and discussed in the previous chapters, CANs display a great potential in the transition towards a circular polymer economy. New and improved CANs are continuously developed. The first commercial CAN composites are slowly entering the market through companies like ATSP Innovations and Mallinda. However, there still remains a lot of research needed before CANs can fully replace commodity plastics.

References

[1] I. S. Golovanov, G. S. Mazeina, Y. V. Nelyubina, R. A. Novikov, A. S. Mazur, S. N. Britvin, V. A. Tartakovsky, S. L. Ioffe, A. Y. Sukhorukov, *J. Org. Chem.* **2018**, *83*, 9756–9773, DOI 10.1021/acs.joc.8b01296.

[2] Y. Spiesschaert, C. Taplan, L. Stricker, M. Guerre, J. M. Winne, F. E. Du Prez, *Polym. Chem.* **2020**, *11*, 5377–5385, DOI 10.1039/d0py00114g.

[3] J. L. Self, N. D. Dolinski, M. S. Zayas, J. Read de Alaniz, C. M. Bates, *ACS Macro. Lett.* **2018**, *7*, 817–821, DOI 10.1021/acsmacrolett.8b00370.

[4] W. Denissen, M. Droesbeke, R. Nicolay, L. Leibler, J. M. Winne, F. E. Du Prez, *Nat. Commun.* **2017**, *8*, 14857, DOI 10.1038/ncomms14857.

[5] L. L. Robinson, E. S. Taddese, J. L. Self, C. M. Bates, J. Read de Alaniz, Z. Geng, C. J. Hawker, *Macromolecules* **2022**, *55*, 9780–9789, DOI 10.1021/acs.macromol.2c01618.

[6] D. Berne, B. Quienne, S. Caillol, E. Leclerc, V. Ladmiral, *J. Mater. Chem. A* **2022**, *10*, 25085–25097, DOI 10.1039/d2ta05067f.

[7] J. H. Bridson, E. C. Gaugler, D. A. Smith, G. L. Northcott, S. Gaw, *J. Hazard. Mater.* **2021**, *414*, 125571, DOI 10.1016/j.jhazmat.2021.125571.

[8] A. Hernández, H. A. Houck, F. Elizalde, M. Guerre, H. Sardon, F. E. Du Prez, *Eur. Polym. J.* **2022**, *168*, 111100, DOI 10.1016/j.eurpolymj.2022.111100.

[9] A. N. Semakin, A. Y. Sukhorukov, A. V. Lesiv, S. L. Ioffe, K. A. Lyssenko, Y. V. Nelyubina, V. A. Tartakovsky, *Org. Lett.* **2009**, *11*, 4072–5, DOI 10.1021/ol9015157.

[10] I. S. Golovanov, A. Y. Sukhorukov, Y. V. Nelyubina, Y. A. Khomutova, S. L. Ioffe, V. A. Tartakovsky, *J. Org. Chem.* **2015**, *80*, 6728–36, DOI 10.1021/acs.joc.5b00892.

[11] A. N. Semakin, I. S. Golovanov, A. Y. Sukhorukov, S. L. Ioffe, V. A. Tartakovsky, *Russ. Chem. Bull.* **2016**, *65*, 2270–2277, DOI 10.1007/s11172-016-1577-7.

[12] A. M. Kirillov, *Coord. Chem. Rev.* **2011**, *255*, 1603–1622, DOI 10.1016/j.ccr.2011.01.023.

[13] S. Zheng, M. Tong, X. Chen, *Coord. Chem. Rev.* **2003**, *246*, 185–202, DOI 10.1016/s0010-8545(03)00116-4.

[14] N. Blažzević, D. Kolbah, B. Belin, V. Šunjić, F. Kajfež, *Synthesis* **1979**, *1979*, 161–176, DOI 10.1055/s-1979-28602.

[15] J. Tian, J. Wu, Y. Lin, J. Geng, J. Shi, W. Lin, W. Hao, C. Ke, J. Yang, W. Sun, Z. Lan, *Energy Technol.* **2023**, *11*, 2201182, DOI 10.1002/ente.202201182.

[16] V. Yesilyurt, A. M. Ayoob, E. A. Appel, J. T. Borenstein, R. Langer, D. G. Anderson, *Adv. Mater.* **2017**, *29*, 1605947, DOI 10.1002/adma.201605947.

[17] D. Oesch, N. W. Luedtke, *Chem. Commun. (Camb)* **2015**, *51*, 12641–4, DOI 10.1039/c5cc03857j.

[18] S. Okamoto, S. Onoue, M. Kobayashi, A. Sudo, *J. Polym. Sci. Part A: Polym. Chem.* **2014**, *52*, n/a–n/a, DOI 10.1002/pola.27414.

[19] J. Desire, J. Prandi, *Carbohydr. Res.* **1999**, *317*, 110–8, DOI 10.1016/s0008-6215(99)00078-6.

[20] S. Mukherjee, M. R. Hill, B. S. Sumerlin, *Soft Matter* **2015**, *11*, 6152–61, DOI 10.1039/c5sm00865d.

[21] O. R. Cromwell, J. Chung, Z. Guan, *J. Am. Chem. Soc.* **2015**, *137*, 6492–5, DOI 10.1021/jacs.5b03551.

[22] H. Gu, T. I. Chio, Z. Lei, R. J. Staples, J. S. Hirschi, S. Bane, *Org. Biomol. Chem.* **2017**, *15*, 7543–7548, DOI 10.1039/c7ob01708a.

[23] H. Gu, S. Ghosh, R. J. Staples, S. L. Bane, *Bioconjug. Chem.* **2019**, *30*, 2604–2613, DOI 10.1021/acs.bioconjchem.9b00534.

[24] A. N. Semakin, I. S. Golovanov, Y. V. Nelyubina, A. Y. Sukhorukov, *Beilstein J. Org. Chem.* **2022**, *18*, 1424–1434, DOI 10.3762/bjoc.18.148.

[25] B. Kang, J. A. Kalow, *ACS Macro. Lett.* **2022**, *11*, 394–401, DOI 10.1021/acsmacrolett.2c00056.

[26] A. Yuchi, J. Sakurai, A. Tatebe, H. Hattori, H. Wada, *Anal. Chim. Acta* **1999**, *387*, 189–195, DOI Doi10.1016/S0003-2670(99)00089-6.

[27] Z. Guo, I. Shin, J. Yoon, *Chem. Commun. (Camb)* **2012**, *48*, 5956–67, DOI 10.1039/c2cc31985c.

[28] C. R. Wade, A. E. Broomsgrove, S. Aldridge, F. P. Gabbai, *Chem. Rev.* **2010**, *110*, 3958–84, DOI 10.1021/cr900401a.

[29] N. SeethaLekshmi, V. R. Pedireddi, *Inorg. Chem.* **2006**, *45*, 2400–2, DOI 10.1021/ic052100h.

[30] J. Ciejka, M. Grzybala, A. Gut, M. Szuwarzynski, K. Pyrc, M. Nowakowska, K. Szczubialka, *Materials (Basel)* **2021**, *14*, 2361, DOI 10.3390/ma14092361.

[31] V. Motta, M. Schäfer, J. Hühn, R. Zierold, R. H. Blick, W. J. Parak, K. Weitzel, *Adv. Mater. Inter.* **2020**, *7*, 2000419, DOI 10.1002/admi.202000419.

[32] M. Capelot, D. Montarnal, F. Tournilhac, L. Leibler, *J. Am. Chem. Soc.* **2012**, *134*, 7664–7667, DOI 10.1021/ja302894k.

[33] L. Zhang, Z. Liu, X. Wu, Q. Guan, S. Chen, L. Sun, Y. Guo, S. Wang, J. Song, E. M. Jeffries, C. He, F. L. Qing, X. Bao, Z. You, *Adv. Mater.* **2019**, *31*, e1901402, DOI 10.1002/adma.201901402.

[34] S. K. Schoustra, M. M. J. Smulders, *Macromol. Rapid. Commun.* **2023**, *44*, e2200790, DOI 10.1002/marc.202200790.

[35] K. Osakada, Y. Nishihara, *Dalton Trans.* **2022**, *51*, 777–796, DOI 10.1039/d1dt02986j.

[36] L. Chen, J. C. Yang, P. Xu, J. J. Zhang, X. H. Duan, L. N. Guo, *J. Org. Chem.* **2020**, *85*, 7515–7525, DOI 10.1021/acs.joc.0c00250.

[37] J. Wang, T. Qin, T. G. Chen, L. Wimmer, J. T. Edwards, J. Cornella, B. Vokits, S. A. Shaw, P. S. Baran, *Angew. Chem. Int. Ed. Engl.* **2016**, *55*, 9676–9, DOI 10.1002/anie.201605463.

[38] J. J. Molloy, K. M. O'Rourke, C. P. Frias, N. L. Sloan, M. J. West, S. L. Pimlott, A. Sutherland, A. J. B. Watson, *Org. Lett.* **2019**, *21*, 2488–2492, DOI 10.1021/acs.orglett.9b00942.

[39] A. Salamé, J. Rio, I. Ciofini, L. Perrin, L. Grimaud, P. Payard, *Molecules* **2022**, *27*, 7517, DOI 10.3390/molecules27217517.

[40] A. Bousher, *J. Coord. Chem.* **2006**, *34*, 1–11, DOI 10.1080/00958979508024298.

[41] G. N. Mukherjee, A. Das, *J. Indian Chem. Soc.* **2002**, *79*, 45–47.

[42] S. Sene, M. A. Pizzoccaro, J. Vezzani, M. Reinholdt, P. Gaveau, D. Berthomieu, S. Bégu, C. Gervais, C. Bonhomme, G. Renaudin, A. Mesbah, A. van der Lee, M. E. Smith, D. Laurencin, *Crystals* **2016**, *6*, 48, DOI 10.3390/cryst6050048.

[43] M. Reinholdt, J. Croissant, L. Di Carlo, D. Granier, P. Gaveau, S. Begu, J. M. Devoisselle, P. H. Mutin, M. E. Smith, C. Bonhomme, C. Gervais, A. van der Lee, D. Laurencin, *Inorg. Chem.* **2011**, *50*, 7802–10, DOI 10.1021/ic200961a.

[44] D. J. Lundberg, C. M. Brown, E. O. Bobylev, N. J. Oldenhuis, Y. S. Alfaraj, J. Zhao, I. Kevlishvili, H. J. Kulik, J. A. Johnson, *Nat. Commun.* **2024**, *15*, 3951, DOI 10.1038/s41467-024-47666-x.

[45] M. Ahmadi, S. Seiffert, *Soft Matter* **2020**, *16*, 2332–2341, DOI 10.1039/c9sm02149c.

[46] W. Chang, W. Song, M. Zhang, P. Yin, *Chempluschem* **2024**, *n/a*, e202400270, DOI 10.1002/cplu.202400270.

[47] R. D. Mukhopadhyay, A. Ajayaghosh, *Chem. Soc. Rev.* **2023**, *52*, 8635–8650, DOI 10.1039/d3cs00692a.

[48] X. Fan, S. Freslon, C. Daiguebonne, L. L. Polles, G. Calvez, K. Bernot, X. Yi, G. Huang, O. Guillou, *Inorg. Chem.* **2015**, *54*, 5534–46, DOI 10.1021/acs.inorgchem.5b00635.

[49] Virender, A. Chauhan, A. Kumar, G. Singh, A. A. Solovev, J. Xiong, X. Liu, B. Mohan, *J. Rare Earth.* **2024**, *42*, 16–27, DOI 10.1016/j.jre.2023.02.006.

[50] Q. Zhang, S. O'Brien, J. Grimm, *Nanotheranostics* **2022**, *6*, 184–194, DOI 10.7150/ntno.65530.

[51] N. S. Chundawat, S. Jadoun, P. Zarrintaj, N. P. S. Chauhan, *Polyhedron* **2021**, *207*, 115387, DOI 10.1016/j.poly.2021.115387.

[52] G. Bao, *J. Lumin.* **2020**, *228*, 117622, DOI 10.1016/j.jlumin.2020.117622.

[53] M. Patyal, K. Kaur, N. Bala, N. Gupta, A. K. Malik, *J. Trace Elem. Med. Biol.* **2023**, *80*, 127277, DOI 10.1016/j.jtemb.2023.127277.

[54] Z. Huang, P. Delparastan, P. Burch, J. Cheng, Y. Cao, P. B. Messersmith, *Biomater. Sci.* **2018**, *6*, 2487–2495, DOI 10.1039/c8bm00453f.

[55] V. Yesilyurt, M. J. Webber, E. A. Appel, C. Godwin, R. Langer, D. G. Anderson, *Adv. Mater.* **2016**, *28*, 86–91, DOI 10.1002/adma.201502902.

[56] Y. Dong, W. Wang, O. Veiseh, E. A. Appel, K. Xue, M. J. Webber, B. C. Tang, X. W. Yang, G. C. Weir, R. Langer, D. G. Anderson, *Langmuir* **2016**, *32*, 8743–7, DOI 10.1021/acs.langmuir.5b04755.

[57] Y. Xiang, B. Su, D. Liu, M. J. Webber, *Adv. Therap.* **2023**, *7*, 2300127, DOI 10.1002/adtp.202300127.

[58] G. Fang, H. Wang, Z. Bian, J. Sun, A. Liu, H. Fang, B. Liu, Q. Yao, Z. Wu, *RSC Adv.* **2018**, *8*, 29400–29427, DOI 10.1039/c8ra04503h.

[59] Y. Chu, D. Wang, K. Wang, Z. L. Liu, B. Weston, B. Wang, *Bioorg. Med. Chem. Lett.* **2013**, *23*, 6307–9, DOI 10.1016/j.bmcl.2013.09.063.

[60] Y. Wang, Y. Zhu, X. Zhang, F. Zhu, Y. Qin, W. Chen, Q. Zheng, *Chem. Eng. J.* **2022**, *450*, 137930, DOI 10.1016/j.cej.2022.137930.

[61] Y. Zhang, L. Zhang, G. Yang, Y. Yao, X. Wei, T. Pan, J. Wu, M. Tian, P. Yin, *J. Mater. Sci. Tech.* **2021**, *92*, 75–87, DOI 10.1016/j.jmst.2021.03.043.

[62] P. Taynton, H. Ni, C. Zhu, K. Yu, S. Loob, Y. Jin, H. J. Qi, W. Zhang, *Adv. Mater.* **2016**, *28*, 2904–9, DOI 10.1002/adma.201505245.

[63] D. A. Kissounko, P. Taynton, C. Kaffer, *Reinforc. Plast.* **2018**, *62*, 162–166, DOI 10.1016/j.repl.2017.06.084.

[64] B. Zhang, T. Cui, X. Jiao, Y. Ma, L. Gao, J. Hu, *Chem. Eng. J.* **2023**, *476*, 146625, DOI 10.1016/j.cej.2023.146625.

[65] C. Cui, X. Chen, L. Ma, Q. Zhong, Z. Li, A. Mariappan, Q. Zhang, Y. Cheng, G. He, X. Chen, Z. Dong, L. An, Y. Zhang, *ACS Appl. Mater. Interfaces.* **2020**, *12*, 47975–47983, DOI 10.1021/acsami.0c14189.

[66] Y. Shi, Y. Hong, J. Hong, A. Yu, M. W. Lee, J. Lee, M. Goh, *Compos. B Eng.* **2022**, *244*, 110181, DOI 10.1016/j.compositesb.2022.110181.

[67] W. Du, A. Deng, J. Guo, J. Chen, H. Li, Y. Gao, *Carbohydr. Polym.* **2019**, *223*, 115084, DOI 10.1016/j.carbpol.2019.115084.

[68] A. D. O'Donnell, S. Salimi, L. R. Hart, T. S. Babra, B. W. Greenland, W. Hayes, *React. Funct. Polym.* **2022**, *172*, 105209, DOI 10.1016/j.reactfunctpolym.2022.105209.

[69] M. Ilyas, S. Imran, M. Ahmad Khan, Z. Ahmad, A. Ihsan, S. Qadir, A. Saba, *J. Mol. Liq.* **2024**, *401*, 124629, DOI 10.1016/j.molliq.2024.124629.

[70] T. Aida, E. W. Meijer, S. I. Stupp, *Science* **2012**, *335*, 813–7, DOI 10.1126/science.1205962.

[71] L. A. Ruppitsch, J. Ecker, T. Koch, K. Ehrmann, J. Stampfl, R. Liska, *J. Polym. Sci.* **2023**, *61*, 1318–1334, DOI 10.1002/pol.20220721.

[72] L. He, Y. Jiang, J. Wei, Z. Zhang, T. Hong, Z. Ren, J. Huang, F. Huang, P. J. Stang, S. Li, *Nat. Commun.* **2024**, *15*, 3050, DOI 10.1038/s41467-024-47333-1.

[73] L. Wang, L. Cheng, G. Li, K. Liu, Z. Zhang, P. Li, S. Dong, W. Yu, F. Huang, X. Yan, *J. Am. Chem. Soc.* **2020**, *142*, 2051–2058, DOI 10.1021/jacs.9b12164.

[74] Y. Liu, J. Wan, X. Zhao, J. Zhao, Y. Guo, R. Bai, Z. Zhang, W. Yu, H. W. Gibson, X. Yan, *Angew. Chem. Int. Ed.* **2023**, *62*, e202302370, DOI 10.1002/anie.202302370.

[75] M. W. Urban, D. Davydovich, Y. Yang, T. Demir, Y. Zhang, L. Casabianca, *Science* **2018**, *362*, 220–225, DOI 10.1126/science.aat2975.

[76] S. Burattini, H. M. Colquhoun, J. D. Fox, D. Friedmann, B. W. Greenland, P. J. Harris, W. Hayes, M. E. Mackay, S. J. Rowan, *Chem. Commun. (Camb)* **2009**, 6717–9, DOI 10.1039/b910648k.

[77] I. Onori, J. A. Berrocal, C. Weder, *Polymer* **2024**, *298*, 126886, DOI 10.1016/j.polymer.2024.126886.

[78] Z. Zhang, L. Cheng, J. Zhao, L. Wang, K. Liu, W. Yu, X. Yan, *Angew. Chem. Int. Ed. Engl.* **2020**, *59*, 12139–12146, DOI 10.1002/anie.202004152.

[79] Z. Zhang, D. Lei, C. Zhang, Z. Wang, Y. Jin, W. Zhang, X. Liu, J. Sun, *Adv. Mater.* **2023**, *35*, e2208619, DOI 10.1002/adma.202208619.

[80] M. Jiang, N. Mahmud, C. B. Koelbl, D. Herr, J. C. Worch, *J. Polym. Sci.* **2024**, *n/a*, DOI 10.1002/pol.20230982.

[81] L. Wimberger, G. Ng, C. Boyer, *Nat. Commun.* **2024**, *15*, 2510, DOI 10.1038/s41467-024-46656-3.

[82] K. Parkatzidis, N. P. Truong, K. Matyjaszewski, A. Anastasaki, *J. Am. Chem. Soc.* **2023**, *145*, 21146–21151, DOI 10.1021/jacs.3c05632.

[83] H. S. Wang, N. P. Truong, Z. Pei, M. L. Coote, A. Anastasaki, *J. Am. Chem. Soc.* **2022**, *144*, 4678–4684, DOI 10.1021/jacs.2c00963.

[84] J. B. Young, R. W. Hughes, A. M. Tamura, L. S. Bailey, K. A. Stewart, B. S. Sumerlin, *Chem* **2023**, *9*, 2669–2682, DOI 10.1016/j.chempr.2023.07.004.

[85] F. De Luca Bossa, G. Yilmaz, K. Matyjaszewski, *ACS Macro. Lett.* **2023**, *12*, 1173–1178, DOI 10.1021/acsmacrolett.3c00389.

[86] L. M. Fenimore, M. J. Suazo, J. M. Torkelson, *Macromolecules* **2024**, *57*, 2756–2772, DOI 10.1021/acs.macromol.3c02515.

Chapter 7

Summary/Samenvatting

English summary

The increasing amount of non-recylable thermosetting polymers is causing more and more environmental problems, due to the accumulating polymer waste. A possible solution to this problem is changing thermosetting polymer networks into covalent adaptable networks (CANs). CANs make use of dynamic covalent chemistry to gain traits of both thermoplastics and thermosets. The dynamic crosslinks allow CANs to be reprocessed and recycled, while retaining most of the mechanical strength of thermosetting polymers.
In this thesis the novel boronate-TetraAzaADamantane (boronate-TAAD) CAN was introduced. This thesis also contains chapters on how the properties of furan-maleimide or boronate-TAAD networks can be tuned through variations in (electronic) aromatic ring substituents. The boronate-TAAD CANs were also tuned using acid catalysis.
In chapter 2 a study was reported on how to test whether varying ring substituents on maleimide linkers could be used to tune the properties of a furan-maleimide network. A series of five differently substituted maleimide linkers (varying in their electronic properties) was prepared and incorporated into furan-maleimide networks. The networks were first analysed using IR, allowing the calculation of $\Delta_r H°$ and $\Delta_r S°$ values through Van 't Hoff plots. Plotting the obtained enthalpy and entropy values against the Hammett (σ_p) values (as a measure for their electronic properties) of the substituents gave a positive trend, suggesting that these networks can indeed be tuned by varying ring substituents. However, when comparing relaxation data obtained from rheological experiments no clear dependence on σ_p was observed. This seems to suggest that variations in the ring substituents of maleimide linkers are not the main contributor in the macroscopic stress relaxation of these networks.

In chapter 3 a novel type of boronate CAN was discussed. The new type involves the use of a TAAD moiety, which is an adamantane-like structure featuring four nitrogen atoms and three hydroxyl groups, as a replacement of the conventionally used diol for boronate ester formation. Stress relaxation experiments, combined with extensional DMA tests on the recycled material, showed that the boronate-TAAD networks are indeed viable as CANs.
In chapter 4 the boronate-TAAD network was compared to a conventional boronic ester network in an effort to better understand the differences between the two systems. The boronate-TAAD networks showed to be stiffer and stronger than the boronic ester networks in rheological testing. Relaxation studies also showed that the boronate-TAAD exchange has a higher activation energy compared to the boronic ester exchange. The boronic ester network did display a higher thermal stability in TGA measurements. Next to this, also the possibility of using ring substituents on phenylboronic acids to tune the macroscopic material properties was demonstrated. A series of variants with different substituents on the *meta*-position relative to the boronic acid was prepared and the resulting networks compared. When comparing the activation energies of the dynamic exchange, as obtained from the relaxation data, and the σ_{m} value of the substituent a linear trend was observed, thus showing the possibility for controlled material tuning in these boronate-TAAD networks.
In chapter 5 the boronate-TAAD motif was implemented into a polystyrene-based material, thus converting the thermoplastic polystyrene into a CAN. The polymer was prepared by polymerising the styrene with a small amount of 4-vinylbenzyl bromide, which was then used to attach the TAAD moiety via quaternisation of the tertiary amine of the TAAD moiety. After crosslinking an insoluble material was obtained. Variations in crosslinking degree of the network were prepared, which all gave swelling materials with high insoluble fractions, indicative of network formation. The T_{g} of the networks was around 83 °C, which is slightly lower than the unmodified polystyrene (≈100 °C). TGA showed the first thermal decomposition step around 180 °C. The effects of crosslinking degree and the addition of an acid catalyst on the relaxation behaviour were also studied. Lower crosslinking degrees generally relaxed faster while higher wt% of acid mixed in resulted in faster relaxation time up until 5 wt% of acid, after which the network did not relax faster. DMA showed that the materials could be reprocessed at least two times. Overall, this study revealed it is possible to transform an existing polymer (polystyrene in this case) into a covalent adaptable network, with properties derived from both the

monomer structure, but also from the dynamic network architecture. Chapter 6 discussed the results of earlier chapters and placed their results in the context of the field of CANs. This chapter also outlined some future research suggestions, mostly based on preliminary experiments performed during the work described in this thesis.

Nederlandse samenvatting

De toenemende hoeveelheid van niet-recyclebare thermohardende polymeren geeft steeds meer milieuproblemen, door het ophopende polymeer afval. Een mogelijke oplossing hiervoor is het vervangen van thermohardende polymeer netwerken door zogenaamde covalent adaptieve netwerken (CANs). CANs gebruiken dynamisch covalente chemie om eigenschappen van zowel thermoplasten en thermoharders te verkrijgen. De dynamische verbindingen zorgen er namelijk voor dat CANs wel verwerkt kunnen worden, terwijl zij grotendeels de mechanische kracht van thermohardende polymeren behouden.

In deze thesis is de nieuwe boronaat-TetraAzaADamantaan (boronaat-TAAD) CAN geïntroduceerd. Deze thesis bevat ook hoofdstukken over hoe de eigenschappen van furan-maleimide of boronaat-TAAD netwerken afgestemd kunnen worden door variaties in (elektronische) aromatische ringsubstituenten. De eigenschappen van de boronaat-TAAD CANs zijn ook verder afgestemd door het gebruik van zuur-gebaseerde katalysatoren.

In hoofdstuk 2 is onderzoek beschreven hoe variaties in ringsubstituenten konden worden gebruikt om eigenschappen van furan-maleimide netwerken af te stemmen. Hiervoor zijn vijf verschillend gesubstitueerde maleimide linkers gemaakt, waarbij met name de elektronische eigenschappen van de substituenten zijn gevarieerd. Deze zijn vervolgens gebruikt in verschillende netwerken. De netwerken werden eerst geanalyseerd met IR. Hierdoor konden $\Delta_r H°$ en $\Delta_r S°$ waarden voor de furan-maleimide reactie berekend worden via zogenaamde Van 't Hoff plots. Wanneer de berekende enthalpie en entropie waardes uitgezet werden tegen de σ_p waarden van de substituenten (als maat voor de elektronsische eigenschappen) werd een positieve trend gevonden. Dit suggereert dat deze netwerken inderdaad afgestemd kunnen worden door variaties in de ringsubstituenten. Maar wanneer gekeken werd naar het relaxatiegedrag van de verschillende netwerken werd geen duidelijk verband gebaseerd op σ_p gevonden. Dit suggereert dat de variatie in ringsubstituenten van maleimide linkers niet de belangrijkste bijdrager is in het afstemmen van macroscopische materiaaleigenschappen.

Hoofdstuk 3 beschreef een nieuw type covalent adaptief netwerk. Dit nieuwe type maakt gebruik van een TAAD groep, een adamantaan-achtige structuur met vier stikstof atomen en drie hydroxyl groepen, als vervanging van de conventionele diol voor boronaat ester vorming. Relaxatie experimenten, gecombineerd met extensie DMA testen op gerecycled materiaal, lieten zien dat boronaat-TAAD netwerken geschikt zijn als covalent adaptieve netwerken.

In Hoofdstuk 4 werden de nieuwe boronaat-TAAD netwerken vergeleken met conventioneel boorzuur ester netwerken in een poging om de verschillen tussen beide netwerken beter te begrijpen. De boronaat-TAAD netwerken bleken stijver en sterker dan de boorzuur ester materialen tijdens de reologische testen. Relaxatiestudies lieten zien dat de boronaat-TAAD uitwisseling een hogere activeringsenergie had dan de boorzuur ester uitwisseling. Darentegen, had het boorzuur ester netwerk een hogere thermische stabiliteit volgens TGA metingen. Deze studie liet ook zien dat het mogelijk is om macroscopische materiaaleigenschappen af te stemmen door het variëren van ringsubstituenten op fenylboorzuren. Een serie van varianten met verschillende substituenten op de *meta*-positie in relatie tot het boorzuur was bereid en de resulterende netwerken zijn vergeleken. Bij het vergelijken van de activerings energieën van de dynamische uitwisselingen, verkregen uit de relaxatie data, met de σ_{m} waarden van de substituenten werd een lineaire trend gevonden. Dit bewees de mogelijkheid van gecontroleerde materiaalafstemming in deze boronaat-TAAD netwerken.

Hoofdstuk 5 beschreef hoe het boronaat-TAAD motief kan worden geïmplementeerd in een materiaal gebaseerd op polystyreen, waardoor het thermoplastische polystyreen veranderd werd in een CAN. Het polymeer werd bereid door het styreen te polymeriseren in aanwezigheid van een kleine hoeveelheid 4-vinylbenzyl bromide, wat vervolgens gebruikt werd om de TAAD groep vast te maken aan het polymeer via reactie met de tertiaire amine groep van TAAD. Na het crosslinken vormde zich een onoplosbaar materiaal. Verschillende materialen met variaties in de hoeveelheid dynamische bindingen in het netwerk gaven allemaal zwelbare materialen met een hoge onoplosbare fractie. De T_{g} van de netwerken lag rond de 83 °C, wat net wat lager ligt dan conventioneel polystyreen (≈100 °C). TGA liet zien dat de eerste stap van thermische degradatie lag rond de 180 °C. De effecten van de mate van verknoping en de additie van een zuur katalysator op de relaxatie zijn ook onderzocht. Minder verbindingen gaven over het algemeen een snellere relaxatie en hogere gewichtsprocenten ingemengd zuur gaven snellere relaxatie tot 5 gewichtsprocent ingemengd zuur, daarna zorgde meer zuur niet voor nog snellere relaxatie. DMA liet zien dat de materialen ten minste twee keer herverwerkt konden worden.

Hoofdstuk 6 besprak de resultaten van voorgaande hoofdstukken en plaatste deze in de context van het CAN veld. Dit hoofdstuk gaf ook een aantal suggesties voor toekomstig onderzoek voornamelijk gebaseerd op verkennende experimenten die uitgevoerd zijn tijdens het werk dat is beschreven in dit proefschrift.

Chapter 8

Acknowledgements

A PhD is a long road with many obstacles to overcome. A lot has to be learned on this road, both about the practices of science and about yourself as a scientist. Fortunately, a lot of people provided much needed support along the way.

First on the list of people to thank for their support is my co-promoter and daily supervisor Maarten Smulders. Thank you for giving me the opportunity to do this PhD and for the support and guidance that you provided over the last few years. Especially also for our weekly meeting where I would deep-dive into a minuscule (please read as molecular) detail within the first few seconds.

I also like to thank my promotor Han Zuilhof for giving me the opportunity to do this PhD and a more general acknowledgement for being the chair of our research department, thus making this research possible.

My sincerest gratitude goes to the thesis committee members for their time and hard work that made it possible to hold a public PhD defence. The same holds true for the board members and the supporting personnel involved in the preparation and execution of the ceremony.

Another big thank you goes out to my paranymphs Natalia Bornosuz and Thijmen van Voorthuizen, who really helped me through my defence.

Sagar, thank you for your help in finishing the experimental work of chapter 5. I would not have been able to finish the chapter without you.

I would also like to thank all the students who worked on the various research projects. The hard work of Thomas Lieshout, Stefan Bontekoe, Marijn Kisters, Irene Hulsen & Thomas Buijsen is greatly appreciated. Wishing you luck in your future studies and/or careers.

The technicians of ORC and PCC also deserve their fair share in this acknowledgement. Thanks go to Barend for support with the NMR and XPS, Hans for support with the GPC systems, Frank for support with the MS measurements and Raoul for fixing problems in the rheological experiments. Herman de Beukelaer is thanked for his help with the DSC and TGA measurements. I would also like to extend the acknowledgements to the staff involved in the many educational duties that ORC has. It was always nice whenever I had to provide education together with you.

The people of lab 8048 also get a well deserved thank you for the nice & supportive atmosphere in the lab. A lot of the time the space between our fume hoods was filled with some rather catchy tunes.

Throughout the years many people came and/or went in our office 8056. We had a really supportive & friendly little environment with our Viking pizza cat mascot. For this I would like to thank everyone who happened to be seated in 8056 over the last few years. I would like to thank Esther, Sybren, Vahid, Bas (+ his 2D friend) and our unofficial office mate Andriy for the pleasant atmosphere. Annemieke, thank you for the nice talks we had. Ellen, thank you for our programming collaboration on the IAST GUI. It really made me feel like a techno-wizard for a moment.

The Wednesday morning workgroup members are thanked for their critical questions and insightful suggestions during the early hours.

I would like to extend my gratitude to all members of the Laboratory of Organic Chemistry and thank them for being around (just in general) and for being nice colleagues. I like to wish all who are still hard at work to complete their PhD a lot of good luck.

Last, but certainly not least, wil ik ook nog mijn familie bedanken voor hun support tijdens mijn PhD traject. Pap, bedankt dat je altijd klaar stond om te helpen en dat je voor wat rust zorgde door taken uit handen te nemen. Frits, bedankt voor de leuke game avonden en uitstapjes om even aan wat anders te denken. Mam, ik weet zeker dat jij het ook mooi en interessant gevonden zou hebben. Speciale dank voor mijn oma die iedere avond een waterval van (semi-)wetenschappelijke termen mocht (lees moest) aanhoren. Ik kan je met zekerheid zeggen dat de stortvloed van termen vaak wel enige betekenis had. Ook de katten moeten bedankt worden voor hun hulp. Felix voor haar dwang om altijd op mijn schoot te liggen, en dus rust af te dwingen. Yoda voor haar eeuwige, luide kreten van steun (neem ik aan). Luigi voor zijn 'subtiele' herinneringen om pauzes in te lassen (en dan natuurlijk meteen het etensbakje te vullen) en zijn liefdevolle, maar keiharde, kopstoten om 's ochtends meteen goed wakker te worden.

Chapter 9

About the author

Simon van Hurne was born on April 19th 1996 in Amersfoort, The Netherlands. In 2014 he started his bachelor in 'Molecular Life Science' at the Wageningen University and Research (WUR) with a minor in bionanotechnology and a thesis on block co-polymer end-cap functionalisation for functionalising the outside of complex coacervate core micelles at the bionanotechnology department under supervision of prof. dr. Aldrik Velders and prof. Vittorio Saggiomo. In 2017 he continued at the WUR with a master in 'Molecular Life Science' with a specialisation in physical chemistry and a thesis on oxidant responsive cyclodextrin-based complex coacervate core micelles under supervison of prof. dr. Aldrik Velders, dr. Vittorio Saggiomo and dr. Camilla Facciotti at the bionanotechnology department. He also did an internship at the Soft Robotics group at AMOLF about the microscale 3D printing of swellable structures under supervision of dr. ir. Bas Overvelde and dr. Augustin Iniguez-Rabago. After graduating in 2019, he started a PhD in organic chemistry on the topic of covalent adaptable networks under dr. ir. Maarten Smulders and prof. dr. Han Zuilhof at the laboratory of organic chemistry at the WUR.

List of publications

- **S. van Hurne***, S. K. Raut, M. M. J. Smulders, *Recyclable Covalent Adaptable Polystyrene-Networks using Boronates and TetraAzaADamantanes*, ACS Applied Polymer Materials, 2024, 6, 13, 7918–7925, 10.1021/acsapm.4c01633
- **S. van Hurne***, T. J. M. Buijssen, M. M. J. Smulders, *Tuning Material Properties of Covalent Adaptable Networks Containing Boronate-TetraAzaADamantane Bonds Through Systematic Variation in Electron Density of Ring Substituents*, Journal of Polymer Science, 2023, 1, 10.1002/pol.20230446
- **S. van Hurne***, M. Kisters, M. M. J. Smulders, *Covalent adaptable networks using boronate linkages by incorporating TetraAzaADamantanes*, Frontiers in Chemistry, 2023, 11, 10.3389/fchem.2023.1148629.
- E. Dautzenberg*, **S. van Hurne***, M. M. J. Smulders, L. C. P. M. de Smet, *GraphIAST: A graphical user interface software for Ideal Adsorption Solution Theory (IAST) calculations*, Computer Physics Communications, 2022, 280, 108494, 10.1016/j.cpc.2022.108494.
- C. Facciotti*, V. Saggiomo, **S. van Hurne**, A. Bunschoten, R. Kaup, A. H. Velders, *Oxidant-responsive ferrocene-based cyclodextrin complex coacervate core micelles*, Supramolecular Chemistry, 2020, 32, 30-38, 10.1080/10610278.2019.1685094.

*first author

Overview of completed training activities

Discipline specific activity	**Organiser(s)**	**Place**	**Year**
Advanced Organic Chemistry	VLAG - ORC	Wageningen	2019-2023
CHAINS 2019	NWO	Veldhoven	2019
CHAINS 2020	NWO	Veldhoven	2020
Rheology: the do's and don'ts	VLAG - PCC	Wageningen	2020
CHAINS 2021*	NWO	Veldhoven	2021
Vitrimat training school 2021 (Vitrimers: high performance materials for cutting edge applications)	Ghent University /Lyon University	Online	2021
Brightlands polymer days 2021	KNCV, BPG, PTN, Brightlands	Veldhoven	2021
CHAINS 2022*	NWO	Veldhoven	2022
18th European School on Rheology	KU Leuven	Leuven	2022
Dutch Polymer Days 2023**	PTN	Lunteren	2023
IUPAC - CHAINS 2023**	KNCV, NWO, IUPAC	Den Haag	2023

General activities	**Organiser(s)**	**Place**	**Year**
Competence Assessment	WGS	Wageningen	2019
Presenting with Impact	WGS	Wageningen	2021
Effective behaviour in your professional surrounding	WGS	Wageningen	2021
Supervising BSc & MSc thesis students	WGS	Wageningen	2021
Scientific Publishing	WGS	Wageningen	2022
Efficient Writing Strategies	WGS	Wageningen	2023
Career perspectives	WGS	Wageningen	2023

Other activities	**Organiser(s)**	**Place**	**Year**
Write Research Proposal	-	Wageningen	2019
Group meetings	ORC	Wageningen	2019-2024
Organisation of PhD excursion 2020-2022 during pandemic	ORC	Wageningen	2020-2022
International PhD excursion	ORC	Wageningen	2023

Teaching activities (code)	**Year(s)**
Organic Chemistry 2 (ORC-12903)	2019-2021
Supervision of BSc/MSc students	2019-2023
Bio-Organic Chemistry for Life Sciences (ORC-13803)	2020-2021
Organic Chemistry 1 (ORC-12803)	2020-2021
Spectroscopy and imaging (BIP-24306)	2020-2023
Organic Chemical Analytical Methods; spectroscopy (ORC-11806)	2021-2022
Exam supervision	2021-2022

The research described in this thesis was financially supported by the Dutch Research Council (NWO, Vidi grant 016.Vidi.189.031 granted to Maarten Smulders).

Financial support from Wageningen University for printing this thesis is gratefully acknowledged.

Cover design by Simon & Frits van Hurne
Layout and inside design was done by the author.

Printed by https://www.proefschriftmaken.nl